ANALYSIS OF THE WATER BALANCE IN THE CALEDON RIVER CATCHMENT USING THE SOIL AND WATER ASSESSMENT TOOL (SWAT) MODEL

MATETE MATHIAS LETSOELA

Dissertation submitted in fulfilment of the requirements for the Degree

MASTER OF ENGINEERING IN
CIVIL ENGINEERING

in the

Department of Civil Engineering
Faculty of Engineering, Built Environment and Information Technology

at the
Central University of Technology, Free State

Supervisor: Prof. Y.E Woyessa, Ph.D.
Co-Supervisor: Dr. G Ndhlovu, DEng

December 2024
Bloemfontein

Central University of Technology, Free State

DECLARATION OF INDEPENDENT WORK

I, MATETE MATHIAS LETSOELA, identity number ### ### ### ### (LESOTHO) and student number ########, do hereby declare that this dissertation submitted to the Central University of Technology, Free State, for the Master of Engineering in Civil Engineering is my own original research work; and complies with the code of Academic Integrity, as well as other relevant policies, procedures, rules and regulations of the Central University of Technology, Free State; and has not been submitted before to any institution by myself or any other person in fulfilment of the requirements for attainment of any qualification.

SIGNATURE OF STUDENT   DATE

DEDICATION

I would like to dedicate this work to my Wife, Mankhethoa 'Mamocansi' Letsoela, whom I am highly indebted to, for her constant love and the motivation she instilled in me through the time of my study. Similarly, I express my deep appreciation to my mother for her love and nurturing me into the man that I am today.

May this collection of engineering work contribute towards the development of my country, the mountain Kingdom of Lesotho.

ACKNOWLEDGEMENTS

First and foremost, I would like to express my sincere gratitude and deep respect to my academic supervisor, Prof. Yali Woyessa, and my co-supervisor, Dr George Ndhlovu, for their patience and invaluable experience throughout this study. Their impeccable supervision enabled me to complete this study, and for that, I will forever be grateful. I am greatly honoured to have been their student, and I hope to emulate their achievements by becoming an acclaimed scholar.

I would also like to extend my heartfelt thanks to the Ministry of Water Affairs, the Food and Agricultural Organisation in Lesotho, and the Lesotho Meteorological Services for providing the much-needed data for my research.

Moreover, I am grateful to my colleagues at Lerotholi Polytechnic, especially the staff of the School of the Built Environment (SOBE), for their support, advice, and constructive criticism. My appreciation also goes to the Central University of Technology for admitting me into their MEng program and for the resources and patience they provided throughout my study.

Finally, I thank my family—my brother, sisters, and my son—and my friends for their unwavering encouragement throughout the course of this study.

ABSTRACT

The Caledon catchment is one of the primary sub-catchments in the Orange Senqu River basin and a crucial hydrological area in both South Africa and Lesotho. The sustainable water resources planning of the Caledon can be achieved through hydrological modelling, given its status as a transboundary catchment shared by Lesotho and South Africa. This study was initiated to critically analyse the water balance components (WBCs) and understand the rainfall-runoff behaviour of the catchment, which are essential for sustainable water resources development and management.

This study presents an application of the SWAT model (Soil and Water Assessment Tool) in the mountainous-agricultural Caledon catchment, which spans Lesotho and parts of South Africa, covering an area of 13 370 km². The watershed area was divided into 31 sub-watersheds, predominantly occupied by agricultural land (42.44%), grassland (42.29%), urban development (5.05%), shrubs (5.74%), and water bodies (4.47%), with the remaining 0.01% being range land. The catchment ranges in longitude from 26°34’46” to 28°49’55” and in latitude from -28°22’53” to -29°43’58”, with an elevation ranging from 1413 m to 3158 m.

The model was set up using observed rainfall from the Lesotho Meteorological Services (LMS) and observed temperature. The SWAT model was calibrated and validated manually by adjusting the curve number (CN2) for the period from 2010 to 2018. Model performance was evaluated using statistical performance indicators such as Nash–Sutcliffe model efficiency (NSE), the ratio of the root mean square error to the standard deviation of measured data (RSR), and the coefficient of determination (R^2). The model, set up with observed rainfall from LMS, produced satisfactory results for both calibration and validation, demonstrating a high capability for estimating runoff in the Caledon catchment when coupled with observed rainfall. The outputs of this study will be used by engineers, scientists, and decision-makers to manage water resources at the sub-watershed level.

Finally, the developed SWAT model analysed important water balance components, including rainfall, direct runoff, evapotranspiration, surface runoff, and water yield at the catchment level for the nine-year period from 2010 to 2018. A drought occurred between 2015 and 2016 due to low precipitation, but there was a significant increase in precipitation thereafter. The monthly rainfall range over the nine years of simulation was from 0 to a maximum of 88.83 mm, evapotranspiration (ET) ranged from 1.44 to 78.00 mm, direct runoff from 0 to 22.51 mm, and water yield from 0.09 to 21.13 mm. It was observed that ET and water yield were the only water balance components consistently above zero, possibly due to groundwater contributing to water yield, resulting in perennial flow throughout the years.

Overall, the performance of the SWAT model in simulating the water balance in the Caledon catchment is rated as good, and the calibrated model could be used for runoff simulation in this agriculture-dominated watershed. The SWAT model application, supported by GIS technology, proved to be a flexible and reliable tool for water resource decision-making.

TABLE OF CONTENTS

LIST OF FIGURES

LIST OF TABLES

ACRONYMS AND ABBREVIATIONS

A	Area
AASHTO	American Association of State Highway and Transportation Officials
Agrl	Agriculture
ARS	Agricultural Research Services
BMP	Best Management Practice
CN	Curve Number
CN2	Curve Number in SWAT
DEM	Digital Elevation Model
DHI	Danish Hydraulic Institute
EPA	Environmental Protection Agency
EPIC	Environmental Policy Integrated Climate
Eq.	Equation
ER	Environmental Reserve
ET	Evapotranspiration
Eα	Evapotranspiration
FAO	Food and Agriculture Organization
GEF	Global Environmental Facility
GIS	Geographical Information System

GLEAMS	Groundwater Loading Effects of Agricultural Management Systems
Gras	Grassland
GW	Groundwater
HEC	Hydrologic Engineering Centre
HEC-HMS	Hydrologic Engineering Centre-Hydrologic Modelling System
HRU	Hydrologic Response Units
IA	International Agreements
IAEA	International Atomic Energy Agency
IFR	Instream Flows Requirements
IHA	Indicators of Hydrologic Alteration
L	Flow Length
LATQ	Lateral Flow
LHDA	Lesotho Highland Development Authority
LHWC	Lesotho Highland Water Commission
LHWP	Lesotho Highland and Water Project
LMS	Lesotho Meteorological Services
LULC	Land Use/ Land Cover
MAP	Mean Annual Precipitation
MIKE-SHE	Mike System Hydrological European

MUSLE	Modified Universal Soil Loss Equation
N	Nitrate
NASA	National Aeronautics and Space Administration
NOAA	National Oceanic and Atmospheric Administration
NSE	Nash-Sutcliffe Efficiency
θ_d	Drainable porosity
ORASECOM	Orange Senqu River Commission
PBIAS	Percent Bias
Prec	Precipitation
Q	Discharge
QGIS	Quantum Geographical Information System
Qgw	Groundwater flow
Qgwj	Groundwater flow into the main channel
Qlat	Lateral Flow
Qsurf	Surface Runoff
QSWAT	Quantum Soil and Water Assessment Tool
R^2	Coefficient of Determination
Rday	Daily Precipitation
Rnge	Rangeland

RSR	Ratio of the mean square error to the standard deviation of measure data
S	Retention Parameter
SADC	Southern African Development Community
SC	Saturated Hydraulic Conductivity
SCS	Soil Conservation Services
SEI	Stockholm Environment Institute
Shrb	Shrub
SURQGEN	Surface Runoff
SWAT	Soil and Water Assessment Tool
SWMM	Storm Water Management Model
Swo	Initial Soil Water Content
Swt	Soil Water Content
SW	Soil Water
TCTA	Trans Caledon Tunnel Authority
Tloss	Transmission loss
UN	United Nations
UN-DESA	United Nations Department of Economic and Social Affairs
UNDP	United Nations Development Programme
Urbn	Urban

USA	United States of America
USCS	Unified Soil Classification System
USDA	United States Department of Agriculture
USGS	United State Geological Survey
V	Volume
WBC	Water Balance Components
WEAP	Water Evaluation and Planning System
WETW	Water
WMS	Watershed Modelling System
Wrchrg	Amount of recharge entering the aquifers
Wseep	Percolation
Wyld	Water Yield
α	Slope of Land
αgw	Baseflow Recession Constant
Δt	Time step

1. INTRODUCTION

1.1. Background

The Orange Senqu River basin covers an area of almost 1 million km^2 and has an estimated natural runoff of 11 300 km^3/annum which flows in a westerly direction 2200 km into the Atlantic Ocean from Lesotho. Of the 11 300 km^3/annum flow, 41% originates from the Lesotho highlands and approximately 900 million m^3/annum from contributing catchment downstream of the orange Vaal confluence which includes part of Namibia and a small portion in Botswana. The remaining natural runoff of 6700 million m^3/annum is generated from areas contributing to the Vaal, Caledon, Kraai and middle orange rivers (Tompkins, 2007; Mare, 2007). Table 1.1 shows contributing river basins from four different countries.

Table 1.1. Contributions to the Orange Senqu River basin by country (Tompkins, 2007).

Item	**Lesotho**	**SA**	**Botswana**	**Namibia**
Basin Area (%)	5	60	12	25
MAP (%)	41	55	0	4

The Lesotho highlands water project is a bilateral agreement between the Governments of Lesotho and South Africa, and water gets transferred from Mohale to Katse via a transfer tunnel of ±32 km long with a width of 3.9 m. Transfer tunnel from Katse to 'Muela is ±45 km long and 4.35 m in diameter, and from 'Muela to Vaal Dam water travels in a 4.6 m diameter delivery tunnel, travelling at a speed of 29 m/s (Mare, 2007).

Water between Lesotho and South Africa must be managed in a sustainable manner and protected from pollution as declining water quality is a global issue of concern because human populations grow, industrial and agricultural activities expand, and climate change threatens to cause major alterations to the hydrological cycle (UN Water, 2015; Heath and Brown, 2007). Serious and increasing pollution of fresh water in both developing and developed countries poses a growing risk to public health, food security, biodiversity and other ecosystem services. However, pollution is strongly linked to economic development with population growth and the expansion of agriculture, industry and energy production all in turn producing wastewater, much of which goes into surface and groundwater bodies uncontrolled or untreated. Major pollutants include nutrients, pathogens, heavy metals, organic pollutants and micro-pollutants found in wastes and wastewater from humans and economic activities such as agriculture, industry, mining, and other sectors such as pharmacy (UN Water, 2016).

Transboundary water resources in Lesotho can be protected nationally by enforcing the Environment Act, which is the framework for implementing the National Environment Policy. The principles of the policy include the following:

i. Ensuring that every person living in Lesotho has a fundamental right to a clean and healthy environment.
ii. Establishing adequate environmental standards.
iii. Polluter pays principle.
iv. Promotion of national, regional and international cooperation for the protection of the environment (Long-Term Water and Sanitation Strategy Volume II Water Sector Programme, 2014).

In this study, the Soil and Water Assessment Tool (SWAT) model was used to analyse the water balance of the Caledon catchment, a watershed drained by the Caledon River, a major tributary of the Senqu-Orange River which is also one of the most important river courses in Southern Africa. This river stretches over Lesotho and South Africa (Chatanga et al., 2018). SWAT is a type of hydrological model used in modern hydrology studies. It is a semi-distributed watershed model which is used to evaluate hydrological parameters such as runoff, transportation of sediment and nutrient, and agricultural management practices, and it operates on a daily or monthly time scale. It is further used for assessing the impact of climate change, chemicals due to agricultural land practice, and sediment yields in large river basins (Arnold et al., 1998 in Kurbah and Jain, 2017; Pohlert et al., 2005; Byakod et al., 2017; Neitsch et al., 2009). It is a physical, conceptual and distributed river basin and deterministic model that operates under different climatic conditions, so it requires a large number of input parameters (Kurbah and Jain, 2017; Ruan, 2016).

Furthermore, it is a tool that is used in conjunction with GIS (Geographical Information System) technology for flexible and reliable outcome in water decision making (Patil et al., 2014).

1.2. Problem statement

Lesotho is a developing country with majority of its catchment poorly managed. This is revealed by the immense erosion of soil in its rural watershed, which is caused by overgrazing and indiscriminate cutting down of trees/forests amongst others. The poor water resource and infrastructure management in the country is also reflected in the quality of its climate stations data (Smith et al., 2012). According to the Lesotho state of water resource report (2016) the Lesotho meteorological station operates a total of 53 rainfall stations in which a given station records a cumulative rainfall amounts on daily basis. In total, there are 90 operational stations in Lesotho and the remaining others are operated by non-government agencies. The effects of this socio-economic problems contribute massively to the general degradation and monitoring of water quantity and quality of the water resources in the country.

The Caledon catchment harbours entirely all the urban area and the industrial activities of Lesotho, including textile industries. In the year 2001, these industries were the second largest employer after the government of Lesotho. The textile industries are categorised under the wet industries, making them the most water demanding type of industries. It is probably for this reason why foreign investment found Lesotho as an ideal location for their placement, as it has abundant water resources which are, however, affected by annual and seasonal variations (Ministry of water resources, 2002; Gibbs and Gibbs, 2002). Despite hosting the industrial and urban activities of the country, little research has been conducted on the state of water resources of the Caledon catchment. However, more sources for research and water infrastructure have been invested towards the water-rich Senqu catchment which houses the Lesotho and South Africa water impoundment and transfer infrastructure, result in less emphasis on the Caledon catchment.

The Millennium Challenge Account compact II, an initiative of the American government, plans to build irrigation infrastructure covering up to 15.8 km^2 of agricultural land within the Caledon catchment. The places to benefit from this initiative are Kolonyama, Peka, Likhakeng and Hlotse in the Leribe district as well as Phamong in the Mohale's Hoek district. This irrigation scheme will bring about the largest irrigation infrastructure to ever take place in the history of Lesotho, and this will place enormous pressure on the water resources in the catchment area (American Embassy, 2022). The pressing environmental, social and economic problems of increasing water demand can potentially be understood better by modelling of hydrological parameters and a thorough water balance analysis of the catchment.

1.3. Aim and Objectives

The main aim of this study is to analyse the water balance and rainfall-runoff behaviour of the Caledon catchment in Lesotho and South Africa.

The specific objectives are:

- To calibrate and validate the SWAT model for the catchment.
- To analyse the water balance of the catchment
- To make recommendations on the management of water resources in the catchment.

1.4. Significance of the study

The significance of this study is to:

- Contribute to sustainable water resources management and planning.
- Assist in effective allocation and efficient utilization of water resources for socio-economic activities.
- Understand the water balance and rainfall-runoff behaviour of the Caledon catchment in both Lesotho and South Africa.
- Determine the water balance of the catchment and verify the simulations the simulations carried out by the government of Lesotho.

1.5. Structure of the dissertation

This dissertation is divided into five chapters as follows:

- Chapter 1: contains a background of the study, an introduction of the aims and objectives of the study, the problem statements, and the significance of the study.
- Chapter 2: contains an extensive review of the past and current literature on catchment environmental hydrology and other contributing factors relevant to the topic of the study.
- Chapter 3: contains an explanation of the research methodology used to conduct this study. The data collection procedures, data preparation strategies, the hydrological model used in the study and the model evaluation techniques used are discussed in this chapter.
- Chapter 4: in this chapter, the analysis of the results of this study is presented including a comprehensive discussion of the results.
- Chapter 5: this chapter contains the summary and conclusions of the study based on the results obtained in relation to the research objectives, and it further provides recommendations for similar future studies.

2. LITERATURE REVIEW

2.1. Introduction

Clean and abundant water forms the foundation for agriculture, energy production, commerce, industry, transportation, and recreation. The global system that supplies and removes water from the Earth's surface is known as the hydrological cycle, which involves the transfer of water to the Earth's atmosphere through evaporation and transpiration processes (Davis and Cornwell, 2013).

According to the US National Research Council (1991), "hydrology is the science that treats the water of the Earth, their occurrence, circulation, and distribution, their chemical and physical properties, and their reaction with the environment, including the relation to living things. The domain of hydrology embraces the full life history of water on Earth." The hydrological cycle explains the continuous motion of water, powered by the sun, which removes water from the oceans into the atmosphere and onto the land, where it is pulled by gravity and flows back to the oceans (Lazaro, 1990). Hydrology is not entirely a pure science, as it has many practical applications and heavily relies on knowledge from other sciences (Sahasrabundhe, 2011). Freshwater constitutes only 2.5% of all the water on Earth, but not all of this is available for human use, as some is locked in polar ice caps, soil moisture, marshes, and biological systems. Groundwater comprises 99% of the Earth's available freshwater, with a volume of 10.5 million km^3. Additionally, there are 91 000 km^3 of freshwater in lakes and 2120 km^3 in rivers (Delleur, 1999; Lazaro, 1990).

The runoff from the Lesotho lowlands drains westward to the Caledon River, while the highlands drain southward via the Senqu River to the Orange River. The lowlands area is susceptible to erosion, and the Caledon River transports large sediment loads, causing extensive sedimentation in dams such as the Welbedacht Dam (Coleman and Van Niekerk, 2007).

2.2. Trans-boundary Water Policies

When countries need to cooperate in managing a shared resource, such as the Orange River, the most effective way is through international agreements. This exercise of sovereignty allows independent states to align their national legal and jurisdictional frameworks with political and geographical realities (Hiddema and Erasmus, 2007). National constitutions often include provisions for the approval, ratification, and incorporation of international agreements. Legal arrangements involving multiple states must be clear and detailed to ensure certainty and predictability (Hiddema and Erasmus, 2007). Cross-boundary policy and legal instruments frequently face enforceability issues due to insufficient mechanisms to handle conflicts adequately. For instance, the Canadian Guidelines for Recreational Water Quality only become legally enforceable if adopted into provincial or territorial legislation (UN Water, 2015). Cooperation enables better ecological management by providing benefits to rivers, aquifers, lakes, wetlands, and related ecosystems, as well as adjacent estuaries, coastal areas, and seas (UN Water, 2008).

There are 263 transboundary lake and river basins globally, covering nearly half of the Earth's land surface and accounting for an estimated 60% of global freshwater flow. These transboundary basins and aquifers link populations of different countries and support the incomes and livelihoods of hundreds of millions of people worldwide. All transboundary water bodies create hydrological, social, and economic interdependencies between societies. While they hold the potential for conflict, they also provide opportunities for cooperation, promoting regional peace, security, and economic growth (UN Water, 2008).

The United Nations agencies involved in transboundary water cooperation include:

1. Food and Agricultural Organization of the United Nations (FAO): FAO helps member countries sharing a transboundary river, lake, or aquifer establish a legal and institutional environment conducive to stable and mutually beneficial cooperation.

2. Global Environment Facility (GEF): Established in 1991, GEF addresses global environmental issues by helping countries sharing transboundary waters establish priorities, adopt policy, legal, and institutional reforms, and test the feasibility of various investments to address conflicts and reverse degradation.

3. International Atomic Energy Agency (IAEA): IAEA is involved in transboundary groundwater management through projects in Africa and Latin America, aiming to enhance cooperation and shared management mechanisms through improved scientific assessment and understanding of aquifer systems and stronger institutional frameworks.

4. United Nations Department of Economic and Social Affairs (UN-DESA): UN-DESA promotes and supports international cooperation to achieve development for all, facilitating intergovernmental debates and providing analytical and technical support to developing countries and countries with economies in transition.

5. United Nations Development Programme (UNDP): Through its GEF International Waters portfolio, Transboundary River Basin Initiative, and other programs, UNDP supports governance reform processes in over 35 shared water bodies, involving over 100 countries (UN Water, 2008).

Each basin state has its own legal, policy, and institutional framework governing the use of both national and international waters, adding significant complexity to water management at the basin level. The Orange-Senqu River Commission (ORASECOM) encourages communication on basin issues among member states through annual meetings of state representatives and stipulates that resources within respective states must be utilized equitably and reasonably. ORASECOM serves as a technical advisor to member states and can conduct feasibility studies to support decision-making (Tompkins, 2007).

The objectives of the Lesotho Water Treaty 1986, signed between Lesotho and South Africa, are to:

- Transfer surplus water from the Lesotho Highlands to South Africa for royalties.
- Generate hydropower in Lesotho.
- Promote the economic development of both states (Tompkins, 2007).

Effective transboundary water management starts at the national level, where coordination and cooperation between different ministries and water-related institutions are needed for sufficient financing and political commitment. Common obstacles include conflicting mandates, fragmented authority, and limited capacity of national institutions (UN Water, 2008). Lesotho, South Africa, Namibia, and Botswana are signatories to the SADC Revised Protocol on Shared Watercourses (2000), initially adopted in 1995 and revised in 2000 to align with the United Nations Convention on the Law of the Non-Navigational Uses of International Watercourses (1998). The protocol provides for management institutions for shared watercourses and sets out five components that limit the use of international watercourses:

- Balancing development with conservation.
- Inter-state cooperation.
- Equitable sharing of watercourses.
- Developing compatible national systems.
- Notification of emergencies (Tompkins, 2007; Hiddema and Erasmus, 2007).

A sound legal framework is essential for stable and reliable cooperation. At the global level, the 1997 Convention on the Non-Navigational Uses of International Watercourses, adopted by the United Nations General Assembly, provides a legal framework for inter-state cooperation on international watercourses. At the transboundary level, the formation of joint bodies with strong enforcement capacity, such as river, lake, and aquifer commissions, is fundamental to ensuring cooperation between various governmental entities and good management of shared resources (UN Water, 2008). The 1997 UN Convention codified international water law as a framework agreement, allowing for adhoc watercourse agreements for specific international watercourses (Hiddema and Erasmus, 2007).

Lesotho is a party to three international institutional agreements:

- Treaty on the Lesotho Highlands Water Project (LHWP) with South Africa (1986).
- The Revised SADC Protocol (2000).
- The ORASECOM agreement with South Africa, Namibia, and Botswana (2000) (Hiddema and Erasmus, 2007).

The Lesotho Highlands Water Commission (LHWC) is a bi-national body that evolved from the Joint Permanent Technical Commission established under the terms of the Lesotho Highlands Water Treaty. This organization is responsible for matters of joint concern to Lesotho and South Africa regarding the implementation of the Lesotho Highlands Water Project (LHWP) (Tompkins, 2007). Activities include the appointment of auditors and consultants, operating and maintenance plans, tendering procedures, the allocation of costs between parties, and the quantities of water to be delivered. Two national institutions are linked with the LHWC: the Trans-Caledon Tunnel Authority (TCTA), which manages and maintains the delivery tunnel transferring water across the border to the Ash River in the Vaal catchment, and the Lesotho Highlands Development Authority, responsible for managing all aspects of the project within Lesotho, including infrastructure and social aspects (Tompkins, 2007).

2.3. Catchment Hydrology

2.3.1. Hydrological cycle

The Earth contains more than 300 million cubic meters of water beneath the land surface, on the surface, and in the atmosphere. This vast amount of water is in constant motion. The hydrologic cycle represents the circulation of water from the oceans to the land via the atmosphere and back to the oceans through overland and river routes (Sahasrabundhe, 2011; Ward and Trimble, 2003). Water evaporates from the oceans and land surfaces to become water vapor, which is carried over the Earth by atmospheric circulation. This water vapor then condenses and precipitates onto the land and oceans. The precipitated water may be intercepted by vegetation, become overland flow across the ground surface, infiltrate the ground, flow through the soil as subsurface flow, or discharge as surface runoff (Larry and Mays, 2005; Chow et al., 2013 in Tetsoane, 2013; Lazaro, 1990). Solar energy drives the hydrological cycle because the conditions that control the net flow of energy determine the amount of energy available for the latent heat of vaporization (Brooks et al., 1997).

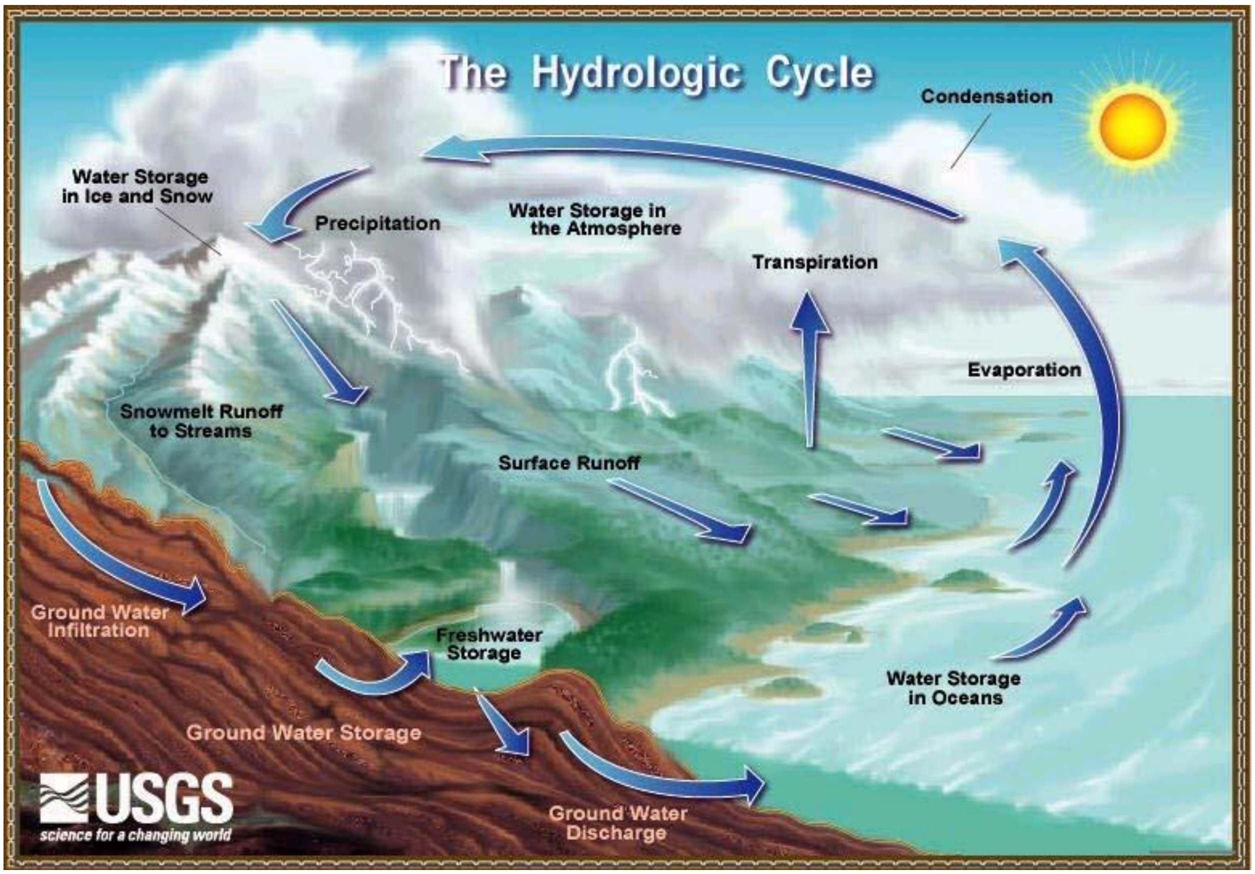

Figure 2.1 Diagrammatical representation of the hydrological cycle (*Source*: https://www.usgs.gov/media/images/natural-water-cycle-jpg)

Water balance is an application of the law of conservation of mass to a spatial unit in which the transportation of pollutants and changes in total water volume, inflow (precipitation), and outflow (abstraction losses and runoff) are in equilibrium. An analysis of the water balance using historical data on climate and physical basin characteristics provides insight into current and future water quantities and forecasts on composite processes affecting catchment runoff (Ivezic et al., 2017; Shruti and Patil, 2016). Surface runoff equals precipitation minus the sum of surface storage and infiltration. Subsurface runoff is rainwater that infiltrates the surface and flows much more slowly on its way to a stream than surface runoff. Streamflow is composed of surface and subsurface runoff, and a small amount comes from rain falling directly into the stream. Streamflow is termed "discharge" and is computed using the formula Q=VA (Lazaro, 1990).

2.3.2. Elements of water balance and hydrometeorology

The study of hydrology requires the collection of data on humidity, temperature, precipitation, radiation, and wind velocity (Wilson, 1990). Atmospheric circulation on Earth is a complex process influenced by many factors, including differences in heating between low and high altitudes, the Earth's rotation, and variations in heat and pressure associated with land and water (Mays, 2001). The relationship among moisture content in the atmosphere, temperature, and vapor pressure determines the occurrence and amounts of evaporation and precipitation (Brooks et al., 1997).

Rainfall varies in space and time due to the general pattern of atmospheric circulation and local factors (Mays, 2001). Air masses moving from oceans to land bring moisture to the land surface, while air masses from polar regions are typically dry and cold. The movement of these air masses modifies the temperature and moisture characteristics of the atmosphere over a watershed, determining the climatic and precipitation conditions (Brooks et al., 1997).

Precipitation occurs when three conditions are met:

1. The atmosphere becomes saturated.
2. Small particles or nuclei are present in the atmosphere (e.g., dust and ocean salt) on which condensation or sublimation can take place.

3. Water or ice particles coalesce and grow large enough to overcome updrafts and fall to the Earth (Brooks et al., 1997).

During the summer, evaporation loss is accelerated from all types of free water surfaces. The water lost in evaporation becomes part of the atmospheric vapor storage (Sahasrabundhe, 2011). Water that evaporates from the Earth's surface is temporarily stored as water vapor in the atmosphere. This vapor forms clouds, and as the atmosphere becomes saturated, water is released back to Earth as precipitation (rain, snow, hail, or sleet) (Ward and Trimble, 2003). Saturation occurs when either the air mass cools to the saturation vapor pressure or moisture is added to the air mass. Precipitation commonly happens when an air mass is lifted, cools, and reaches its saturation vapor pressure (Brooks et al., 1997).

Precipitation can occur in various forms, including drizzle, rain, snow, and hail. Drizzle and rain consist of liquid water droplets, snow is composed of ice crystals, and hail contains solid ice stones (Akan and Houghtalen, 2003). The precipitation process begins when water molecules concentrate on condensation nuclei such as smoke, dust, or sea salt particles. As the air cools, the amount of condensed water increases, leading to precipitation when the condensed water droplets or ice crystals grow large enough to fall to the Earth's surface (Ward and Trimble, 2003). The following two main reasons cause the change from vapor to precipitation:

1. When a hot, moist air mass cools, its capacity to hold vapor decreases, leading to rainfall.
2. Variations in pressure can also cause the change from vapor to precipitation (Sahasrabundhe, 2011).

Interception refers to the amount of water caught and stored on the leaves and stems of vegetation. Part of the precipitation, whether rainfall or snowfall, is intercepted by vegetative cover before reaching the ground. Raindrops are retained in thin layers on the leaves, and once this storage capacity is exhausted, the rate of interception decreases significantly and equals the amount evaporated from the vegetation (Sahasrabundhe, 2011).

According to Sahasrabundhe (2011), there are different types of rainfall:

1. Cyclonic precipitation occurs from the lifting of air converging into a low-pressure area or cyclone.
2. Front precipitation occurs when a moving warm, moist air mass is obstructed by a stationary cold air mass, causing the warm air to rise, cool, and precipitate.
3. Non-frontal precipitation occurs when a moving cold air mass meets a warm, moist air mass, lifting and cooling it to cause precipitation.
4. Convective precipitation occurs when local effects heat the air, causing it to rise and store more vapor particles.
5. Orographic precipitation occurs when a moving warm, moist air mass is obstructed by a barrier such as a mountain, forcing it to rise, cool, and precipitate.

Determining the depth of precipitation over watersheds requires measurements at selected points within the watershed and extrapolating these to estimate precipitation depth over ungauged areas (Brooks et al., 1997). Gauges should be located throughout the watershed to measure spatial and elevation differences in precipitation. Factors such as topographic barriers, elevation differences, and storm track patterns should be considered when developing a rain gauge network. Generally, the number of rain gauges should increase with the size of the watershed and precipitation variability (Mays, 2001).

Rainfall intensity refers to the rate of rainfall over time, varying spatially and temporally during a storm. Rainfall depth is usually highest near the storm center and decreases with distance from it. A spatially averaged depth over the storm-covered area is often used to characterize a storm (Akan and Houghtalen, 2003). Precipitation data are essential for most land use and hydrologic planning (Ward and Trimble, 2003).

2.3.3. Geology

Geology plays a crucial role in shaping topography and influencing groundwater movement. The underlying rock of an area forms the groundwater zone where infiltrated water slowly moves through aquifers to rivers and the sea (Wilson, 1990). The inorganic part of the Earth consists of rocks and their weathering products. A rock is composed of one or more minerals, and a mineral, as defined by Gerbert (1971), is a natural, inorganic chemical element or compound with atoms in definite ratios, allowing its composition to be expressed by a chemical formula (Delleur, 1999).

Soil comprises three phases: solid, liquid, and gaseous. The solid phase includes mineral particles such as gravel, sand, silt, and clay. Gravels are pieces of rock with occasional quartz, feldspar, and other minerals. Sand particles are primarily quartz and feldspar. Silts are microscopic soil fractions consisting of very fine quartz grains and flake-shaped particles from micaceous minerals. Clays are mainly flake-shaped microscopic and sub-microscopic particles of mica, clay minerals, and other minerals (Delleur, 1999; Das, 2006).

To characterize fine-grained soils, it's essential to identify the types and contents of minerals present. Common descriptive terms like gravel, sand, silt, and clay help identify specific soil textures. Residual soils remain at the site of weathering, retaining many elements of the parent rock. Alluvial or fluvial soils are transported by rivers and streams (Bhudu, 2000).

Soils with similar properties can be classified into groups and subgroups based on their engineering behaviour. Two widely used classification systems are:

a) AASHTO Classification System: Developed in 1929, this American system classifies soil into seven groups (A1 through A7). Groups A1, A2, and A3 are granular materials, with 35% or less passing through the No. 200 sieve. Groups A4, A5, A6, and A7 include silts and clays, with more than 35% passing through the No. 200 sieve.

b) Unified Soil Classification System (USCS): Proposed by Casagrande in 1942, this system classifies soils into coarse-grained (gravelly and sandy, with less than 50% passing through the No. 200 sieve) and fine-grained (50% or more passing through the No. 200 sieve) categories. USCS uses particle size, plasticity index, and liquid limit for classification. The soil matrix consists of mineral particles and interconnecting pores and may also include organic material such as peat (Delleur, 1999).

Groundwater reserves are found in all three rock classes, with sedimentary rocks holding the greatest volume due to their higher porosity. Among the three rock types, igneous rocks are industrially significant, formed when hot molten rock crystallizes and solidifies, or when molten rock fuses into other formations and cools. Delayed cooling causes various minerals to crystallize into an interconnected solid mass, characteristic of rocks like granite (Delleur, 1999).

Sedimentary rocks form from the accumulation of grains of rocks and minerals transported by air or water. These sediments result from the weathering of igneous, metamorphic, or other sedimentary rocks. All three rock classes can be subjected to extreme heat and pressure, transforming them into metamorphic rocks. Metamorphic rocks, altered by heat and pressure, may retain the same chemical composition as their precursor but undergo significant changes in mineral composition and structure (Delleur, 1999).

2.3.4. Soil moisture

Crushing rocks into fine fragments does not directly produce soil but can accelerate soil formation. Rock fragments decompose into soil primarily through physical and chemical weathering, as well as biological processes involving microorganisms, plant root action, and other life forms within the soil ecosystem (Ward and Trimble, 2003; Das, 2006).

Soil particles and organic matter consist of solid matter, water, and voids or pores. Water occupying these voids is known as soil water. When all pores are completely filled with water, the soil is saturated. In unsaturated conditions, a small amount of water, called hygroscopic soil water, is held tightly to soil particles by molecular attraction and cannot be removed by normal drying (Ward and Trimble, 2003). Water travels through interconnected pores from areas of high energy to low energy. In soil pores, water generally flows laminarly, while in fractured rocks and coarse aggregates, turbulent flow can occur. This variability causes different soil types to have different infiltration rates, measured in mm/h (Wilson, 1990; Das, 2006).

The hydraulic conductivity of soils depends on several factors:

a) Viscosity of the fluid

b) Pore size

c) Void ratio

d) Roughness of mineral particles

e) Degree of soil saturation (Das, 2006).

Physical weathering reduces the size of rock fragments without altering their original composition. The main agents responsible for this process are:

a) Exfoliation

b) Unloading

c) Erosion

d) Freezing and thawing (Bhudu, 2000).

Chemical weathering reduces rock size and transforms the chemical composition of the parent rock. The main agents responsible for chemical weathering are:

a) Hydration

b) Carbonation

c) Oxidation (Bhudu, 2000).

Apart from weathering, soil can form from unconsolidated and decomposed materials. Peat forms from the accumulation of decomposed vegetation or organic matter, typically found in low-altitude areas where the water table is close to or above the ground surface.

This constant supply of groundwater supports aquatic plant growth, and as these plants decompose, peat forms. When a large amount of peat mixes with inorganic soil, it is called organic soil, which typically has a natural moisture content ranging from 200% to 300%, is highly compressive, and supports a rich ecosystem of microorganisms (Das, 2006).

Most unconsolidated materials are young and near the Earth's surface, meaning they haven't been fused by heat and pressure. Consequently, they generally have high porosity and serve as sources for groundwater storage (Delleur, 1999; Busacca and Sweeney, 2004). These unconsolidated materials include:

a) Glacial Drift: Sedimentary material deposited directly by glaciers or their meltwater, varying in texture from fine silt to large boulders, and a mixture of all sizes.
b) Glacial Till: A diverse mixture of minerals, rock structures, and particle sizes, typically not used for groundwater storage due to poor water retention.
c) Lacustrine Deposits: Silt and clay deposited in still bodies of water such as lakes and lagoons, with poor groundwater retention.
d) Peat: Brown, porous remains of water plants accumulating in stagnant water and marshes, compacting with depth and occasionally filtering water.
e) Limestone: A carbonate sedimentary rock composed primarily of calcite, with potential inclusions of silt, clay, and aragonite, formed by sediment accumulation.
f) Ancient Dunes: Sometimes found as sandstone deposits, coarse aggregates that may hold groundwater, though fine-grained wind-blown deposits have low porosity and permeability.
g) Loess: An unstratified sediment deposited by wind, often reworked by frost action to form columnar structures with vertical fractures (Delleur, 1999; Busacca and Sweeney, 2004).

In the upper part of unsaturated soil, especially in the root zone, there is constant competition for water between soil capillary forces and plant root osmotic suction. When capillary forces exceed osmotic forces, the wilting point is reached, and plants cease to take in water and begin to wilt. Capillary forces are greater in fine-grained materials due to fewer void spaces compared to coarse-grained materials. The wilting point is reached more quickly in high temperatures and insufficient rainfall, as capillary forces drive water to the surface for evaporation (Delleur, 1999; Ward and Trimble, 2003).

Soil water content increases with continuous light rainfall, allowing air bubbles to escape upward through the soil profile. During dry periods, crusting occurs when clay and silt dominate the upper soil profile. If moisture reduction continues, water is held as thin films around grains by adhesive forces. The crust impedes water infiltration, but wormholes, coarse-grained materials, and dry organic matter extending to the soil surface can accelerate infiltration (Ward and Trimble, 2003).

Soil water storage changes throughout the year due to various meteorological and hydrological factors. Increases occur from infiltration, while depletion is caused by deep percolation, groundwater recharge, gravitational drainage, and evaporation. Water movement into and out of the soil matrix is controlled by tension forces, but accurately measuring soil tension is complex (Ward and Trimble, 2003).

When rock cools and solidifies, it is characterized by inherent porosity, known as primary porosity. This porosity may later be reduced by geohydrological and mechanical processes, forming secondary porosity through pores and fractures. The total porosity of a rock sample is the sum of primary and secondary porosities, reflecting the packing arrangement of its grains (Delleur, 1999).

The upper soil horizon typically has greater permeability than the lower horizon due to human activities, root activity, and soil fauna, which alter the structure of soil particles. This imbalance can lead to lateral flow if the hydraulic conductivity in the upper horizon is greater. Water may travel through the subsurface zone to a stream or discharge along the way at lower elevations (Delleur, 1999; Ward and Trimble, 2003). Various methods, both ancient and recent, have been developed to estimate and quantify hydraulic conductivity from physical soil properties such as texture, porosity, and bulk density.

Notable studies on this topic include those by Rawls et al. (1982), Puckett et al. (1985), Wang et al. (1985), Bouma (1986), and Baumer et al. (1987).

2.3.5. Infiltration

Infiltration rate is the maximum rate at which water enters the soil surface through small pores. It differs from **percolation**, which is the vertical movement of infiltrated water through larger soil pores driven by gravity. Typically, both the size and amount of pore space in soil decrease with increasing depth (Sahasrabundhe, 2011; Lazaro, 1990; Ward and Trimble, 2003; Brooks et al., 1997).

When rain falls, it first wets the vegetation or bare soil before infiltrating deeper until it reaches the zone of saturation, contributing to groundwater storage. This water may eventually flow from springs or seep into streams due to the combined forces of capillarity and gravity. Infiltration directly impacts deep percolation, groundwater flow, and surface runoff contributions to the water balance. When water is applied to dry, unfrozen soil, a fast initial infiltration rate occurs, which typically drops and stabilizes as the soil becomes saturated (Mays, 2001; Brooks et al., 1997; Ward and Trimble, 2003; Wilson).

The importance of the infiltration process lies not only in its contribution to groundwater recharge but also in the changes it induces in the soil, such as aggregate dispersion, surface layer puddling, colloid swelling, and soil crack closure (Sahasrabundhe, 2011). The rate at which net precipitation enters the soil depends on the conditions of the upper soil horizon and the soil's physical properties. Plant debris impacts infiltration by slowing surface runoff, allowing water to penetrate the soil and significantly increasing water storage in the lower layer (Brooks et al., 1997).

Several factors affect infiltration, as described by Sahasrabundhe (2011), Brooks et al. (1997), Kruger (2013), and Ward and Trimble (2003):

- Soil texture and structure: Coarse-textured soils in the upper horizon allow rapid infiltration, leaving no excess water for runoff. Conversely, clayey soils, which swell after soaking, significantly reduce infiltration.
- Conditions at the soil surface: Blockages in subsoil pores from turbid water or in-wash sediments, or the accumulation of salts like sodium chloride (NaCl), can collapse soil structure and reduce infiltration.
- Soil moisture content: As soil moisture storage capacity fills, infiltration decreases. When the soil dries, infiltration rates increase.
- Vegetation root systems: Extensive root systems increase soil porosity, providing pathways for water and significantly influencing infiltration.
- Frozen soil: Severe low temperatures cause pores in the upper soil horizon to fill with solid ice, making the soil nearly impermeable.
- Human activities: Compaction from human activities decreases soil porosity and infiltration rates.
- Water viscosity: Low temperatures increase water viscosity, reducing infiltration rates.
- Long-term soil conservation management: Changes in organic material, faunal activity, and soil structure from conservation efforts can increase bulk density, reducing infiltration capacity.

Roberts and Klingeman (1970) conducted experiments testing the effects of 0%, 50%, and 100% porous surfaces on hydrological unit hydrographs. They found that the rising limbs of the hydrographs for the 0% and 50% permeable surfaces were similar for about half their lengths, at which point the 50% permeable surface lagged behind the impervious one due to water infiltrating the top half of the 50% permeable sample. The 100% permeable sample showed a considerably slower rise time, demonstrating the effects of increased storage and infiltration. Similar experiments by Black (1970), cited in Lazaro (1990), confirmed these findings.

Infiltration rates of soils are measured using different techniques. Two widely used methods, as described by Sahasrabundhe (2011), are:

- Indirect methods: Using infiltrometers, water is applied over an artificial sample area within a cylinder placed into the soil. Water is added to a specific depth in the cylinder, and the amount needed to maintain that depth is recorded over time.
- Direct methods: Analysing surface runoff hydrographs resulting from rainfall over a study watershed.

2.3.6 Evapotranspiration

Evaporation is the net loss of water from a surface due to the change from liquid to vapor. It can occur directly from soil and vegetation surfaces. The loss of water vapor through plant leaves is termed **transpiration**. In field conditions, it is nearly impossible to distinguish between evaporation and transpiration when the ground is covered with vegetation. These processes are collectively referred to as **evapotranspiration** (Wilson, 1990; Mays, 2001; Ward and Trimble, 2003; Brooks et al., 1997). The pressure resulting from evaporation at the water-air interface is called the vapor pressure of water, and when net evaporation ceases, the air reaches the saturation vapor pressure (Brooks et al., 1997; Ward and Trimble, 2003).

The amount of evapotranspiration is crucial for planning and designing irrigation schemes, dam bathymetry, bio-monitoring, and other environmental concerns. It is a key factor in developing watershed policies and is important in negotiations involving water resources (Ward and Trimble, 2003).

Potential evapotranspiration is the amount that would occur with unlimited water, while actual evapotranspiration is the amount that occurs with limited water. Evapotranspiration affects water yield and largely determines the proportion of precipitation that becomes streamflow (Brooks et al., 1997; Ward and Trimble, 2003). Rates of evapotranspiration influence water yield by affecting the antecedent water status of a watershed, the necessary capacity of reservoirs, the size of pumping plants, the consumptive use of water by crops, and the yield of underground supplies. High evapotranspiration rates deplete water in soil and surface water impoundments, making more storage space available for precipitation. Low rates leave less storage in soil and surface water impoundments (Brooks et al., 1997; Wilson, 1990).

Evaporation and transpiration processes in most watersheds are controlled by water flow through unsaturated soils. The driving force is the difference in water potential between two points, with water flowing from regions of higher to lower free energy. Both energy in the form of solar radiation and conditions that allow water vapor to move away from evaporating or transpiring surfaces are needed. Water molecules migrate from the liquid surface due to their kinetic energy. Gravitational potential exerts a downward pressure determined by the height of the water column, gravity, and density (Brooks et al., 1997; Wilson, 1990).

Evapotranspiration is influenced by increases in air and water temperature, wind, and solar radiation, while a high-water vapor percentage in the air decreases evaporation potential. According to Sahasrabundhe (2011) and Ward and Trimble (2003), evaporation occurs in three scenarios:

1. From free water surfaces
2. From land surfaces
3. From vegetative cover

The rate at which water moves through a plant is critical because water carries nutrients and minerals into the plant. Water that falls on leaves from precipitation or irrigation and then evaporates is not associated with transpiration. The needed energy primarily comes from direct solar radiation. Increased evaporation raises vapor pressure in the intercellular space, creating a vapor pressure gradient between the leaf and the atmosphere under most conditions (Ward and Trimble, 2003).

The rate of evaporation varies with the colour and reflective properties of the surface and differs between surfaces exposed to or shaded from solar radiation. The amount of moisture lost by evapotranspiration primarily depends on precipitation incidence and secondarily on climatic factors like temperature, humidity, crop growth stage, cultivation manner, and vegetation extent. Changes in vegetation that reduce annual evapotranspiration (ET) will increase streamflow or groundwater recharge, while an increase in annual ET has the opposite effect (Brooks et al., 1997; Wilson, 1990; Sahasrabundhe, 2011).

The amount of evaporation depends on energy supply and vapor pressure gradient. Under open atmospheric conditions, sufficient vapor pressure gradients usually exist. Two essential requirements for evaporation are:

- Availability of a heat energy source to vaporize the water, which could be solar radiation, air blowing over the surface, or heat from within the underlying surface.
- Existence of a vapor concentration gradient between the evaporating surface and the surrounding air. Evaporation can only occur if the vapor concentration at the evaporating surface is greater than in the overlying air (Sahasrabundhe, 2011; Brooks et al., 1997).

Transpiration benefits plants by bringing essential nutrients from the soil into the plant and helping cool the leaves. While more water may be available to lower roots, the energy required to pull that water up to the plant is significant, so only a smaller amount is extracted. Plants transpire at maximum rates at soil field capacity and stop at the wilting point. Wind can increase transpiration rates by breaking up the saturated air layer closest to the leaf (Ward and Trimble, 2003).

Evaporation occurs on the surfaces of open water such as lakes, reservoirs, or puddles, as well as from vegetation and ground surfaces. Transpiration involves the removal of water from the soil by plant roots, transport through the plant into the leaf, and evaporation from the leaf's stomata into the atmosphere (Ward and Trimble, 2003).

Sahasrabundhe (2011) lists factors affecting evaporation from free water surfaces as follows:

Meteorological factors:

- Temperature: Rising temperatures increase the air's capacity to hold vapor molecules.
- Wind: Incoming fresh air removes vapor molecules, making space for more.
- Atmospheric pressure: Higher altitudes have decreased atmospheric pressure, increasing the rate of escaping water molecules as the air above has fewer molecules to prevent entry of new ones.

Physical factors:

- Nature of the evaporating surface: As soil dries, evaporation decreases and eventually stops since water cannot reach the surface from great depth.
- Shape of the evaporating surface: Maximum evaporation occurs from a convex surface, followed by flat, then concave surfaces.
- Water quality: Evaporation rates decrease with an increase in the specific gravity of the solutions.

Evaporation rates from saturated soils are nearly identical to those from free water surfaces. As the surface soil moisture content decreases, evaporation losses decrease, and when it becomes very low, evaporation nearly ceases.

Transpiration is the process by which water vapor leaves the living plant body and enters the atmosphere. It involves continuous movement of water from the soil into the roots, through the stems, and out through the leaves. Factors affecting transpiration include:

- Climatic factors: Light intensity, atmospheric vapor pressure, temperature, and wind.
- Soil factors: Conditions governing water supply to the roots.
- Plant factors: Root system efficiency, leaf area, leaf arrangement and structure, and stomatal behaviour. Vegetation virtually ceases to transpire at night due to stomatal closure. The term **consumptive use** refers to water losses due to evapotranspiration and the water used by the plant for metabolic activities, generally equivalent to ET (Sahasrabundhe, 2011).

Methods of measuring transpiration have been developed for crop plants, though few are applicable for field measurements of larger trees and shrubs relevant in forest hydrology. Evaporation from lakes or reservoirs can be estimated using wind speed, relative humidity, and temperature data (Ward and Trimble, 2003; Brooks et al., 1997). Actual evapotranspiration from watersheds cannot be measured directly by any practical field method. The best estimates come from water budget analyses and paired-watershed experiments or climatological data (Sahasrabundhe, 2011; Brooks et al., 1997).

2.3.7 Groundwater

Groundwater study involves a comprehensive examination of its distribution and evolution over time and space, influenced by regional geology. Groundwater exists below the surface, confined under a pressure equal to or greater than atmospheric, saturating the rock medium through which it moves and is stored (Prasad, 2002). It accounts for more than 99% of all liquid freshwater on Earth. However, significant quantities of this valuable resource can become unusable due to contamination or excessive deep pumping, rendering further extraction economically unfeasible (Brooks et al., 1997).

The process of infiltration and the subsequent movement of water through the soil result from both capillary forces and gravity. Capillary forces, representing the physical attraction of soil and rock particles to water, drive water from wetter particles (higher energy potential) to drier particles (lower energy potential). As the spaces between particles fill with water, gravity becomes more dominant. Once the field capacity of well-drained soil is exceeded, water begins to flow downward, continuing through pores in the soil, parent material, and underlying rock (Brooks et al., 1997).

Subsurface water is generally divided into two major types: phreatic water (or soil moisture) in the unsaturated zone, and groundwater in the saturated zone. In saturated pores, adhesion forces are equal in all directions, so there is no directional attraction. The only active forces are gravity and the gradient of the fluid potential (Delleur, 1999). Groundwater movement and storage depend on the thickness, texture, and structure of the Earth's crust and the physical ability of water to move through a permeable medium. In highland areas, numerous springs occur at various levels, mainly from weathered basalt horizons at inter-basalt flow zones and adjacent to dolerite dykes. Some boreholes in these formations yield high amounts of water, with strikes occurring in weathered mantles, inter-flow zones, and fractured areas. For instance, in the Likalaneng area, water strikes have been recorded at depths greater than 150 meters with low yields exceeding 10 litres per second (UN Water, 2007; Prasad, 2002; Viles, 2007).

Groundwater may flow over a wide area in a laminar state, but as it approaches a discharge point (e.g., a spring or well), the streamlines crowd together, and the flow velocity increases to maintain the same volumetric discharge rate. Near or at the discharge point, the velocity often becomes turbulent. Turbulent flow into the well requires more energy and a steeper gradient than laminar flow (Delleur, 1999). Groundwater moves in response to a hydraulic gradient, similar to water flowing in an open channel or pipe. However, groundwater flow is restricted by friction with the porous media through which it flows (Sahasrabundhe, 2011). Groundwater flow through porous material occurs under the influence of energy, moving from regions of high energy to low energy. The energy a water particle possesses at any position within a flow system is the sum of its elevation energy, pressure energy, and velocity energy. The energy from the movement of flowing groundwater is negligible and can be ignored (Sahasrabundhe, 2011; Ward and Trimble, 2003). Head drop or head loss is undesirable, as it requires extra energy, reducing the efficiency of the pumping system and increasing pumping costs (Delleur, 1999).

The uppermost surface or top level of the saturated zone is called the water table. The water table's elevation fluctuates in response to changes in precipitation and evapotranspiration patterns. It can be defined as the level at and below which soil particles are completely saturated. Excessive rainfall and subsequent infiltration can cause the water table to rise rapidly, reaching the ground surface and completely filling the root zone, rendering the soil useless for crop production. This phenomenon is known as waterlogging (Sahasrabundhe, 2011; Brooks et al., 1997).

Groundwater occupies open spaces in lithological units such as gaps between crystals or grains, faults, joints, lithological contacts, and other discontinuities, as well as rock cavities caused by cooling and dissolution due to weathering. Surface features generally do not reveal the location, depth, and extent of water-bearing materials or strata. The quantity of water accommodated underground depends on the porosity of the sub-surface strata (Brooks et al., 1997; Prasad, 2002). Lithological units with a high capacity to store and yield water are called aquifers. Aquifers, which can range from a few meters to hundreds of meters thick and can underlie a few hectares to thousands of square kilometres, yield significant amounts of water to wells (Brooks et al., 1997; Prasad, 2002). Upland forest watersheds are commonly seen as important recharge zones for aquifers due to their high annual precipitation and soils with high infiltration capacities (Brooks et al., 1997).

Grain-size distribution and shape are the primary factors controlling pore size distribution and the rate of gravity drainage. Groundwater flow patterns are influenced by several factors, including the elevation and location of recharge and discharge areas, the heterogeneity of geologic materials, the thickness of these materials, and the water table configuration (Ward and Trimble, 2003). A geologic formation that bears water, is saturated with it, and can yield sufficient quantities for economic use is called an aquifer. The lateral continuity and vertical boundaries of these reservoirs are often ill-defined due to subsurface formation complexities. Water in the zone of saturation is referred to as groundwater, and the geologic formation containing it is called an aquifer. The upper surface of the saturated zone, if not confined by impermeable material, is called the water table (Davis and Cornwell, 2013; Sahasrabundhe, 2011). An unconfined aquifer has infiltrating water moving through the unsaturated zone under less-than-atmospheric pressure until it reaches the fully saturated pores, possessing a pressure equal to atmospheric pressure at the water table (Ward and Trimble, 2003).

A confined aquifer does not receive direct infiltration from precipitation because it is overlain by a layer of low hydraulic conductivity. As such, it lacks a water table, and the water within is confined under sufficient pressure to rise above the base of the overlying confining layer (Ward and Trimble, 2003). Confined aquifers, or artesian aquifers, contain water under pressure, sometimes sufficient to produce freely flowing wells (Brooks et al., 1997). According to Sahasrabundhe (2011), aquifers can be classified as follows:

a) Unconfined aquifer: Not overlain by any confining layer but has one at its bottom. It is normally exposed to the atmosphere, with its upper portion partly saturated with water. The upper surface of saturation, under atmospheric pressure, is called the water table, hence this aquifer is called a phreatic aquifer.
b) Perched aquifer: Occurs when an impervious or relatively impervious layer of limited area forms a lens within an unconfined aquifer.
c) Confined aquifer: Also called an artesian aquifer, it is overlain and underlain by confining layers. Water within is held under pressure, and water from such wells reaches the surface without pumping.
d) Leaky aquifer: Rarely truly confined, as confining layers are not entirely impervious. An aquifer overlain or underlain by a semi-pervious layer (aquitard) through which vertical leakage occurs due to head difference is called a leaky or semi-confined aquifer.

Groundwater can be managed using the concept of safe yield, which refers to the annual draft of groundwater at levels that do not produce undesirable effects. Groundwater should not be withdrawn at rates that result in excessive lowering of the water table, high pumping costs, or saltwater intrusion, especially in coastal regions. Depletion of groundwater storage not only affects groundwater use but also impacts surface water supplies by reducing groundwater contributions to lakes and streams. To sustain water yields from wells, the extraction or pumping rate must not exceed the recharge rate over long periods. The permeability of the aquifer and its recharge determine the discharge of a spring (Brooks et al., 1997).

The amount of water extracted from aquifers can always be recharged through natural processes:

a) Deep percolation from precipitation: The amount of recharge in a particular area is influenced by vegetative cover, topography, soil nature, and precipitation type, intensity, and frequency.
b) Seepage from streams and lakes: Seepage from streams, lakes, and other water bodies is another important source of recharge (Sahasrabundhe, 2011).

2.3.8. Surface water hydrology

Runoff is the portion of precipitation, snowmelt, or irrigation water that flows over and through the soils eventually making its way to surface water systems. Saturation and consequent surface runoff occur relatively rapidly in the urban watershed, since storage and infiltration have been reduced to practically zero. Incoming rainwater quickly fills any depressions and becomes readily available for surface runoff (Ward and Trimble, 2003). Rainwater reaching the surface of the earth may be intercepted, may infiltrate the soil, or flow into streams through a natural run-off process. The soil type, as well as the plant growth in the catchment area has a great influence on the volume of rain that eventually does run-off (Burgher et al., 2003). While runoff is usually benevolent under extreme conditions of rainfall or land use, it can cause extensive damage by eroding soils and stream banks by carrying off valuable agricultural nutrients and pollutants. It can destroy bridges, utilities, and urban developments, and it can also cause flooding and sediment deposits in recreational, industrial, and residential areas along stream systems (Ward and Trimble, 2003).

Base flow is responsible for maintaining a sustained flow throughout the year, and it is mainly derived from groundwater storage. Direct runoff on the one hand, is made up of overland flow or surface runoff and that part of infiltration which flows laterally through the unsaturated zone of soil mass and joins the stream flow promptly (Sahasrabundhe, 2011). On the other hand, base flow is made up of groundwater contribution and that portion of infiltration which moves laterally but joins the stream flow quite late after the precipitation has stopped. Now it may be appreciated that only part of the rainfall is available for producing overland flow or surface runoff. This portion of total rainfall which produces surface runoff is called rainfall excess (Sahasrabundhe, 2011). It is important to note that overland flow occurs as soon as the infiltration rate is less than the water application rate, and surface depressions have been filled with water (Ward and Trimble, 2003).

The watershed factors affecting runoff are drainage area size, topography, shape, orientation, geology, interflow, and perhaps most important, the soil and land use, and a few of them are elaborated below:

(a) Rainfall pattern: if the rainfall is very heavy the consequent runoff will also be more. If the rainfall is just showery type with low intensity there may not be runoff at all as the rainwater is completely lost in infiltration.
(b) Character of catchment surface: if the surface is rocky then the surface absorption will be practically nil, and the runoff will be more. If the surface is compact clayey type runoff will be more, but if the surface is sandy then the absorption losses will be more and runoff will be less.
(c) Topography: if the surface slope is steep runoff will be more as water will pass over the surface rapidly before losses take place.
(d) Shape and size of the catchment: if the catchment area is large, runoff will be more. If the catchment is fan shaped runoff at outlet will be more as all other contributes to the stream practically at the same time. If the catchment is fern shaped the runoff will be less.
(e) Vegetal cover: if there is vegetal cover over the catchment then evaporation loss will be reduced as sun rays cannot reach the ground surface.
(f) Geology of the area: if there are fissures, cracks, fault zones present in the catchment then the rainwater find its way out through these openings.
(g) Weather conditions: temperature of the region also largely also affects the runoff. If the temperature is more, it renders surface dry and when the rain occurs more water is absorbed by the ground surface (Sahasrabundhe, 2011; Ward and Trimble, 2003).

Some excessive runoffs can result in turbulent flows that can endanger people’s lives and damage property. These turbulent flows are called floods, and they are unusual high stage of a river due to runoff from rainfall and/or melting of snow in quantities too great to be confined in the normal water surface elevations of the river or stream due to the result of infrequent meteorological combination. The maximum flood that any structure can safely pass is called the ‘design flood’, and it is selected after consideration of economic and hydrologic factors (Raghunath, 2006).

2.3.9. Topographical factors

Firstly, the hydrology of a region is primarily influenced by its climate and, secondly, by its topography and geology. Climate is largely dependent on the region's topographical position on the Earth’s surface. Topography significantly affects precipitation patterns and the occurrence of lakes, marshlands, and varied runoff rates (Wilson, 1990). Surface runoff follows the land's slope, usually flowing perpendicular to contour lines. Overland flow slopes can be determined by measuring the lateral change in distance between contours. The land slope has minimal impact on infiltration rates or runoff depth (Ward and Trimble, 2003).

In larger catchment areas, there are proportionally fewer runoff-producing rain showers compared to smaller catchments, as water must travel further before reaching the dam site, increasing opportunities for infiltration, stream formation, and surface storage. Consequently, in smaller catchment areas, the mean annual runoff (MAR) may be proportionally higher. South Africa is divided into several catchment areas for which runoff data is available, known as reference catchment areas (Burgher et al., 2003).

Catchment shapes significantly influence runoff characteristics. For instance, fan-shaped catchments result in higher peak flows than long, narrow catchments. However, the slope of the main watercourse and other factors can mitigate this effect. Circular or fan-shaped watersheds have high runoff rates because runoff from various points tends to reach the outlet simultaneously (Ward and Trimble, 2003; Burgher et al., 2003). In elongated watersheds, tributaries join the mainstream at intervals along its length, so high flows from downstream tributaries pass before those from upstream tributaries arrive, leading to lower peak discharges (Ward and Trimble, 2003).

Steep slopes facilitate faster water flow and shorten the critical duration of flood-causing storms, necessitating the use of higher rainfall intensities in runoff calculations. On steep slopes, vegetation is generally sparser due to shallower soil layers, resulting in fewer depressions and faster runoff. Well-drained catchments have shorter times of concentration, leading to higher peak flows. Meandering watercourses, marshes, and flow outside riverbanks slow down flood progression and increase flood peak attenuation (Kruger et al., 2013).

2.3.10. Developmental Influences

Urbanization increases impervious land surfaces, reducing infiltration and causing more runoff and higher peak discharges (Ward and Trimble, 2003). The effects of urbanization depend on the percentage of impermeable surface area and changes in drainage patterns due to stormwater systems. Urbanization usually increases flood peak sizes by 20-50% compared to natural conditions (Kruger et al., 2013).

Various studies have shown that streams respond to urbanization by incision and bed widening (Ward and Trimble, 2003). Catchment depressions fill up on the ground surface in pans, lakes, vleis, and marshes, significantly affecting flood peak attenuation and translation (Kruger et al., 2013).

2.4. Hydrological Modelling

Hydrological modelling represents natural processes involving the cyclic movement of water in a catchment mathematically (Srinivas and Naik, 2017; Patil et al., 2014). Hydrologists and engineers predominantly use these models to understand watershed hydrology and assist in planning and developing water resource management programs (Irvem and Sadek, 2018; Kurbah and Jain, 2017). Models can represent simplified systems defining real systems like an entire river basin or sub-basin (Ranit et al., 2004).

Traditional methods for estimating hydrologic responses using tables, charts, and graphs are being replaced by computer models in research. Government and university researchers with access to mainframe computers have developed models to describe climate, infiltration, runoff, erosion, soil water movement, drainage, groundwater flow, and water quality (Ward and Trimble, 2003). Many computer simulation models have been developed to simulate watershed-scale processes and the hydrologic effects of different management scenarios. Watershed models are effective tools for investigating the complex processes affecting surface and subsurface hydrology, soil erosion, and the transport and fate of chemical constituents in watersheds (Golmohammadi et al., 2014).

Models can be empirical, deterministic, or stochastic. Empirical models are developed by analysing large data sets to create statistical relationships between inputs and outputs and are not easily transferable between regions. Deterministic models mathematically describe the processes modelled, such as runoff, while stochastic models identify statistical probabilities of hydrologic events like rainfall or flood flows to predict outcomes (Ward and Trimble, 2003). Due to their integrative power, predictive abilities, and demonstration utility, computer-based decision support models can play a significant role in water management operations (McKenzie and Seago, 2007).

2.4.1. WEAP model

The Water Evaluation and Planning System (WEAP) model, developed by the Stockholm Environment Institute (SEI) at the Tellus Institute, USA, has the capacity to model hydrologic processes. It is a semi-theoretical, continuous-time, semi-distributed, deterministic model requiring calibration and verification. WEAP provides a comprehensive, flexible, and user-friendly framework for developing water balances, scenario generation, planning, and policy analyses (Dimova et al., 2013; Abrishamchi, 2007).

The WEAP tool was used to model surface water resources allocation in the Didessa Sub-Basin, West Ethiopia. Existing demand sites were collected from irrigation and water supply sectors. CROPWAT 8.0 and Indicators of Hydrologic Alteration (IHA) programs were used to estimate crop water requirements and instream flow requirements (IFR), respectively. The model sufficiently represented the sub-basin's surface water flow (Adgolign, 2015). In South Africa's Olifants River Basin, WEAP was used to estimate the water balance and impacts of future water demands, incorporating scenarios for changes in water demand evolution and implementation of the Environmental Reserve (ER), International Agreements (IAs), water conservation programs, and population growth (Arranz and McCartney, 2007).

WEAP's integrative approach considers hydrological processes, water allocation, and management systems, making it widely used globally and freely accessible (Abrishamchi, 2007). Unlike other models, WEAP offers scenario analyses in a user-friendly manner, providing a wide range of model results. The model is also scalable and can be updated anytime, allowing for future improvements (Metobwa et al., 2018).

2.4.2. HEC-HMS

The Hydrologic Engineering Centre's Hydrologic Modelling System (HEC-HMS), developed by the US Army Corps of Engineers Hydrologic Engineering Centre (HEC) in 1992, is a hydrologic modelling software used to estimate a basin's hydrological response due to precipitation. It is a physically based and conceptual semi-distributed model capable of simulating rainfall-runoff routing processes in various geographic areas, from large river basins to small urban and natural watersheds (Choudhari, 2014; Sahu et al., 2020; Hamdan, 2021).

Chu et al. (2009) utilized HEC-HMS for both event-based and continuous rainfall-runoff modelling in the Mona Lake catchment, West Michigan, USA, employing the Soil Conservation Service-Curve Number model and soil moisture accounting method for loss estimation. The Clark UH model transformed excess precipitation into direct hydrograph. The model outcomes showed that fine-scale event models provided better results in coarse-scale continuous models. In another study, Majidi et al. (2012) performed Rainfall-

Runoff modelling on Iran's Abnama basin using HEC-HMS. The Green-Ampt method estimated losses, the SCS unit hydrograph method transformed excess rainfall into direct runoff, and the Muskingum method was used for routing. The correlation between observed and simulated discharge was 0.89, indicating a strong match and demonstrating the model's capability for runoff simulation.

The HEC-HMS model was applied to estimate both gauged and ungauged runoff contributions to Cahora Bassa's water balance using GIS techniques. Rivers considered in the study included the Zambezi, Kafue, Luangwa, Chongwe, Musengezi, and Manyame. Missing data were generated using the mean value infilling method, and the DEM hydro-processing technique determined the spatial extent of the ungauged area. The study showed that the ungauged catchment contributed about 12% of total inflows into the Cahora Bassa Dam, aiding in its operation and artificial flood management (Gumindoga et al., 2016).

HEC-HMS has been widely used due to its simplicity and reliability in simulating runoff accurately across different river basins. It saves time and money by providing runoff data without direct measurement and can be used for runoff simulation in ungauged basins for water resource planning, development, management, and decision-making (Halwatura and Najim, 2013; Sahu et al., 2020; Sheth, 2018).

2.4.3. MIKE-SHE

MIKE System Hydrological European (MIKE-SHE), developed by the Danish Hydraulic Institute in 2007, is a deterministic, fully distributed, and physically based hydrological and water quality modelling system. It addresses various water environment challenges through consultancy services (Agrawal and Desmukh, 2016). MIKE-SHE has been effectively used in watershed studies where conventional models cannot represent the entire water cycle (Sandu and Virsta, 2015).

Hydrological processes in MIKE-SHE are modelled using finite difference representations of partial differential equations for mass, momentum, and energy conservation, along with some empirical equations. The model is widely applied in water supply design, management, planning, irrigation, soil and water management, groundwater management, environmental impact assessments, land use and climate change studies, flood forecasting and management, and water quality modelling (Agrawal and Desmukh, 2016; Ayana et al., 2012; Erlingis, 2017).

Zhang et al. (2011) coupled MIKE-SHE and SWAT models to develop a sediment budget in the Zijingguan watershed, China, using parameters derived from GIS and remote sensing. The coupled model accurately predicted the distribution of annual mean soil erosion and sediment yield. In another study, Gumindoga et al. (2016) evaluated water balance components for the Upper Gilgel Abay River Basin using MIKE-SHE and validated the simulated river flows at various gauging stations. The model reproduced streamflows within acceptable ranges, indicating satisfactory performance for runoff simulation in the study area. Moreover, MIKE-SHE has proven effective in simulating runoff, evapotranspiration, and soil moisture content at various time scales for different land uses and soil types.

The model's complexity and high data requirements make it suitable for applications in well-monitored basins. It offers flexibility in simulating various hydrological processes and integrates GIS and remote sensing data, making it a valuable tool for detailed hydrological studies and water resource management (Erlingis, 2017; Sandu and Virsta, 2015).

2.4.4. SWMM

The Storm Water Management Model (SWMM) is a dynamic tool widely used to predict flows and pollutant concentrations for both single-event and long-term (continuous) simulations in urban areas. It is also useful for designing drainage systems (Wu et al., 2013; Jiang et al., 2015; Maharjan et al., 2017).

Jiang et al. (2015) applied the SWMM model to simulate urban flooding in Dongguan City, a rapidly urbanized area in southern China. The SWMM setup involved the use of Digital Elevation Models (DEM), digital maps, and the underground pipeline network. Parameters were derived from the properties of the sub-catchment and storm sewer conduits. A parameter sensitivity analysis demonstrated robustness. The simulation results indicated that the area would not flood with a 1-year return period precipitation but would be inundated with 2, 5, 10, and 20-year return period precipitation. Although promising for urban flood forecasting, the absence of surface runoff routing in SWMM limits its precision in predicting urban flooding.

Zakizadeh et al. (2022) calibrated and validated the SWMM model using field measurements of rainfall and runoff in an urban watershed of Tehran metropolis, Iran. They evaluated the model's performance based on statistical criteria and graphical techniques. A local sensitivity analysis identified the percentage of impervious surface in each sub-watershed as the most influential parameter. The results indicated satisfactory calibration and validation, with goodness-of-fit indices for simulating runoff quality and quantity within acceptable ranges.

SWMM is an open-source software tool widely available for research and practical applications in addressing urban flood problems (Kim et al., 2015). Numerous studies have demonstrated the model's reasonable accuracy when calibrated and validated properly (Temprano et al., 2006; Yang et al., 2020).

2.4.5. SWAT

The Soil and Water Assessment Tool (SWAT), developed by the USDA Agricultural Research Service, is a comprehensive, semi-distributed, and continuous-time model designed to simulate the impact of land management practices on water, sediment, and agricultural chemical yields in large, complex watersheds with varying soils, land use, and management conditions over long periods (Arnold et al., 2012).

SWAT has been widely used to assess water resources and nonpoint source pollution management at the watershed scale (Neitsch et al., 2011). The model operates on a daily time step and can simulate a wide range of watershed processes, including hydrology, soil erosion, nutrient cycling, pesticide transport, and crop growth. SWAT divides a watershed into sub-basins and further into hydrologic response units (HRUs) based on unique land use, soil, and slope combinations (Arnold et al., 2012).

The model's flexibility and extensive use have led to numerous successful applications worldwide. For instance, Singh et al. (2014) used SWAT to evaluate the impact of best management practices (BMPs) on water quality in the upper Ganges basin, India. The study showed that implementing BMPs significantly reduced sediment and nutrient loads, highlighting SWAT's effectiveness in watershed management planning. Similarly, Parajuli et al. (2009) used SWAT to assess the effects of land use changes on water quality in the Upper Pearl River basin, Mississippi, USA. The model accurately simulated streamflow and water quality parameters, demonstrating its utility in evaluating land use impacts.

SWAT's ability to integrate various data sources, including GIS and remote sensing, and its extensive documentation and support have made it a preferred tool for watershed-scale hydrological modelling and management. However, the model's complexity and data requirements necessitate careful calibration and validation to ensure accurate predictions (Gassman et al., 2007; Neitsch et al., 2011).

The SWAT model was applied to investigate the water availability of the Holetta River using Geographical Information Systems (GIS) tools. The watershed was divided into six sub-basins and 33 hydrological response units (HRUs) according to SWAT classification. The performance of the SWAT model was evaluated using statistical methods (coefficient of determination [R2], Nash-Sutcliffe Efficiency Coefficient [NSE], and Index of Volumetric Fit) and graphical methods. The results showed a good fit, indicating that the SWAT model performed well in simulating the hydrology of the watershed (Tibebe et al., 2016).

Kurbah and Jain (2017) tested the performance of the SWAT model on the Sher River at Belkheri in the Narsimhpur District of Madhya Pradesh, India. They concluded that the model's accuracy could be optimized with good quality gridded rainfall data. Byakod et al. (2017) applied SWAT for simulating rainfall-runoff and estimating water availability in the Balehounur Catchment. The model produced encouraging results, generating water balance components such as precipitation, evapotranspiration, water yields, surface flow, lateral flow, and groundwater flow in each HRU, and accurately predicting the catchment's water availability.

Pohlert et al. (2005) used SWAT to simulate point and non-point source pollution of nitrate in a mesoscale mountainous catchment, successfully simulating the water balance components for each HRU. However, an analysis of the internal fluxes and cycles of nitrogen revealed weaknesses in the model's conceptualization of nitrogen modules. While the seasonal cycle was simulated accurately, the temporal patterns of the daily loads showed a poor fit. Marcinkowski et al. (2013) demonstrated the application of SWAT in an agricultural coastal watershed to study the model's accuracy in simulating daily discharge and water quality parameters (nitrate-nitrogen). The results were satisfactory, indicating that SWAT can be used for water resources management in Polish watersheds.

Smarzynska and Miatkowski (2016) applied SWAT to analyse the water balance and nitrogen load pathways in a small agricultural watershed in the lowlands of central Poland. The daily and monthly water balance simulations showed a very good fit, and the monthly nitrate load simulations also expressed a good fit.

Kateb et al. (2019) stated that the SWAT model has gained considerable attention from researchers worldwide due to its effectiveness and feasibility in different types of watersheds. Despite its widespread use, there has been no published research on the SWAT model in the Caledon catchment.

2.5. Model Performance Evaluation

Model evaluation involves both operational and scientific examination, serving as a critical measure to verify the robustness of the model (Willmott et al., 1985; Moriasi et al., 2007). Evaluating model performance should include both statistical criteria and graphical displays. Researchers recommend using a combination of graphical techniques and quantitative statistics in model evaluation, as this combined approach facilitates comparative evaluations of performance between alternative or competing models (Loague & Green, 1991; Moriasi et al., 2007).

According to Moriasi et al. (2007), the most popular methods for evaluating model performance are the Nash-Sutcliffe Efficiency (NSE), the coefficient of determination (R^2), percent bias (PBIAS), and the ratio of the root mean square error to the standard deviation of measured data (RSR).

The Nash-Sutcliffe Efficiency (NSE) is computed as the ratio of residual variance to measured data variance (Nash & Sutcliffe, 1970). It is calculated as follows:

$$\boldsymbol{NSE} = 1 - \left[\frac{\sum_{i=1}^{n}\left(Qi^{obs} - Qi^{sim}\right)^2}{\sum_{i=1}^{n}\left(Qi^{obs} - Qi^{mean}\right)^2}\right] \quad (2.1)$$

The NSE is interpreted as the proportion of variation in the observed values explained by the model, ranging between -∞ and 1, where 1 indicates perfect agreement between observed and simulated values.

The coefficient of determination (R^2) indicates the quality of the relationship between observed and simulated results and is calculated as follows:

$$\boldsymbol{R^2} = \frac{\left[\sum_i (Q_{m,i} - \bar{Q}_m)(Q_{s,i} - \bar{Q}_s)\right]^2}{\sum_i (Q_{m,i} - \bar{Q}_m)\sum_i (Q_{s,i} - \bar{Q}_s)^2} \quad (2.2)$$

Where Q is a variable (e.g., discharge), and m and s stand for measured and simulated, respectively. A higher R^2 value indicates better model accuracy and lower error variance, with the range from 0 to 1, where 1 signifies an ideal fit between observed and simulated values (Moriasi et al., 2007).

Percent bias (PBIAS) measures the average tendency of the simulated data to be larger or smaller than their observed counterparts (Gupta et al., 1999)

$$\boldsymbol{PBIAS} = \left[\frac{\sum_{i=1}^{n}(Qi^{obs} - Qi^{sim})\ x\ 100}{\sum_{i=1}^{n}(Q_i^{obs})}\right] \tag{2.3}$$

Where Q is discharge, m and s stand for measured and simulated, respectively. The optimal value of PBIAS is 0.0, indicating accurate model simulation. PBIAS is commonly used to quantify water balance errors and can be extended to load errors (Moriasi et al., 2007).

The RSR standardizes RMSE using the observations' standard deviation and is calculated as follows.

$$\boldsymbol{RSR} = \sqrt{\frac{\sum_{i=1}^{n}(Q_m - \bar{Q}_s)_i^2}{\sum_{i=1}^{n}\left(Q_{m,i} - \bar{Q}_m\right)^2}} \tag{2.4}$$

Where Q is a variable (e.g., discharge), and m and s stand for measured and simulated, respectively. A model simulation is considered satisfactory if RSR is less than 0.70 (Moriasi et al., 2007). RSR incorporates the benefits of error index statistics and includes a scaling/normalization factor, so a lower RSR indicates a lower RMSE and better model simulation performance (Singh et al., 2004; Chai & Draxler, 2014).

Table 2.1. Classification of model performance statistical indices.

Performance rating	**PBIAS**	**R^2**	**NSE**	**RSR**
Very good	PBIAS < ±10	0.75 < R2 < 1	0.75 < NSE	0 ≤ RSR ≤ 0.5
Good	±10 ≤ PBIAS < ±15	0.6 < R2 ≤ 0.75	0.65 < NSE ≤0.75	0.5 < RSR ≤ 0.6
Satisfactory	±15 ≤ PBIAS < ±25	0.5 < R2 ≤ 0.6	0.5 < NSE ≤ 0.65	0.6 < RSR ≤ 0.7
Unsatisfactory	PBIAS ≥ ±25	0.25 < R2 ≤ 0.5	NSE < 0.5	RSR > 0.7

3. MATERIAL AND METHODS

3.1. Introduction

This study focuses on analysing the water balance of the Caledon catchment using the SWAT hydrological model. The model setup, calibration, and validation will cover the period from 2008 to 2018. Its performance will be assessed using the root mean square error standard deviation ratio (RSR), Nash-Sutcliffe efficiency (NSE), and the coefficient of determination (R^2). To facilitate model use, it has been coupled with GIS software through the QSWAT extension in QGIS.

3.2. Description of Study Area

3.2.1. Location

The study focuses on the Caledon watershed, a sub-watershed of the Orange-Senqu River basin, with an approximate drainage area of 13 370 km². The watershed spans a longitude range from 26°34'46" to 28°49'55" and a latitude range from -28°22'53" to -29°43'58" (State of Water Resources Report Fiscal Year, 2016).

The Caledon watershed is drained by the Caledon River, a major tributary of the Senqu-Orange River, one of the most important river courses in Southern Africa. The river flows through Lesotho and South Africa and is a vital water source for the city of Maseru. The Caledon River passes through several administrative districts in Lesotho, including Leribe, Berea, Maseru (the capital), and Mafeteng. From Mafeteng, the river continues into South Africa, where its water is used for various purposes in the municipalities of Dihlabeng, Mantsopa, Naledi, and Setsoto in the Free State province (Chatanga et al., 2018; State of Water Resources Report Fiscal Year, 2016).

Figure 3.1 below shows the study area, which is a transboundary catchment that falls within both Lesotho and South Africa.

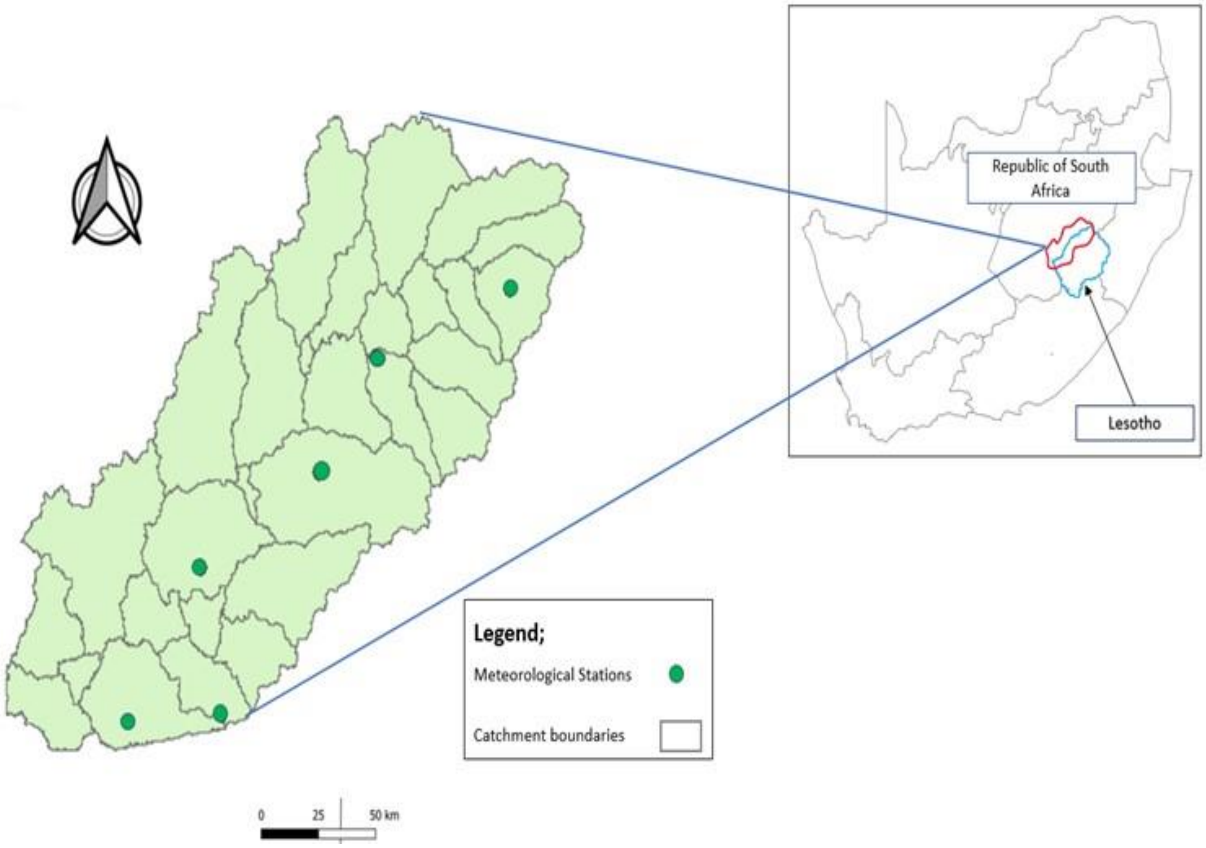

Figure 3.1. Location of the study area and meteorological stations used in the SWAT model

3.2.2. Climate

The mean annual precipitation (MAP) in the Caledon watershed varies significantly, ranging from as high as 800 mm in the northern-upper parts of the catchment, including the Butha-Buthe district, to less than 600 mm in the lower-southern part of the catchment (Mare, 2007; Viles, 2007; State of Water Resources Report Fiscal Year, 2016). As shown in Figure 3.2, the monthly average rainfall distribution from the Butha-Buthe observation station indicates that the northern-upper part of the Caledon catchment experiences high rainfall during the summer season, with an average of 155 mm recorded in January.

The catchment area is predominantly agricultural land (42.44%), followed by grassland (42.29%), urban development (5.05%), shrubs (5.74%), and water bodies (4.47%), with rangeland accounting for the remaining 0.01%. The region exhibits large spatiotemporal variability, experiencing a dry and cold climate in winter and a moist and hot climate in summer. Temperature data from the Butha-Buthe observation station, shown in Figure 3.2, indicates that average monthly temperatures drop to 0 °C in winter, while summer temperatures reach an average of 25 °C. The Butha-Buthe district's high altitude of around 2,050 m contributes to its relatively cool climate.

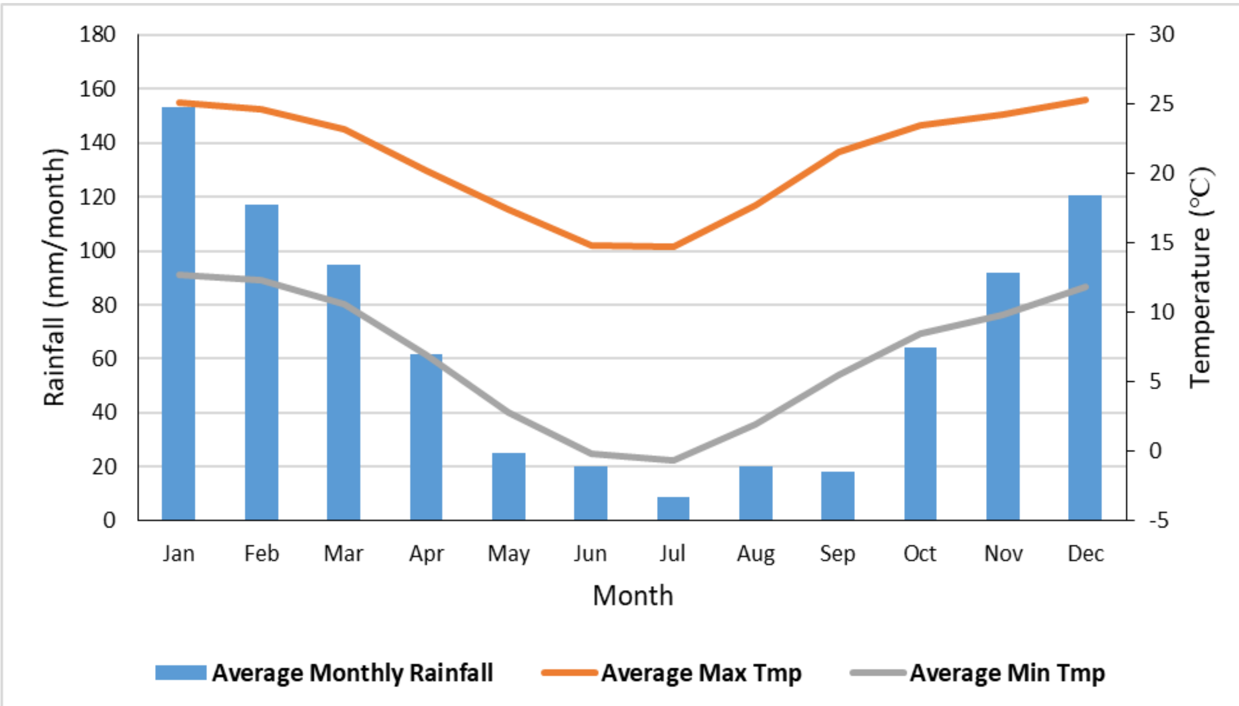

Figure 3.2 Average monthly max & min temperature and rainfall (2000-2018) of the northern-upper Caledon catchment, Butha-Buthe district

In contrast, the southern-lower part of the Caledon catchment, including the Mafeteng district, records relatively lower rainfall compared to the northern-upper catchment. Figure 3.3 shows historical monthly average rainfall data from the Ts'akholo observation station in the southern part of the catchment. This data indicates low rainfall during the winter season and a reduced monthly average of about 102 mm in December. Temperature data from the Ts'akholo observation station, shown in Figure 3.3, indicates that average monthly temperatures drop to 0 °C during the cold, dry season, while maximum average monthly temperatures reach highs of 28 °C during the warm summer months.

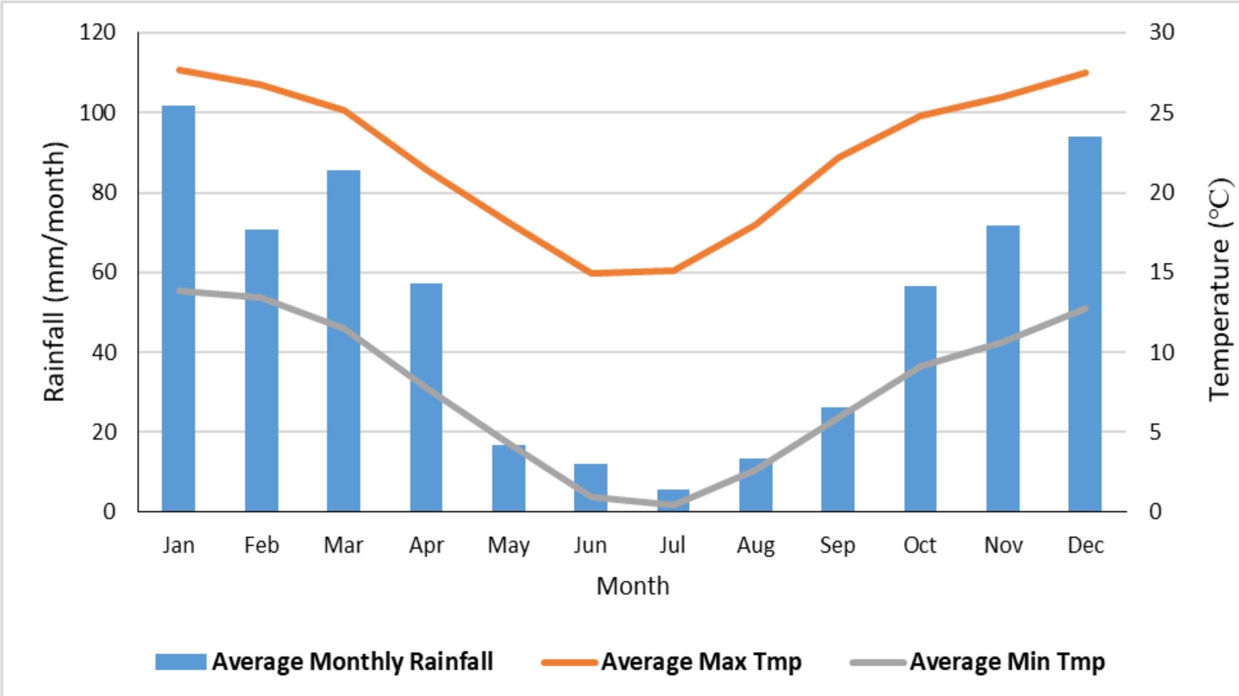

Figure 3.3 Average monthly max & min temperature and rainfall (2000-2018) southern-lower Caledon catchment, Mafeteng district

3.2.3. Bio-physical factors

Topography and Soil

The topography of the Caledon catchment ranges from 1413 m to 3158 m (Figure 3.6). This variation is a critical property as it influences flow rates and directions. The catchment features gentle and moderate slopes predominantly in the southwestern part, which lies mostly in South Africa. In contrast, the eastern and northeastern parts, located in Lesotho, consist of steeper slopes (Devito et al., 2005; State of Water Resources Report Fiscal Year, 2016). Groundwater in the catchment occurs within the fractured Stormberg Group and a smaller portion is underlain by the Drakensberg Group. Both groups belong to the Karoo Supergroup, which comprises sedimentary and basalt rock aquifers, alluvial sediments, and fracture and dolerite intrusion zones. Groundwater is primarily used in the rural parts of the catchment for domestic water supply and agricultural activities (Mare, 2007; Viles, 2007). The catchment is mainly covered by clayey loam in the north and southeast, with loam soils dominating a smaller area in the northeast. These soils have a balanced distribution of sand, clay, and silt particles. The clay loam soils are associated with the basalt of the Drakensberg Group, while the loam soils, containing 30-50% sand, are linked to the mudstones and siltstones of the Stormberg Group (Midgley et al., 1994).

Vegetation

According to Nusser (2001), the vegetation in the Caledon catchment comprises long grassland and dwarf scrub sparsely distributed around the area. The dominant rangeland in the high-altitude regions is established by grasses such as Merxmuellera disticha, Festuca caprina, Helichrysum trilineatum, and Harpachloa falx.

Streamflow

The annual streamflow of the Caledon River during the observation period varied significantly, ranging from 0.129 to 572.871 m^3/s, as shown in Figure 3.4. The highest streamflows are typically observed from November to February, while the winter season (June to August) is characterized by decreased streamflow.

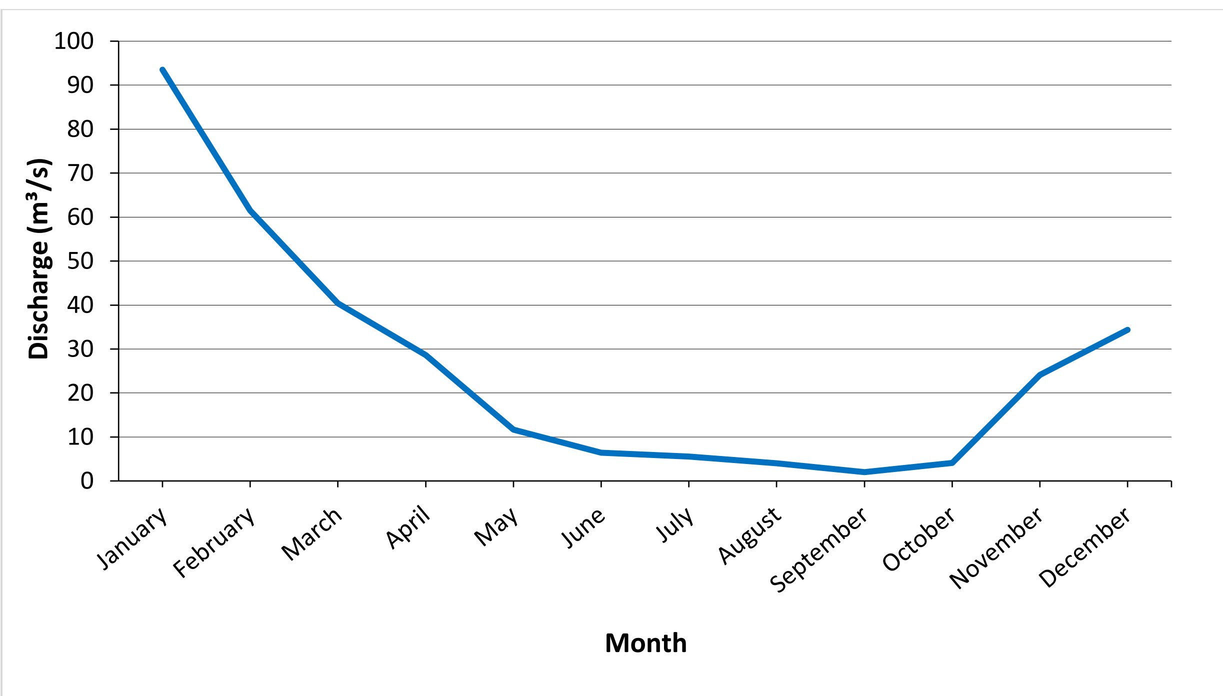

Figure 3.4. Average monthly discharges of CG 22 observed station (2010 to 2018)

3.3. SWAT Model Description

The SWAT hydrological model will be used in this study to analyse the water balance. SWAT model is a comprehensive conceptual, continuous time, distributed river basin and deterministic model that requires vast input data varying widely in space and time while changing input into output variables (Kurbah and Jain, 2017). SWAT has capabilities to capture various hydrological processes such as precipitation, surface runoff, soil storage, evapotranspiration, infiltration, subsurface flow, and groundwater flow. The pollutants that can be currently modelled in SWAT are sediment, Nitrogen, Phosphorus, pesticide, and bacteria loads (Dakhlalla and Parajuli, 2018). SWAT capability of simulating hydrologic processes, soil erosion and sediment yield at each HRU is dependent on the following water balance and Modified Universal Soil Loss Equation (MUSLE) (Williams, 1975). The model's equations are as follows:

$$SW_t = SW_0 + \sum_{i=1}^{n}\left(R_{day} - Q_{surf} - E_\alpha - W_{seep} - Q_{gw}\right) \qquad (3.1)$$

Where, SW_t is soil water content (mm), $SW_0$0 is initial soil water content (mm), R_{day} is daily precipitation (mm), Q_{surf} is surface runoff (mm), E_α is evapotranspiration (mm), W_{seep} is percolation (mm), and Q_{gw} is groundwater flow (mm).

Water yield is a critical parameter that should be evaluated for sustainable water resources management, it is the aggregate sum of water leaving the HRU and entering principal channel during the time step (Arnold et al., 2011). Water yield of a within a watershed is evaluated by the model based on Eq. 3.2.

$$\boldsymbol{W_{yld}} = Q_{surf} + Q_{lat} + Q_{gw} - T_{loss} \qquad (3.2)$$

Where W $_{yld}$ is the measure of water yield (mm), Q $_{surf}$ is the surface runoff (mm), Q $_{lat}$ is the lateral flow contribution to stream (mm), Q $_{gw}$ is the groundwater contribution to streamflow (mm), and T loss is the transmission losses (mm) from tributary in the HRU by means of transmission through the bed. The estimation of surface runoff can be performed by the model using the SCS curve number system by the USDA Soil Conservation Service.

$$\boldsymbol{Q_{surf}} = \frac{(R_{day} - 0.2S)^2}{(R_{day} + 0.8S)} \quad (3.3)$$

Q $_{surf}$ is the accumulated runoff or rainfall excess (mm), R $_{day}$ is the rainfall depth for the day (mm), S is the retention parameter (mm). The retention parameter S and the prediction of lateral flow by SWAT model are defined in Eqs. (3.4) and (3.5), respectively

$$\boldsymbol{S} = 25.4\left(\frac{100}{CN} - 10\right) \quad (3.4)$$

$$\boldsymbol{Q_{lat}} = 0.024\,\frac{(2SCsin\alpha)}{(\theta_d L)} \quad (3.5)$$

Where, Q $_{lat}$ = lateral flow (mm/day); S = drainable volume of soil water per unit area of saturated thickness (mm/day); SC = saturated hydraulic conductivity (mm/h); L = flow length, α ¼ slope of the land, θ $_{d}$ = drainable porosity and CN is the soil curve number. The estimation of the base flow was done using Eq. 3.6.

$$Q_{gwj} = Q_{gwj-1.}e^{(-\alpha gw.\Delta t)} + W_{rchrg}\left(1 - e^{(-\alpha gw.\Delta t)}\right) \quad (3.6)$$

Where Q $_{gwj}$ = groundwater flow into the main channel on day j; α $_{gw}$ = base flow recession constant; Δt = time step; and W $_{rchrg}$ = the amount of recharge entering the aquifers (mm/day).

A watershed in SWAT is divided into multiple sub-basins or sub watersheds as part of the discretisation process. The strategy of sub-basins is particularly useful when the watershed is grouped by land uses, slope and category of soils dissimilar enough in properties to impact hydrology. The total runoff generated by a sub-basin will be mainly dependent on the hydrologic condition of each land cover, soil type and slope present in the watershed. Therefore, the impact of each type of land use is crucial in the modelling of runoff of the basin. After the overlay of the land-use, soil maps and slope, the distributions of the Hydrological Response Units (HRUs) were determined. HRUs divide the sub-basin into the area of similar land use, soil type and slope. Runoff is predicted separately for each HRU and routed to obtain the total runoff of the watershed (Kangsabanik et al., 2017; Tibebe et al., 2017). Figure 3.5 shows the flow chart of modelling using QGIS with QSWAT interface.

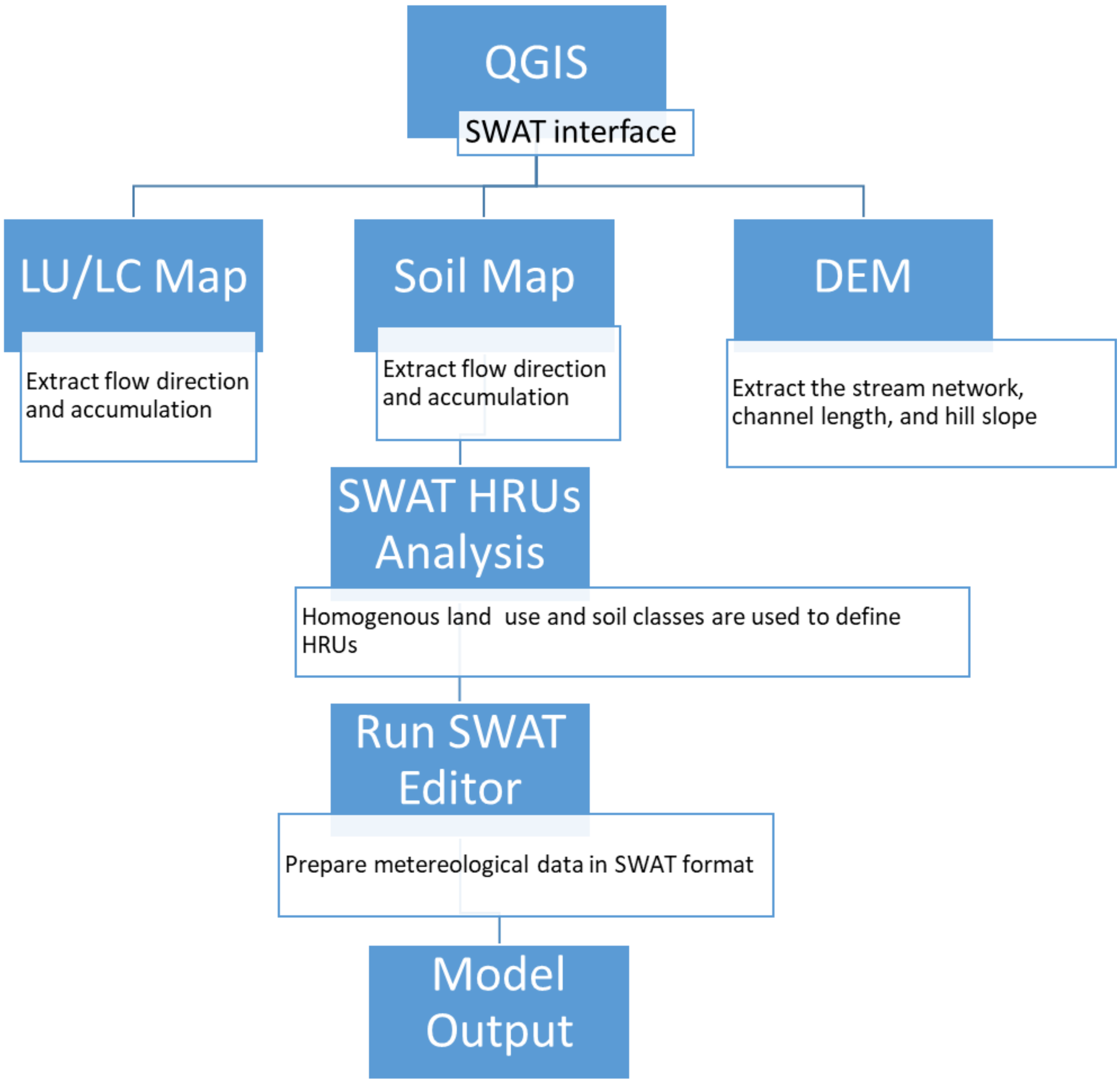

Figure 3.5 SWAT Model Flow Chart

The SWAT model divides sub-basin components into several key processes: hydrology, weather, sedimentation, soil temperature, crop growth, nutrients, pesticides, and agricultural management.

Hydrology

Hydrologic processes in the SWAT model include:

- Surface runoff: Generated from daily rainfall using the SCS curve number method.
- Percolation: Modelled with a layered storage routing technique combined with a crack flow model.
- Lateral subsurface flow: Simulated using the Hargreaves method.
- Groundwater flow: From shallow aquifers to streams.
- Potential evapotranspiration: Calculated using the Priestley-Taylor and Penman-Monteith methods.
- Snowmelt: Included in the hydrology processes.
- Transmission losses: From streams.
- Water storage and losses: From ponds.

Weather

The SWAT model is driven by weather variables, including daily precipitation, maximum and minimum air temperatures, solar radiation, wind speed, and relative humidity. A weather generator can simulate these variables based on monthly climate statistics calculated from long-term measured data.

Sedimentation

Sediment yield for each sub-basin is computed using the Modified Universal Soil Loss Equation (MUSLE).

Soil Temperature

Soil temperature is updated daily for each soil layer as a function of air temperatures, snow, plant and residue cover, damping depth, and mean annual temperature.

Crop Growth

Crop growth is simulated using the EPIC crop model, which operates on a daily time step. It estimates phenological development based on daily accumulation of heat units, harvest index for partitioning grain yield, Monteith's approach for potential biomass, and adjustments for water and temperature stress. Various crops, both annual and perennial, can be simulated using crop-specific input parameters.

Nutrients

Nitrate losses in runoff, percolation, and lateral subsurface flow are simulated. Organic nitrogen losses dissolved in soil are estimated from soil losses and an enrichment ratio. The nitrogen transformation model, modified from EPIC, includes residue mineralization, humus mineralization, nitrification, denitrification, volatilization, fertilization, and plant uptake. Phosphorus processes include residue and humus mineralization, losses with runoff water and sediment, fertilization, fixation by soil particles, and plant uptake.

Pesticides

Pesticide transformations are simulated with a simplified GLEAMS model approach, including interception by the crop canopy, volatilization, degradation in soils and from foliage, and losses in runoff, percolation, and sediment.

Agricultural Management

Simulated agricultural management practices include tillage effects on soil and residue mixing, bulk density, and residue decomposition. Irrigation can be scheduled by the user or applied automatically according to user-specified rules. Fertilization with nitrogen and phosphorus can also be scheduled by the user or applied automatically. Pesticide applications are scheduled by the user. Grazing is simulated as a daily harvest operation.

Stream Processes

Simulated stream processes include channel flood routing, channel sediment routing, and nutrient and pesticide routing and transformations modified from the QUAL2E model. Components include algae as chlorophyll-a, dissolved oxygen, organic oxygen demand, organic nitrogen, ammonium nitrogen, nitrite nitrogen, organic phosphorus, and soluble phosphorus. In-stream pesticide transformations include reactions, volatilization, settling, diffusion, resuspension, and burial.

Ponds and Reservoirs

The ponds and reservoirs component includes water balance, routing, sediment settling, and simplified nutrient and pesticide transformation routines. Water diversions into, out of, or within the basin can be simulated to represent irrigation and other withdrawals from the system (Srinivasan et al., 2010).

3.4. Model Set-Up

3.4.1. Model input data

The basic inputs required for a SWAT simulation includes a topography, land-use map, soil map, and weather data. The topography data, which is a 30 m resolution Digital Elevation Model (DEM), the LULC map and soil map are spatial data, whereas the Climate data are observed records collected from the Lesotho Meteorological Services (LMS).

3.4.1.1. Climate data

The climate data used in the SWAT model as an input consist of the observed daily rainfall (mm) and daily temperature (°C) data from the Lesotho Meteorological Services (LMS) from 2008 to 2018 from six (6) weather stations as listed in Table 3.1 below. The wind speed (m/s) from 2008 to 2018 were obtained as spatial data from National Oceanic and Atmospheric Administration (NOAA) (https://www.noaa.gov/) downloaded on daily time step. All observed daily rainfall (mm) and daily temperature (°C) data were obtained from the stations listed below.

Table 3.1. Meteorological stations of Caledon catchment

ID	Station Name	Latitude	Longitude	Altitude (m)
1	Ts'akholo	-29.6831	27.2322	1717.33
2	Teya-teyaneng	-29.1136	27.8722	1920.80
3	Butha-buthe	-28.7362	28.4764	2050.42
4	Mejametalana	-29.3068	27.4990	1544.00
5	Hlotse	-28.8785	28.0532	1633.00
6	Matsieng	-29.6066	27.5644	1710.00

3.4.1.2. Digital Elevation Model (DEM)

To incorporate elevation data in the model, a 30 m by 30 m, DEM grid was downloaded from the National Elevation Dataset from the United State Geological Survey (USGS) (https://earthexplorer.usgs.gov/), and it was used to delineate the watershed. Figure 3.6 shows the Caledon catchment DEM.

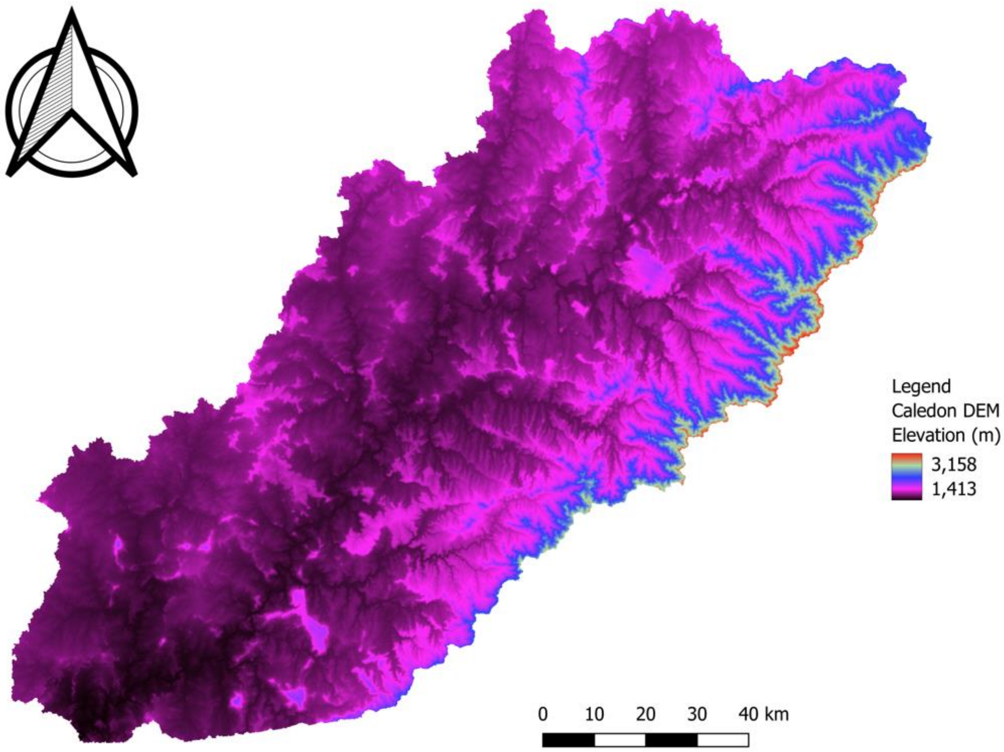

Figure 3.6. Caledon Catchment Digital Elevation Model (DEM)

3.4.1.3. Soil Map

Soil data for the watershed was downloaded from FAO Digital Soil Map (https://data.apps.fao.org/map/catalog/srv/eng/catalog.search#/metadata/cc45a270-88fd-11da-a88f-000d939bc5d8) of the world having scale of 1: 5,000,000. The soil map of the study area was prepared in QGIS in order to correspond with the parameters in the SWAT user soil database. Figure 3.7 shows the Caledon catchment soil map.

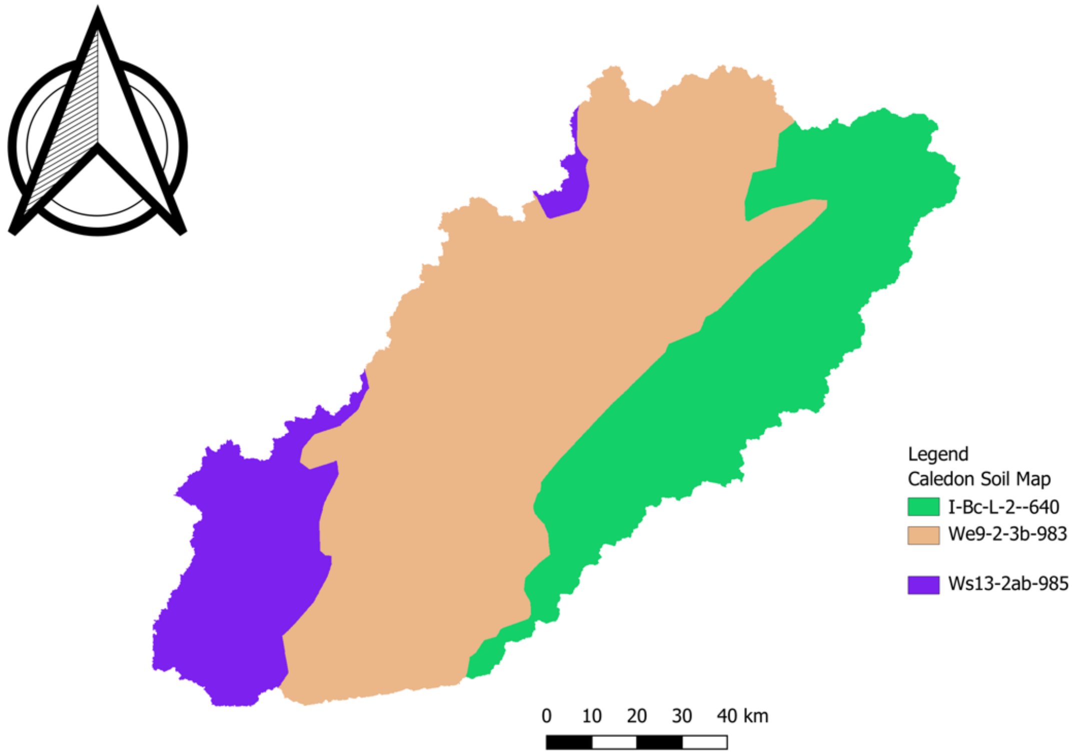

Figure 3.7. Caledon Catchment Soils

Table 3.2 shows the SWAT soil dataset which consists of three (3) soil classes found in the Caledon catchment, which are mostly of clay loam textural class.

Table 3.2. Caledon SWAT model soil summary

SWAT soil code	Soil Texture	Area (km^2)	Area Percentage (%) watershed
We9-2-3b-983	CLAY_LOAM	7323.28	57.84
I-Bc-L-2-640	CLAY_LOAM	3575.89	28.24
Ws13-2ab-985	LOAM	1762.77	13.92
TOTAL		**12 661.95**	**100.00**

3.4.1.4. Land use/ Land cover Map

Land use data was also used to develop the SWAT model, which was downloaded from the LANDSAT of the United State Geological Survey (USGS) (https://earthexplorer.usgs.gov/), the land use maps were based on the 1 : 250,000 topographic from 2009. On the origin of land use and land cover map, the map of the study area was prepared in QGIS in order to correspond with the parameters of other raster files. Figure 3.8 shows the Caledon catchment land cover classification.

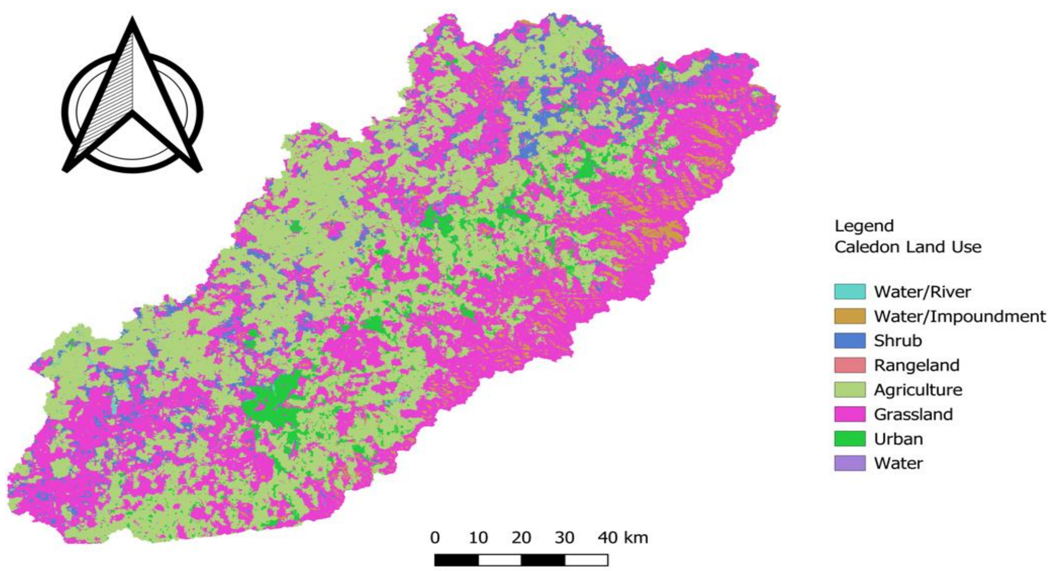

Figure 3.8. Caledon Catchment Land use/Land cover (LU/LC)

The reclassified land use and percentage cover area are presented in Table 3.3 below. Agricultural land (42.44%), grassland (42.29%), urban development (5.05%), shrubs (5.74%), water bodies (4.47%), whereas the share of range land yields the remaining 0.01%. Table 3.3 shows areal distribution of the catchment land use classifications.

Table 3.3. SWAT land use types and percentage area for the study site.

Land Use Classification	**SWAT Land Use Code**	**Area (ha)**	**Area percentage (%) Watershed**
Grass land	Gras	5355.24	42.29
Shrub	Shrb	727.32	5.74
Water	WETW	566.01	4.47
Agriculture	Agrl	5373.15	42.44
Urban	Urbn	639.05	5.05
Range land	Rnge	1.18	0.01
TOTAL		**12,661.95**	**100.00**

3.4.2. Data processing

The pre-processing of the spatially distributed data will be done in two phases. Firstly, the digital elevation model (DEM) is analysed to extract the sub-basins, the stream network, channel length, and hill slope (Pohlert et al., 2005). Secondly, to represent spatial variability, homogenous land use and soil classes are used to define several hydrological response units (HRU) within each sub-watershed based on the concept of flow direction and accumulation (Pohlert et al., 2005; Adu and Kumarusamy, 2017; Abebe and Gebremariam, 2019; Irvem and Sadek, 2019; Ruan, 2016). In SWAT model, surface runoff is determined by the SCS curve number approach, which estimates the surface runoff based on the hydrological soil group, land cover, and antecedent moisture condition. Potential evapotranspiration will be determined by the Penman-Moneith method (Kurbah and Jain, 2017 Shruti and Patil, 2016; Irvem and Sadek, 2019; MSA Professional Services, 2015; Neitsch et al., 2009).

After that, land use/soil/slop definition and HRU definition was performed by using the land use and soil map in combination with look up tables. By using these data, SWAT classified the watershed. Then, writing of input tables was continued by defining weather data. The first step to proceed was to define the weather generator data. To define the weather generator data, the user weather station was created through edit SWAT database section. Then, the weather station parameters were fitted in the new station. To finalise the weather writing part, all sections written in the weather-writing window were selected and then all the watershed data was written, and the model was made ready to be run.

3.5. Calibration and Validation of the SWAT Model

For accurate results, the model was calibrated against discharge measurement. This is a demonstration that the model is capable of reproducing field observed values of various hydrological variable (Marcinkowski et al., 2013; Ranit et al., 2014). The model was used to simulate for a period of 10 years (2009–2018). The calibration period is from 2012 to 2018. The observed data consists of daily streamflow obtained from the Lesotho Ministry of Water Affairs, at a gage station in the district of Maseru, station CG22. First time SWAT users are recommended to carry out manual calibration over the semi-calibrated tool.

3.6. Model Performance Evaluation

Model evaluation techniques include subjective and/or objective estimates of how close model predictions fit to the observations. For objective evaluation, mathematical estimation of errors between observed and predicted values must be conducted using different model evaluation statistics (Krause et al., 2005).

The model performance will be assessed by comparing the observed flow versus simulated monthly flows during calibration and validation periods. For proper evaluation, mathematical estimation of errors between observed and simulated values, must be conducted by the use of different model evaluation statistics. The model performance and evaluation will be analysed using statistical parameters such as root mean square error standard deviation ratio (RSR), Nash Sutcliffe efficiency (NSE) and the coefficients of determination (R^2) to meet these demands (Legates and McCabe, 1999; Dakhlalla and Parajuli, 2018; Abbaspour, 2007).

4. RESULTS AND DISCUSSION

4.1. Model Calibration and Validation

The model was manually calibrated on a monthly time step for the period from 2010 to 2015, and validation was conducted on a monthly time step for the period from 2016 to 2018, with a two-year warming-up period from 2008 to 2009. These time steps were chosen based on periods with minimal missing data. Before beginning manual calibration, the simulation results from the SWAT model run were plotted against the observed flow to analyse the patterns and variance in the data. Once a thorough analysis was completed, a decision was made on which parameters to adjust and by how much.

The initial simulation results from the SWAT model run showed lower flow peaks compared to the observed flows, a common issue in mountainous catchments. This was supported by a study conducted in the middle of Portugal by Demirel et al. (2009), which found that the process-based model SWAT simulations in the Pracana basin were not effective in forecasting peak flow values. Consequently, the calibration process involved manually adjusting the CN2 parameter until an acceptable result was achieved between observed and simulated data. The CN2 was adjusted by 50% to yield higher flows in the calibrated model, which almost matched the observed flow.

Despite manual calibration, the SWAT model generally failed to predict high flows, especially during the wet seasons (October to February). The hydrographs of the simulated flows lagged behind those of the observed flows; however, there was a slight correlation between the simulated and observed hydrographs during the dry seasons (May to August). The recession limbs of both the observed and simulated hydrographs ran concurrently from 2010 to 2014. Multiple studies have shown that the SWAT model poorly predicts high flows, often due to ungauged catchments with poor rainfall data and numerous water impoundments (Mango et al., 2011; Ndomba et al., 2009; Maliehe and Mulungu, 2017). This study's results are supported by Tibebe et al. (2016), who found that the model did not capture peak values accurately in the Holetta catchment in Ethiopia, due to poor rainfall data records. According to Bartley et al. (2002), small water impoundments can significantly impact the hydrological response of a catchment, increasing evapotranspiration and ground infiltration rates, and reducing the volume of water contributing to high peaks (Bao-qing et al., 2004).

The monthly graphs indicated that the model validation satisfactorily fitted the observed flow measurements. While the model still showed lower predictions of peak flows, there was no significant lagging in the validated model. Figure 4.1 below displays the calibration and validation of monthly mean discharges for the Caledon catchment.

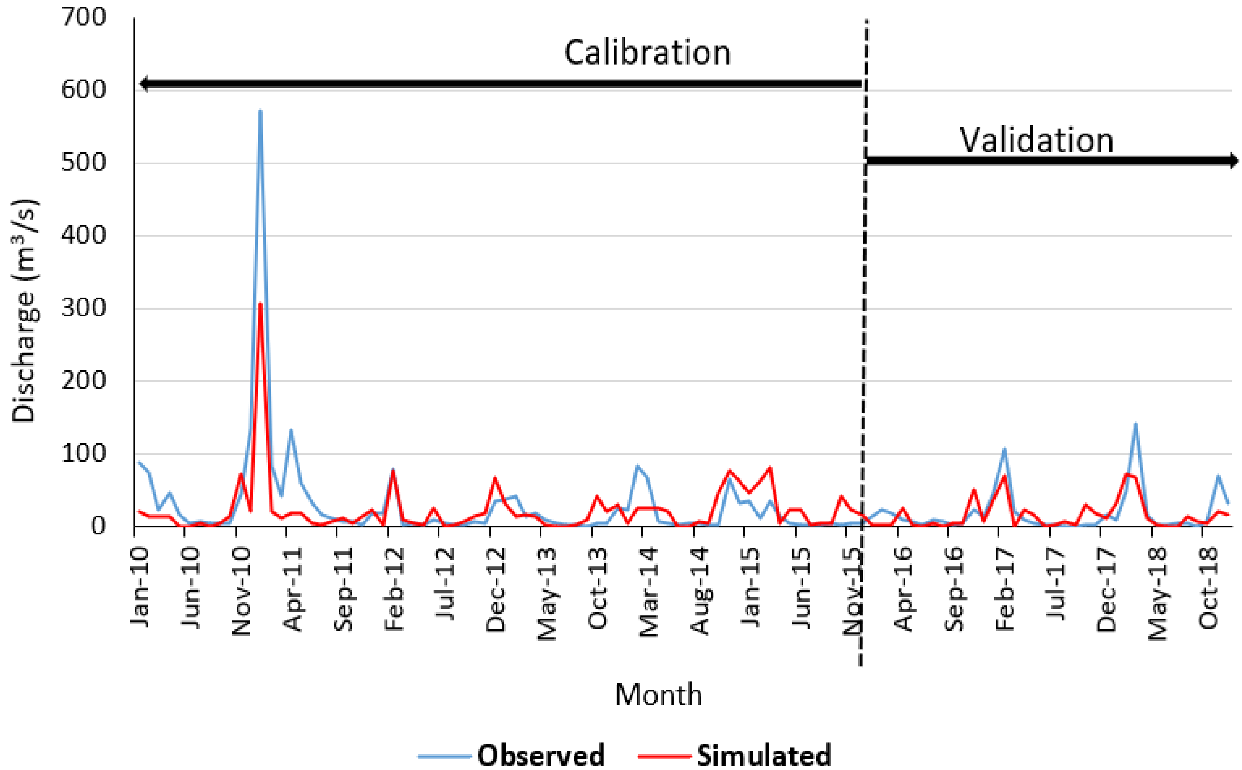

Figure 4.1. Calibration and validation of the model using monthly discharges for the Caledon catchment.

Manual calibration of SWAT model is challenging and time consuming in many large-scale applications. However, manual calibration is most effective in ensuring that the user understands the model well, the important processes in the watershed, and the parameter sensitivity (Arnold et al., 2012).

As stated in the preceding section, the catchment is a transboundary area spanning both Lesotho and South Africa, with an elevation ranging from 1413 m to 3158 m. This indicates that it is a mountainous catchment with a mix of lowlands. According to Smarzynska and Miatkowski (2016), the curve number (CN2) is the most sensitive parameter in mountainous areas and greatly affects surface runoff. Therefore, the curve number was treated as the most sensitive parameter.

4.2. Model Performance and Limitations

The coefficients of determination (R^2), ratio of the root mean square error to the standard deviation of measured data (RSR) and Nash-Sutcliffe (NSE) efficiency were used to analyse the adjustment of the values predicted by the model to the observed data. The model performance results obtained through the objective functions are indicated in Table 4.1 below.

Table 4.1. The performance rating of R^2, RSR and NSE of the Caledon catchment.

Model Evaluation Criterion	Calibration	Validation
NSE	0.62	0.54
R^2	0.68	0.56
RSR	0.61	0.68

The efficiency coefficients of Nash-Sutcliffe (NSE) and RSR during the monthly calibration of the SWAT model, as shown in Table 4.3, are considered satisfactory. The correlation coefficient (R^2) presented a higher value of 0.68, as shown in Figure 4.2, which is considered a good fit. A possible reason for the lower performance of the model under the NSE and RSR criteria is that these evaluations place a higher weight on peak events during assessment, making the model more reliable in estimating peaks (Abbaspour, 2007).

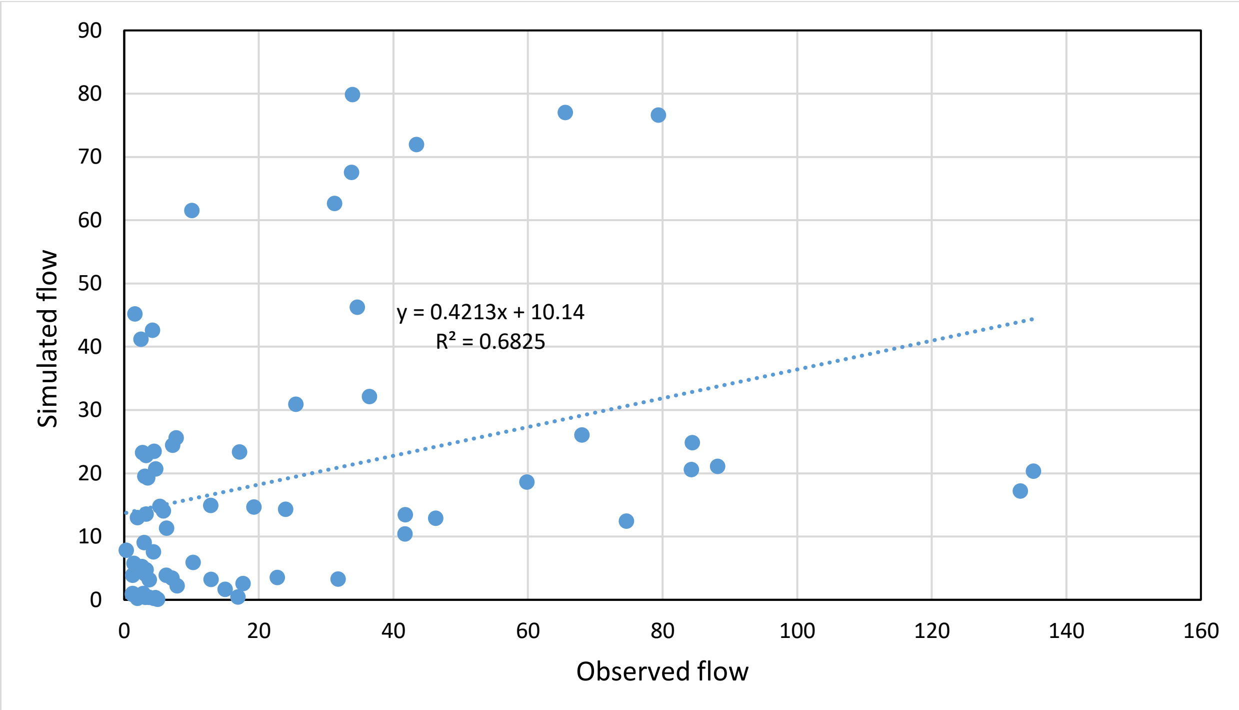

Figure 4.2. Comparison of observed and simulated flow during calibration phase

The results obtained for validation show that the SWAT model performed satisfactorily across all evaluation criteria. The efficiency coefficient of Nash-Sutcliffe (NSE) during the monthly validation of the SWAT model, along with the correlation coefficient (R^2) presented in Table 4.3, indicate a good fit. The RSR was 0.68, demonstrating that the SWAT model performed well in all statistical assessments. Therefore, SWAT can be an important tool for integrated basin management and simulating surface runoff, aiding in the proper planning and management of water resources. Figure 4.3 below shows the coefficient of determination (R^2) correlation between the validated flow and observed flow of the Caledon catchment.

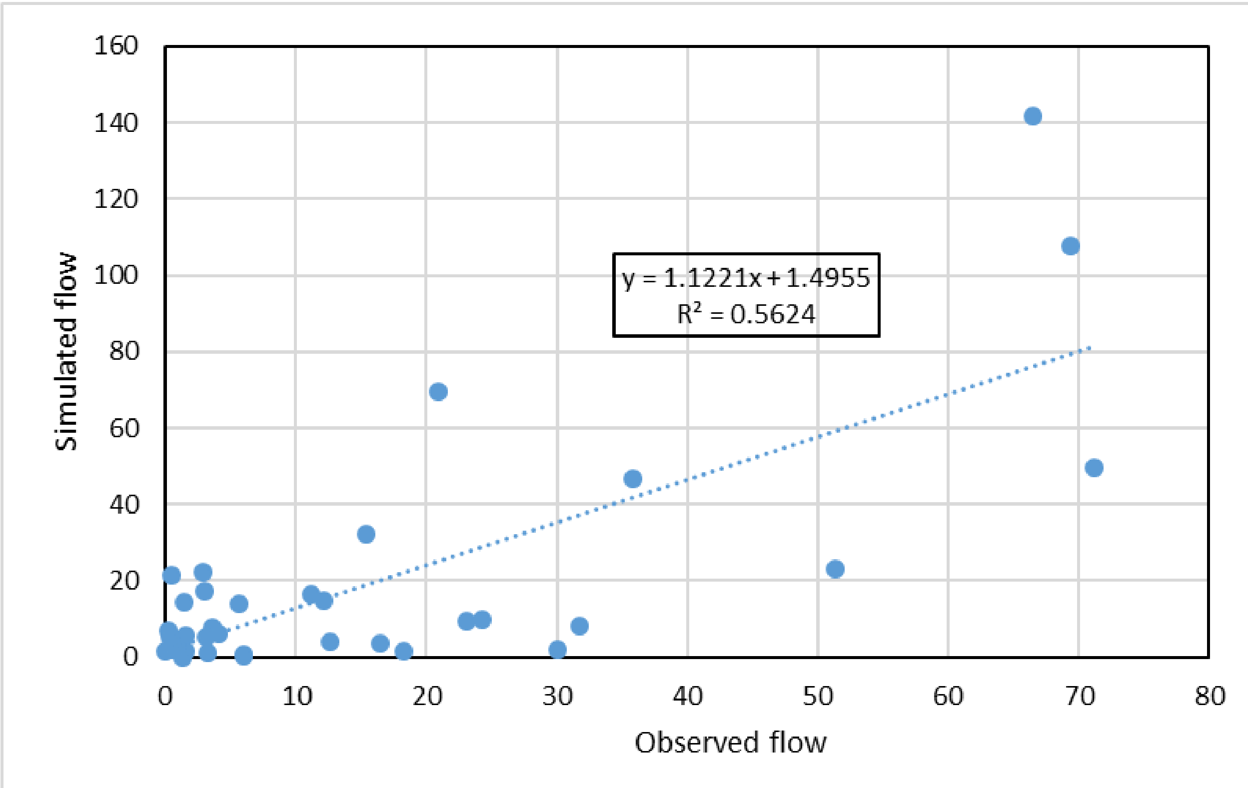

Figure 4.3. Comparison of observed and simulated flow during the validation phase.

4.3. Analysis of Water Balance Components

The SWAT model estimated important water balance components in addition to the simulated monthly discharge of the watershed. To address water management issues, it is crucial to analyse and quantify the diverse components of hydrological processes occurring within the study area. The estimated average monthly basin values for the different water balance components simulated are as follows:

i. Evapotranspiration (ET)

ii. Direct Runoff

iii. Water Yield (WYLD)

iv. Groundwater (GWQ)

v. Surface Flow (SURQGEN)

Direct runoff is the combined lateral flow of water in the subsurface zone and surface flow (SURQGEN) of water into a stream or reservoir within a specific time period under the influence of gravitational force. It is important in hydrological research as it provides insights into stream flow estimation, irrigation, and flood management (Ward and Trimble, 2003; Ayivi and Jha, 2018). Water yield, the amount of streamflow at the catchment outlet during the time step, is a key parameter estimated by the model for efficient water management and planning. It differs from direct runoff as it incorporates transmission losses, including evaporation from flowing river flow and infiltration losses into the riverbed/banks (Ayivi and Jha, 2018; Shawul et al., 2013).

According to Hussainzada and Lee (2021), SWAT simulates groundwater into shallow and deep aquifers, with water entering the deep aquifer not accounted for in the water balance computations as it does not return to the hydrological cycle. Surface runoff is the unconfined overland flow that moves over the Earth's surface into catchment depressions and streams, generated by the SCS curve number in the SWAT model (Srinivasan et al., 2010; Ward and Trimble, 2003).

The simulated water balance components, such as evapotranspiration, direct runoff, surface runoff, and water yield at the catchment level, are measured in millimetres (mm) and are presented from January 2010 to December 2018. The monthly range of rainfall throughout the nine years of simulation is 0 to a maximum of 88.83 mm. ET ranged from 1.44 to 78.00 mm, total runoff ranged from 0 to 22.51 mm, and water yield ranged from 0.09 to 21.13 mm. It was observed that ET and water yield were the only two water balance components to consistently show values above zero. This may be due to groundwater contributing to water yield, as groundwater flows over a wide area in a laminar state, resulting in perennial flow throughout the years and sustaining the components it contributes to throughout the year.

4.3.1. Analysis of rainfall and evapotranspiration

Evapotranspiration is influenced by various climatic parameters, including solar radiation, humidity, temperature, and other general catchment factors such as landscape, vegetation type, soil properties, and land use management practices. This makes ET a highly variable parameter, and its modelling is important for water resources planning (Mahasa et al., 2023; Moeletsi et al., 2013). ET was simulated for a period of 9 years. According to Figure 4.4, November showed higher simulations for both rainfall and ET, with rainfall recording a monthly average of 72 mm and ET 64.47 mm. In contrast, July showed lower records, with rainfall simulations at 10.01 mm and ET at 10.44 mm. This is also reflected in Figure 3.4 (Monthly discharges of CG 22 observed station), which shows an extremely flat hydrograph during July over the 9-year observation period.

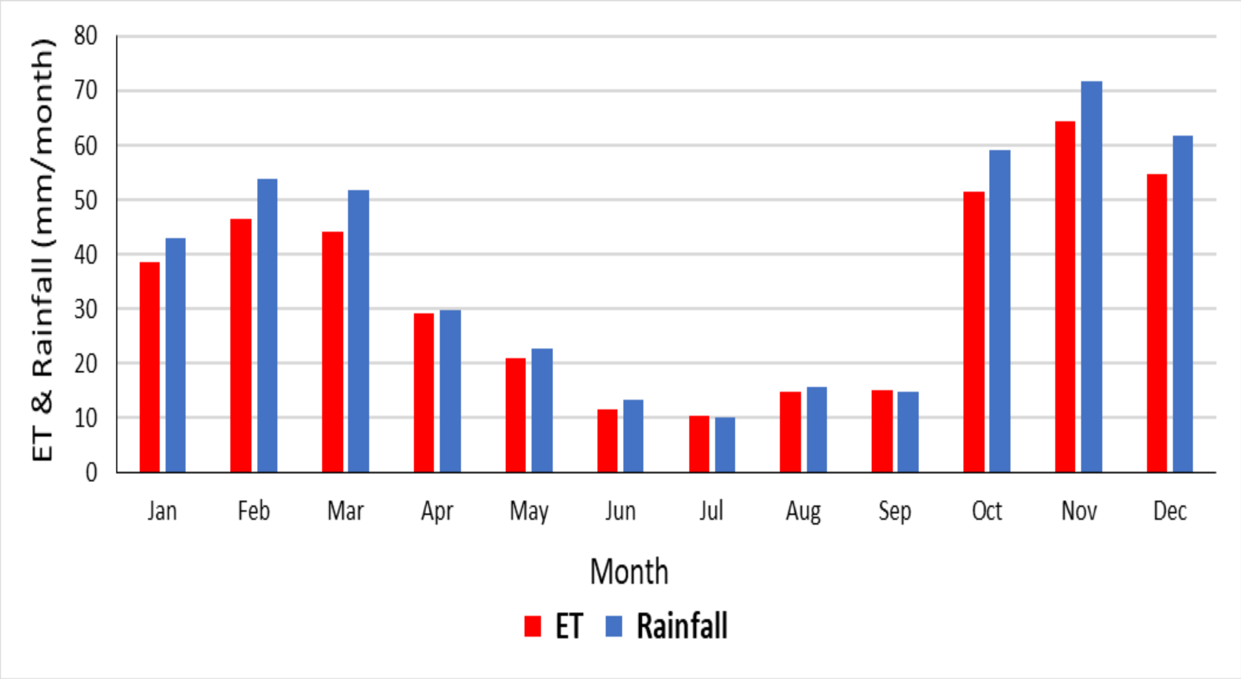

Figure 4.4. Average monthly evapotranspiration (ET) and rainfall (2010-2018)

Figure 4.5 shows the mean annual ET and rainfall records for a 9-year period. The years 2010, 2011, and 2016 recorded mean annual rainfall below 400 mm. These periods were marked by drought, especially during the winter season of 2016. As shown in Figure 4.6, average ET simulations from June to September recorded 13.29 mm, while average rainfall was 12.77 mm. This dominance of ET over rainfall indicates that the catchment lost more water than it received during these four months. The low rainfall in 2010, 2011, and 2016 is explained by Mahasa et al. (2023), who noted that the 2010 and 2015/2016 periods experienced a series of El Niño-driven droughts throughout Southern Africa.

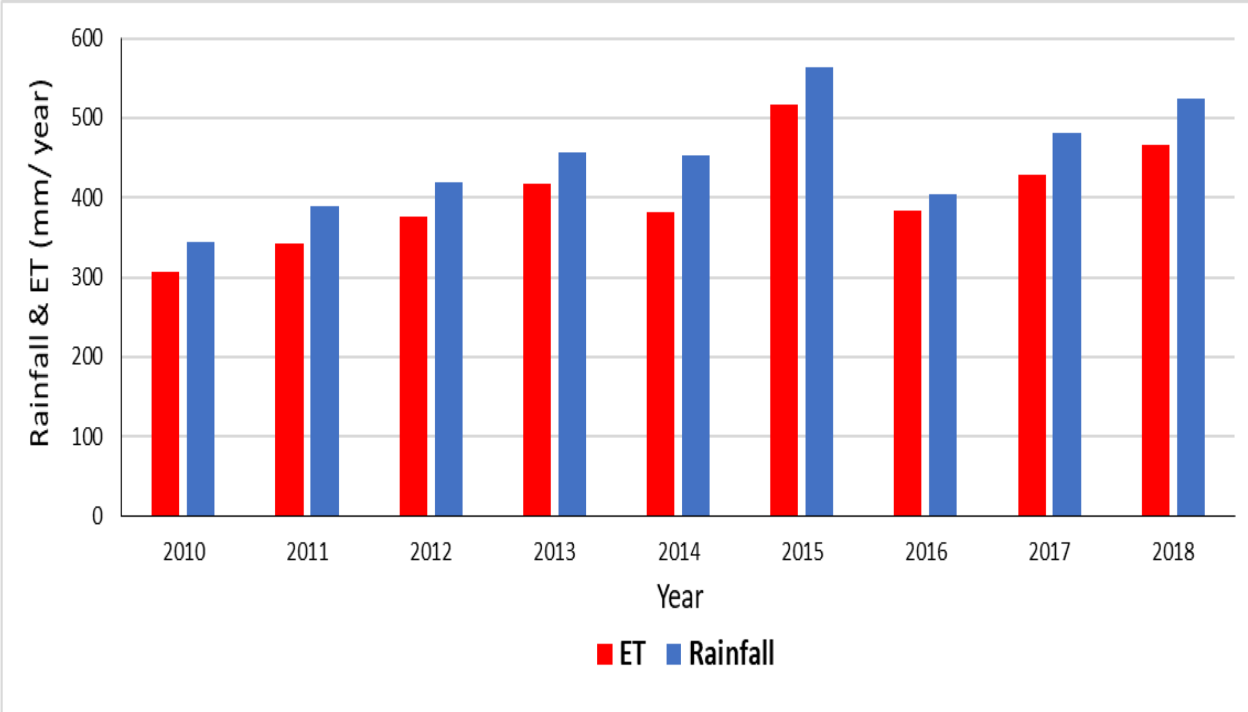

Figure 4.5. Mean annual evapotranspiration (ET) and rainfall (2010-2018)

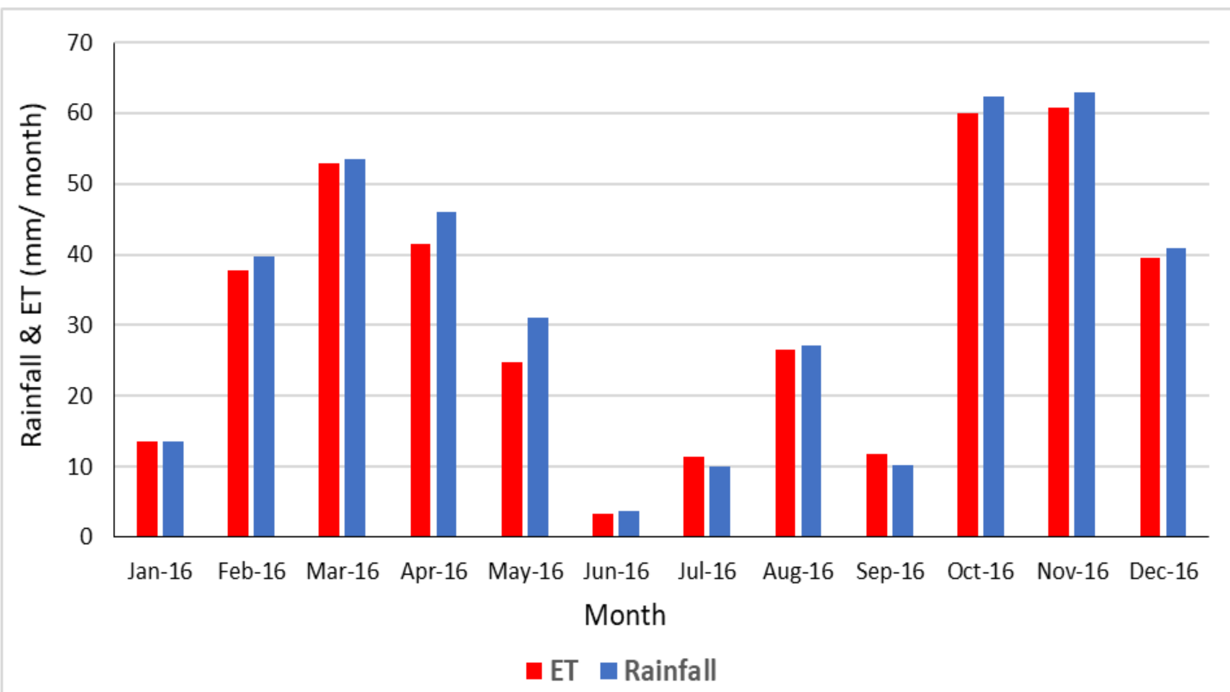

Figure 4.6. Total monthly evapotranspiration (ET) and rainfall (2016)

These high ET records in the catchment can likely be attributed to the land cover proportion. According to Table 3.3, agricultural space, grassland, and water bodies collectively occupy almost 90% of the catchment area, and these land cover/use categories are where evaporation and transpiration occur in greater amounts. The study reported that, on average, the Caledon catchment loses about 80% of monthly rainfall to ET, which is significantly higher compared to reports by other researchers. Bennie and Hensley (2001) stated that between 50% and 75% of annual precipitation is lost through evaporation from the soil surface in South Africa. It is important to note that this study was limited to simulations of evaporation, with no findings presented on the general loss of water from both the soil surface and vegetative cover.

4.3.2. Analysis of rainfall, direct runoff and water yield

Both water yield and direct runoff were simulated over a period of 9 years on a monthly time step and rainfall is the most dominant water balance component and directly affects all other components, acting as the water recharge engine of the entire catchment. It is responsible for generating runoff and water yield. These two components, water yield and direct runoff, exhibited similar patterns in both magnitude and spatial variability. The simulations show a clear statistical relationship of linear correlation with rainfall, as evidenced by Figures 4.7. An increase in rainfall results in an increase in direct runoff and water yield (WYLD), and a decrease in rainfall leads to a decrease in direct runoff and WYLD. November typically experiences high rainfall, which can result in flash floods and increased surface runoff, a primary contributor to water yield. The high rainfall event of 72 mm in November resulted in a higher water yield of 7.7 mm, while the winter season, characterized by low rainfall, resulted in lower water yields. For instance, August recorded a low water yield of 0.78 mm.

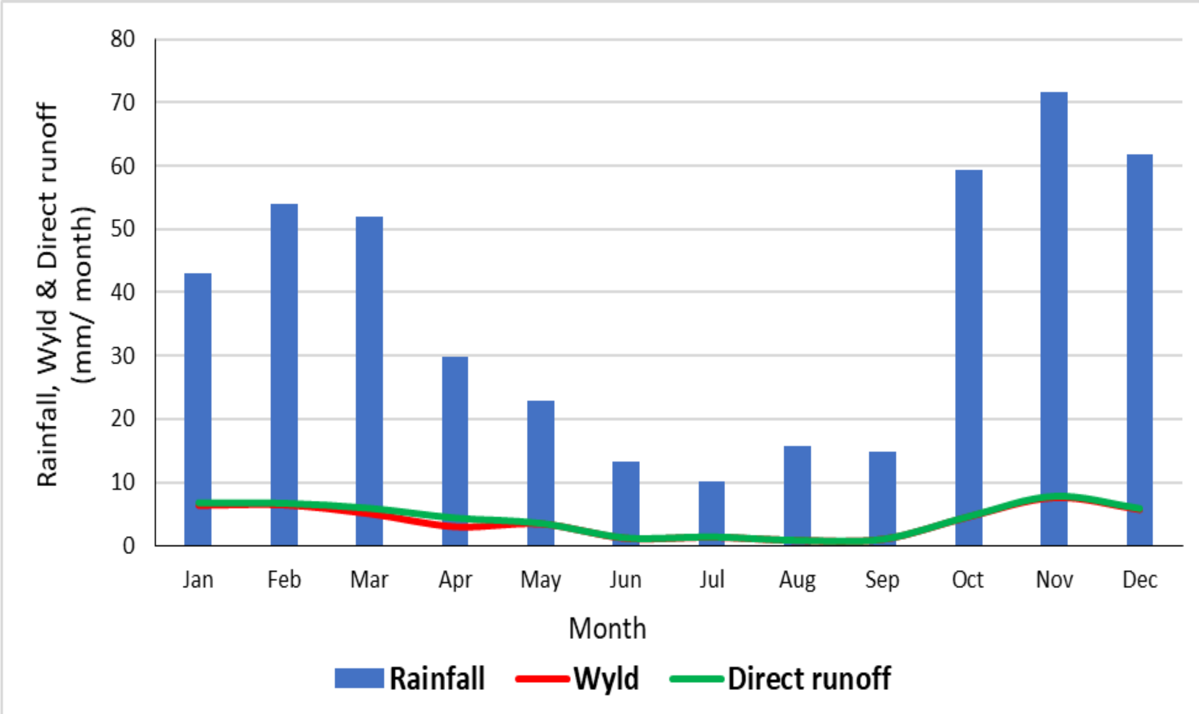

Figure 4.7. Average monthly water yield (WYLD), total runoff and rainfall (2010-2018)

The direct runoff and water yield (WYLD) exhibit similar trends to precipitation. When direct runoff and WYLD are at their maximum, rainfall is also at its peak, and vice versa. Examining these three water balance components—rainfall, water yield, and total runoff—over the 9-year period from 2010 to 2018 revealed that water yield consistently falls between 8.5% and 11% of total rainfall, while direct runoff ranges from 9.2% to 12.13%. The lower simulation in WYLD can be attributed to transmission losses, which arise due to infiltration and evaporation losses in the river stream.

According to Figure 4.8, the 2010, 2013 and 2016 period resulted in low mean annual WYLD of 33.85 mm, 34.74 mm and 20.7 mm, respectively, and the 2018 resulted in the highest mean annual WYLD, with a record high of 66.9 mm.

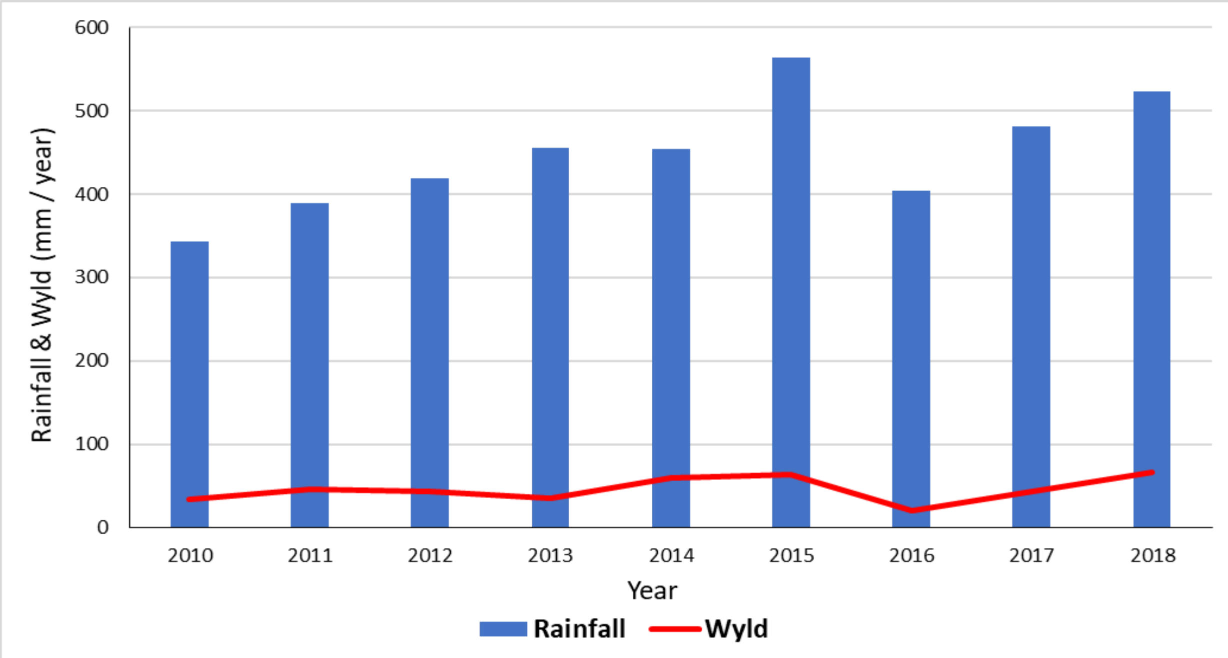

Figure 4.8. Mean annual water yield (WYLD) and rainfall (2010-2018)

The 2016 period experienced moderate water yield records during April and May, with a monthly average of 4 mm. However, a steep decline in WYLD simulation was observed during the winter and spring seasons, with June to October recording a monthly average of 0.89 mm, as illustrated in Figure 4.9. This 5-month period is considered the longest dry period based on the simulation records. This finding is supported by Mahasa et al. (2023), who noted that the 2016 period was severely affected by drought in South Africa and Lesotho.

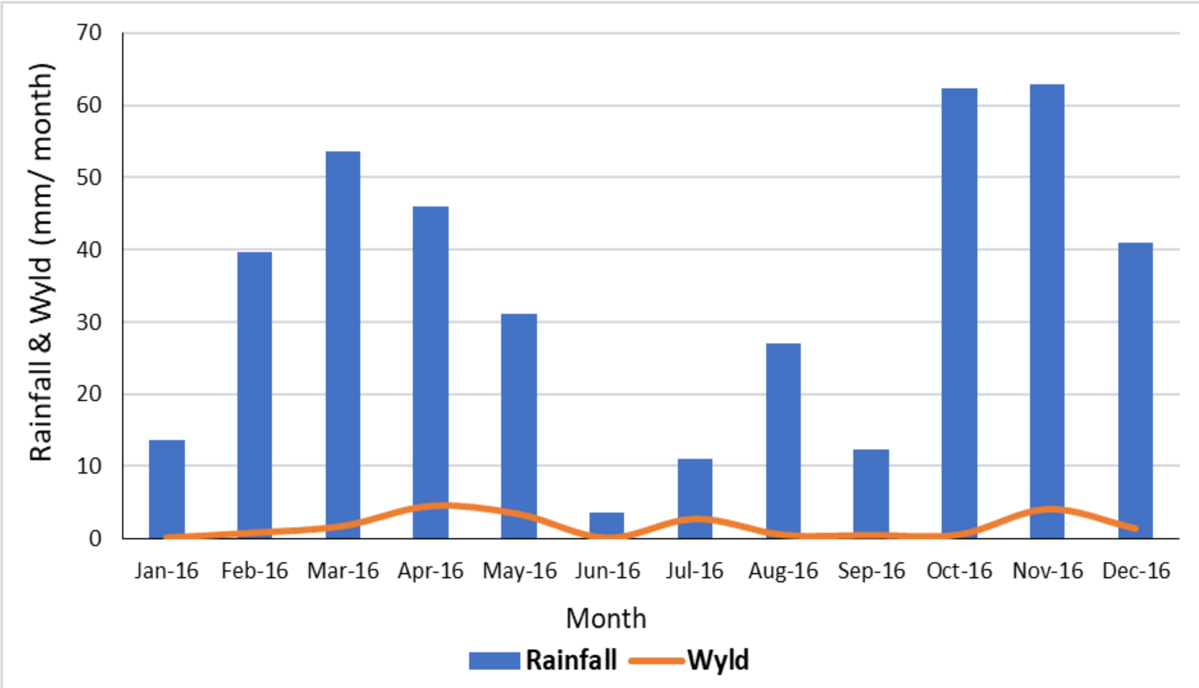

Figure 4.9. Mean annual water yield (WYLD) and rainfall (2016)

In 2018, moderately high WYLD was recorded, as shown in Figure 4.10. During the winter period, characterized by typically low WYLD, a seasonal average of 2.24 mm was recorded. In contrast, Figure 4.7 shows a seasonal average of 1.06 mm for the winter period over the 9-year span from 2010 to 2018. Notably, November 2018 recorded a WYLD high of 16.18 mm, attributed to the high rainfall of 88.83 mm during the same month, which is also the highest average monthly rainfall observed during the 9-year period.

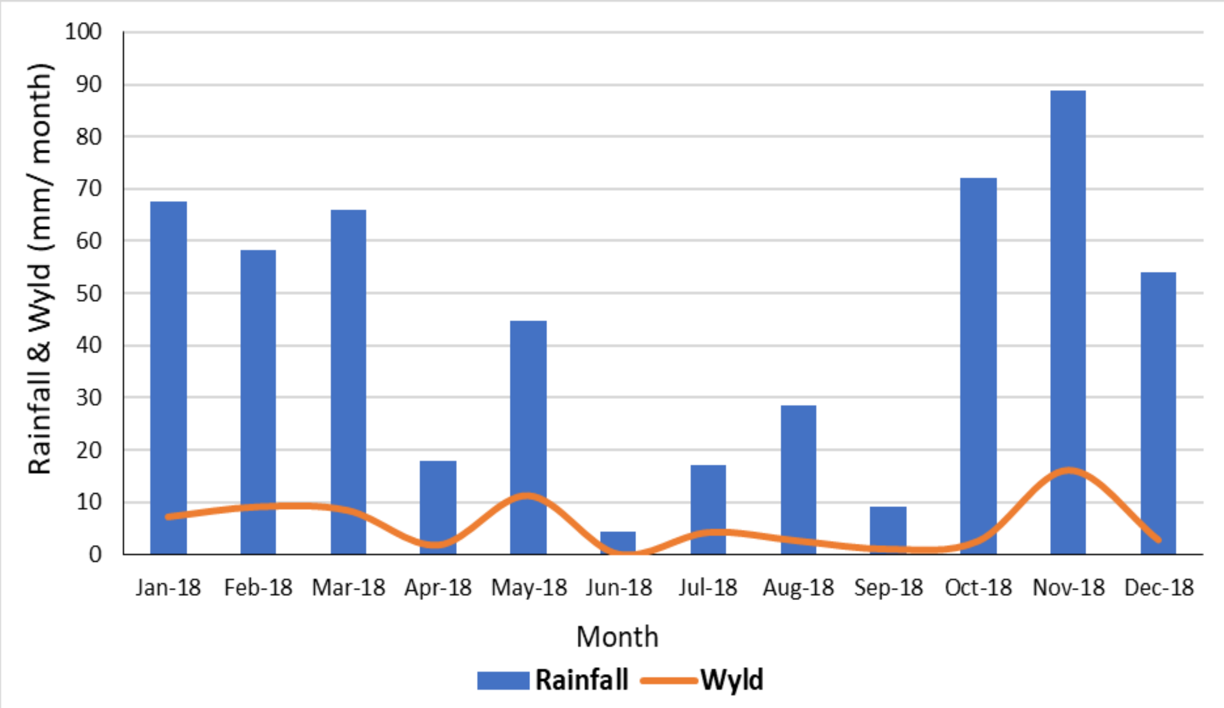

Figure 4.10. Mean annual water yield (WYLD) and rainfall (2018)

Generally, it was found that the WYLD represented 9.15% of the total rainfall, aligning with the regional study by Alexander (1985), who reported a national average of 8.6% for South Africa. This indicates that the Caledon catchment receives a significant amount of rainfall contributing to stream flow, which may lead to reliable and accessible water resources in the area.

4.3.3. Analysis of rainfall and direct runoff

Direct runoff was simulated over a 9-year period from 2010 to 2018 on a monthly time step, combining SURQGEN and lateral flow. As shown in Figure 4.11, the winter period generally experienced low rainfall, with a seasonal average of 12.98 mm. These low rainfall simulations negatively affected direct runoff, resulting in a low average seasonal simulation of 0.97 mm. In contrast, the wet season recorded an average seasonal rainfall simulation of 52.67 mm, with the corresponding direct runoff averaging 6.67 mm.

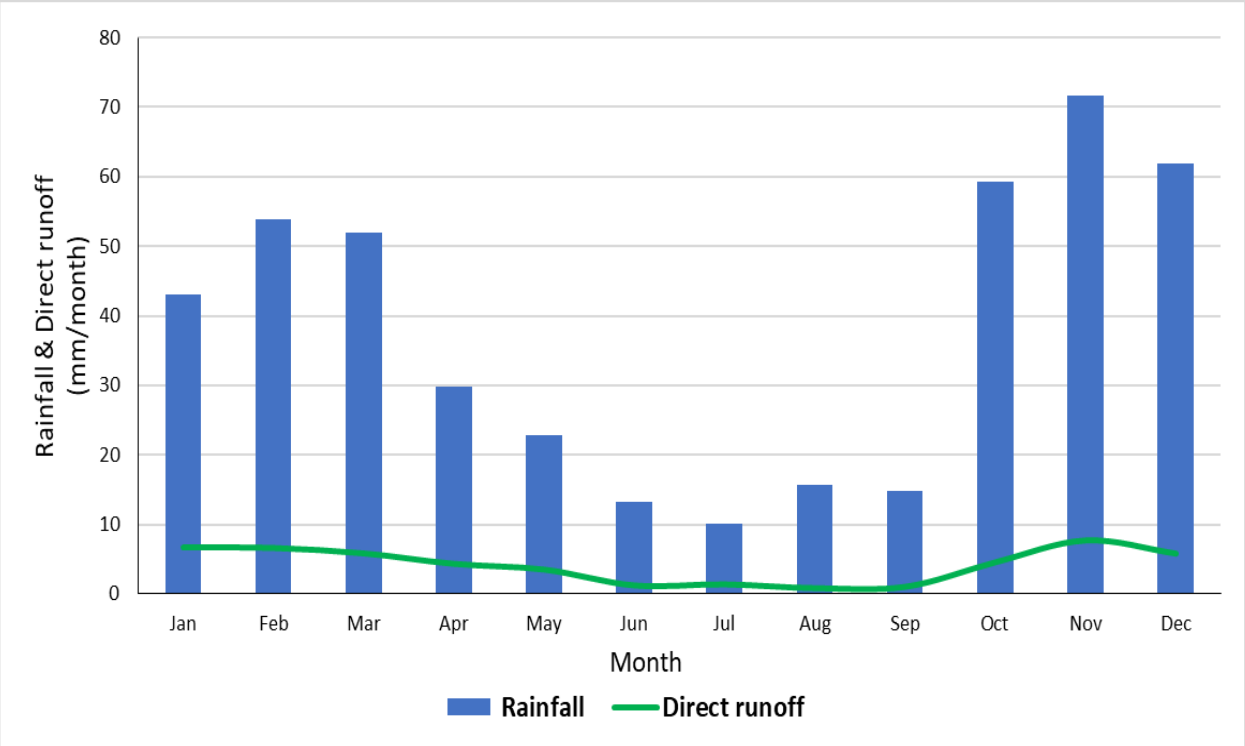

Figure 4.11. Average monthly total runoff and rainfall (2010-2018)

Figure 4.12 shows that the 2010, 2013 and 2016 generated the lowest records of direct runoff of 33.31 mm, 35.81 mm and 21.02 mm, respectively. An exceptional case in these periods of low direct runoff is the year 2016, where direct runoff represented 5.2 % of the mean annual rainfall whereas the 2010 and 2013 direct runoff represented 9.98 % and 7.85% of the rainfall, respectively. These simulation results demonstrates that the 2016 period generated the least runoff from the rainfall received in the year, this might be caused by the 93% of rainfall lost to evapotranspiration (ET), as shown in Figure 4.5, this further demonstrates that the 2016 period was severely affected by the El Niňo-driven droughts as mentioned by Mahasa et al. (2023).

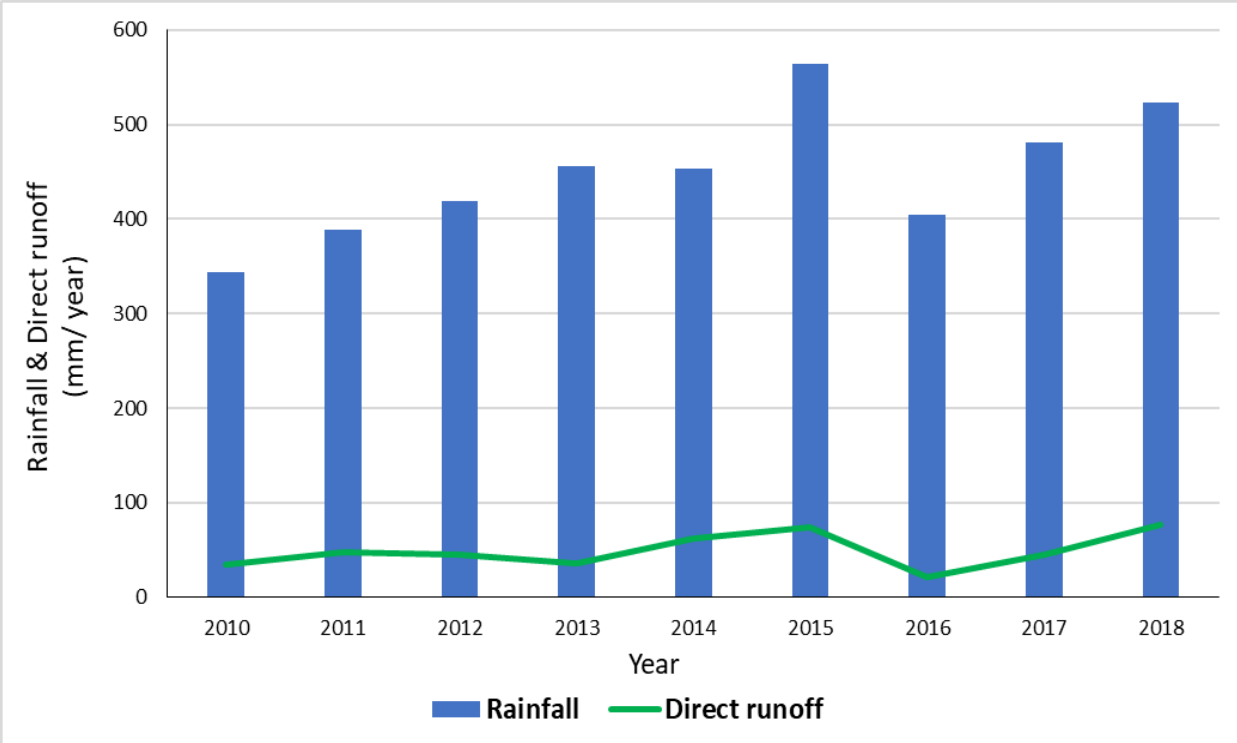

Figure 4.12. Mean annual direct runoff and rainfall (2010-2018)

Figure 4.13 shows the linear correlation of the rainfall-runoff relationship, this illustrates that 9.54 % of the Caledon catchment rainfall is converted to direct runoff. This is a justifiable result as illustrated by Figure 4.7, which demonstrates that the wyld and direct runoff have a similar pattern, both in their magnitude and spatial variability.

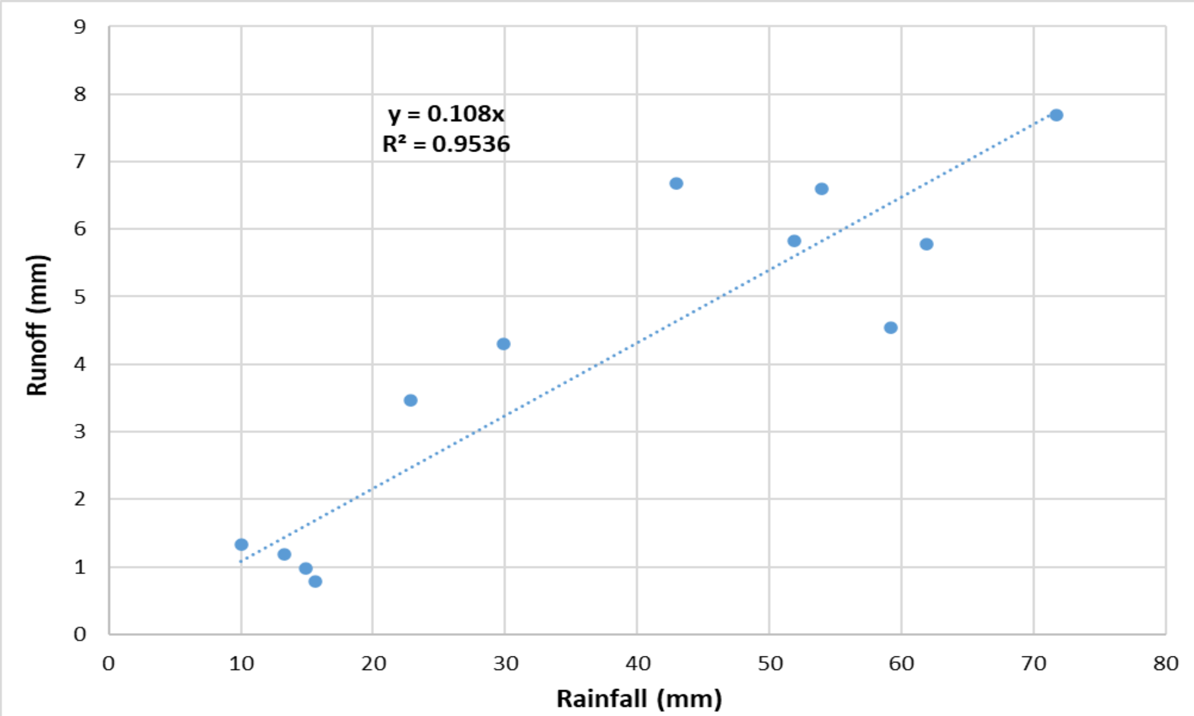

Figure 4.13. Linear correlation of rainfall and runoff

Figure 4.14 presents a comparison of the two components contributing to the direct runoff in this study. It reveals that surface runoff (SURQGEN) is the dominant contributor, accounting for 98.7% of the direct runoff. This predominance is likely due to the steep terrain in most parts of the catchment, which increases the velocity of rainwater upon impact, preventing sufficient infiltration into the ground. Additionally, the impermeable surface of the Drakensberg group, underlain by basaltic rocks, exacerbates surface runoff due to its geological properties that hinder water penetration.

The remaining 1.3% of direct runoff is attributed to lateral flow (LATQ). According to Sahasrabundhe (2011), lateral flow occurs when the rapid downward movement of water passing the Earth's surface increases soil moisture, forcing the water to travel laterally above the subsurface zone. The minimal contribution from lateral flow is likely due to the steep slopes and loamy clay soils in the catchment, both of which impede water infiltration into the soil.

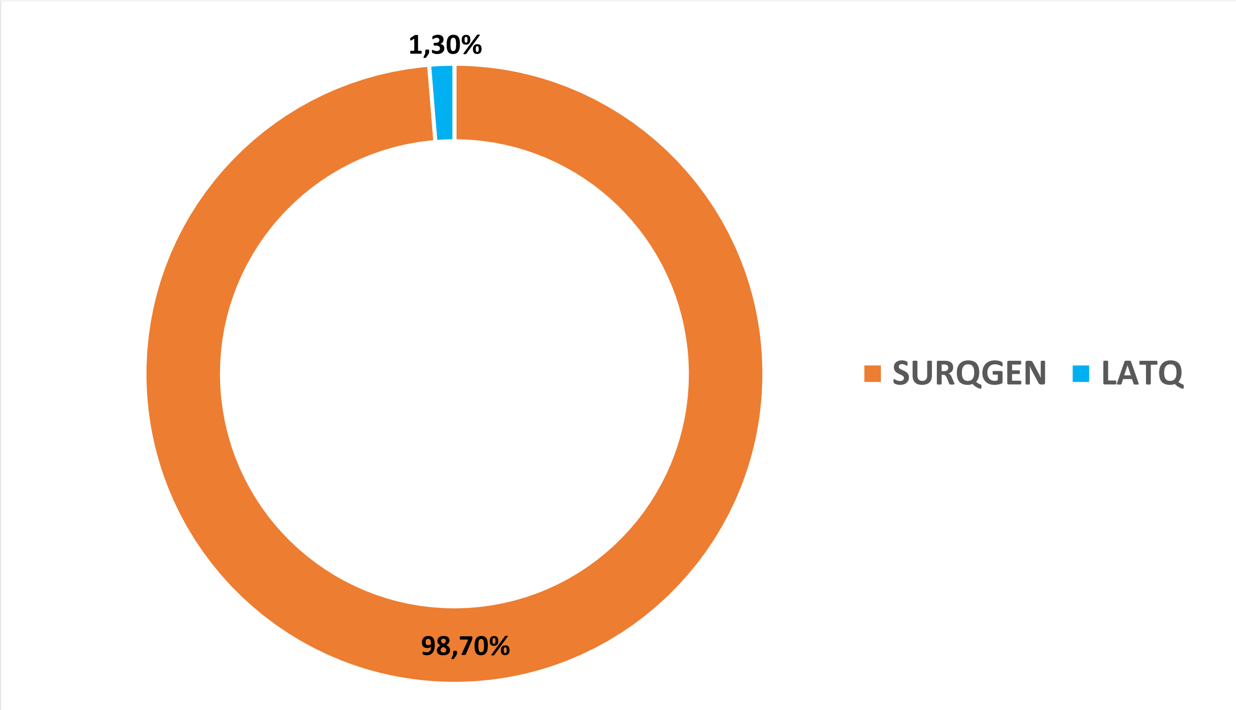

Figure 4.14. Proportion of water balance components contributing to direct runoff

4.3.4. Analysis of rainfall and surface runoff

The surface runoff (SURQGEN) was simulated over a period of 9 years, from 2010 to 2018, on a monthly time step. Figure 4.15 shows that November generally exhibited higher surface runoff, with a maximum of 7.6 mm. This sharp peak in surface runoff is attributed to the high rainfall recorded in November. As Jain et al. (2010) validate, the amount of water generated by a catchment is an index of the rainfall's amount and intensity as well as the land use practices within the catchment.

During the summer, rainfall and surface runoff appear to occur concurrently, with an immediate rise in SURQGEN following an increase in rainfall, and a similar decline in SURQGEN when rainfall decreases. However, the opposite trend is observed in the winter season. In June, rainfall was recorded at 12 mm while SURQGEN was low at 1.05 mm. In July, despite a drop in rainfall to 10 mm, SURQGEN increased to 1.2 mm. August further supports this pattern, with rainfall reaching a winter high of 15 mm, but SURQGEN decreasing to 0.8 mm.

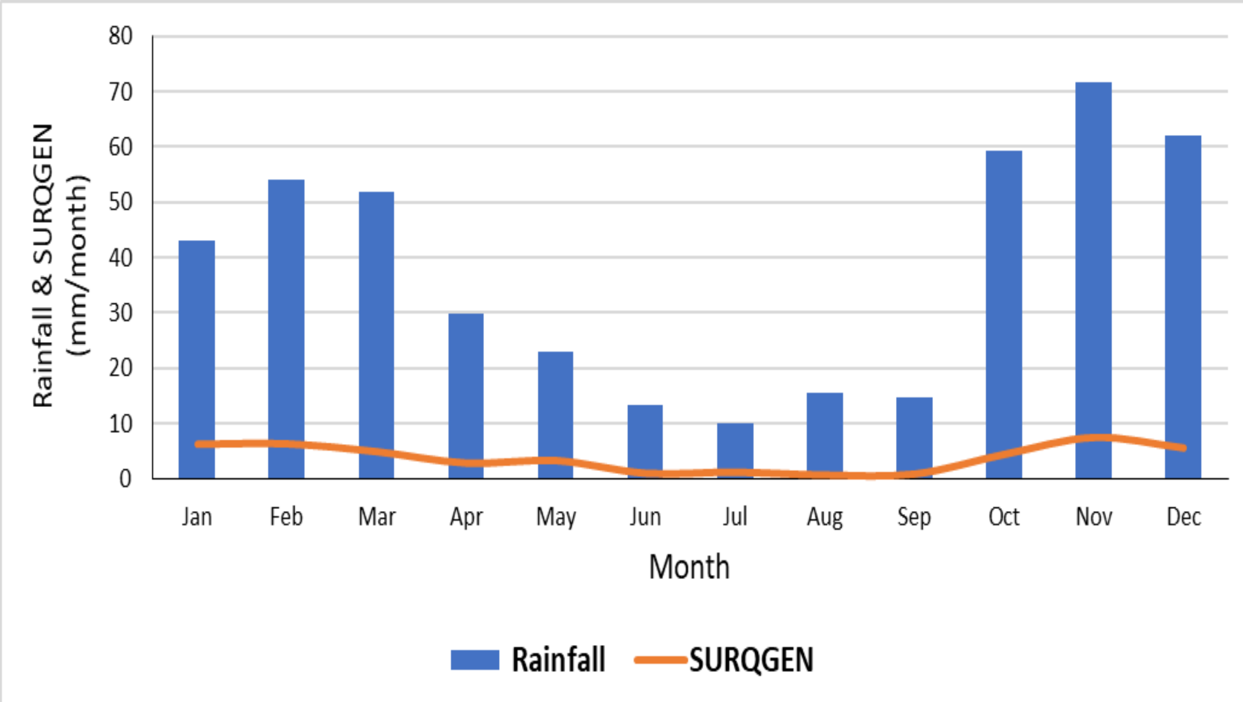

Figure 4.15. Average monthly rainfall and SURQGEN (2010-2018)

4.3.5. Analysis of rainfall and groundwater flow

Groundwater from the shallow aquifers was simulated over a period of 9 years, from 2010 to 2018, with variations in average monthly groundwater flow ranging from 0.84 mm to 4.37 mm, as displayed in Figure 4.16. The groundwater flow generally follows the rainfall trend; increases in rainfall lead to increases in groundwater flow and decreases in rainfall result in corresponding decreases in groundwater flow. However, an exception to this pattern was observed during the winter season. In July, rainfall was recorded at 10.12 mm, corresponding to a groundwater flow of 10.98%. In contrast, September saw a higher rainfall of 14.86 mm, but the groundwater flow was lower at 5.65%.

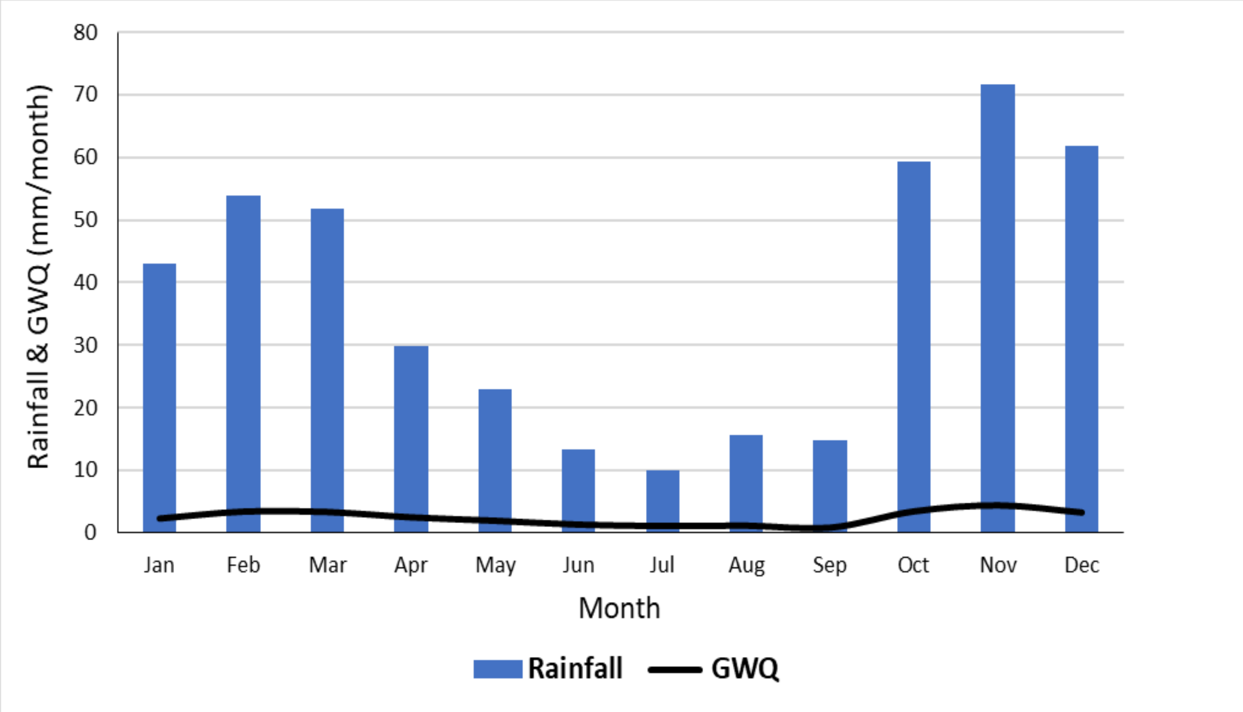

Figure 4.16. Average monthly rainfall and GWQ (2010-2018)

According to Figure 4.17, 2015 generated the highest records of groundwater flow (GWQ), with an annual high of 40.68 mm. In contrast, 2010 recorded the lowest groundwater flow during the 9-year simulation period, with a mean annual value of 18.55 mm. This low simulation can be linked to the exceptionally low rainfall recorded in 2010, where, according to Figure 4.18, the summer rainfall had a seasonal average of 43.7 mm. The period from May to August yielded low simulations, with a GWQ average of 0.3 mm over these four months.

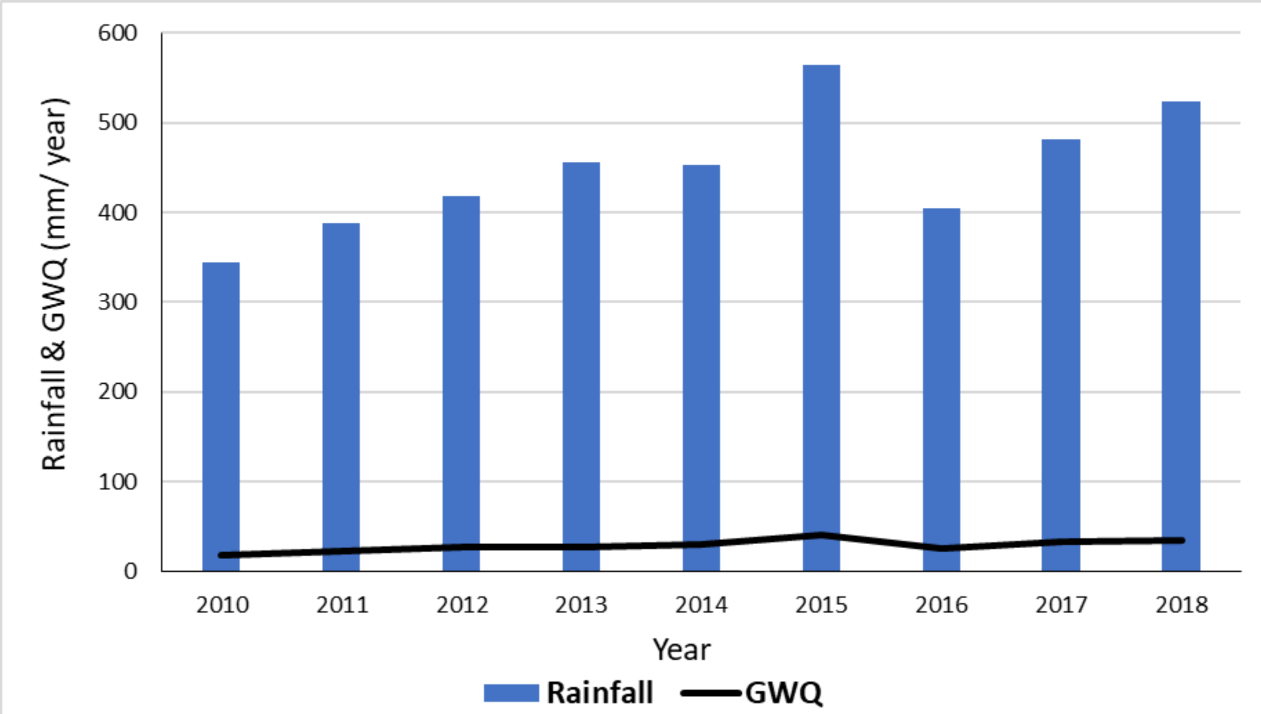

Figure 4.17. Mean annual groundwater (GWQ) and rainfall (2010-2018)

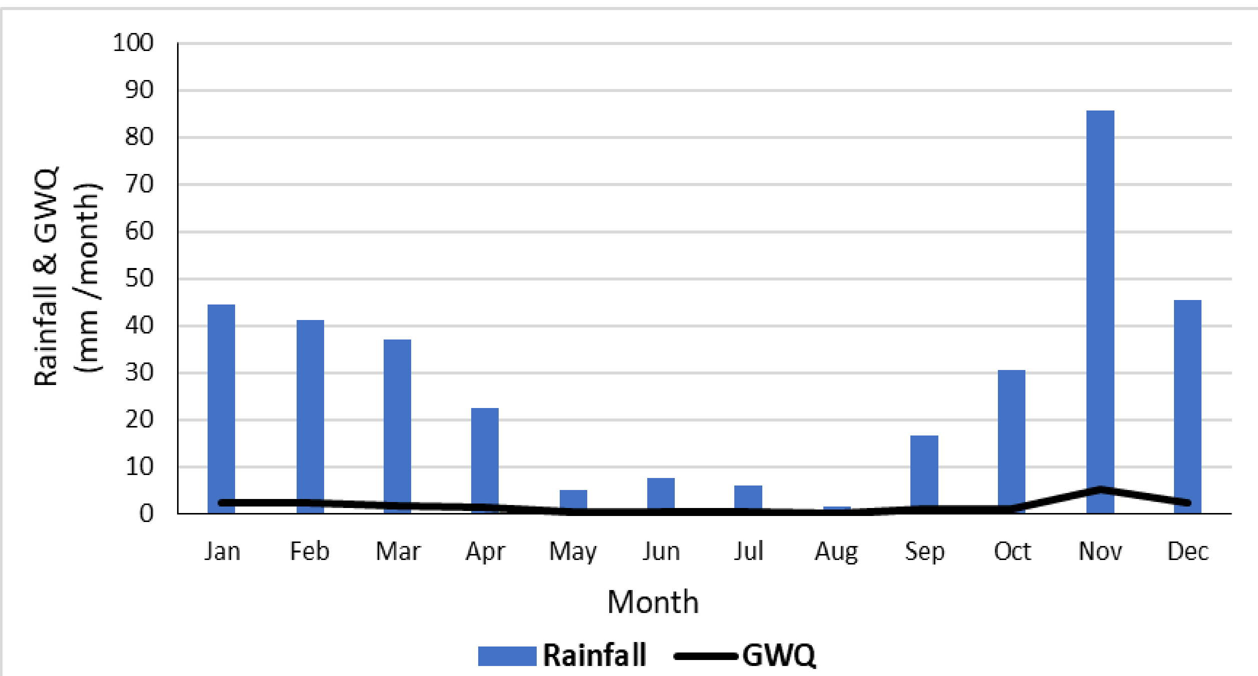

Figure 4.18. Total monthly rainfall and GWQ (2010)

The 2015 period, as displayed in Figure 4.19, recorded the highest groundwater flow during the 9-year simulation, with a mean annual value of 40.67 mm, nearly double that of 2010. The period yielded moderately high rainfall from January to March, resulting in correspondingly high groundwater flow. Additionally, record-high simulations were observed during the winter season, with a peak of 5.17 mm recorded in July.

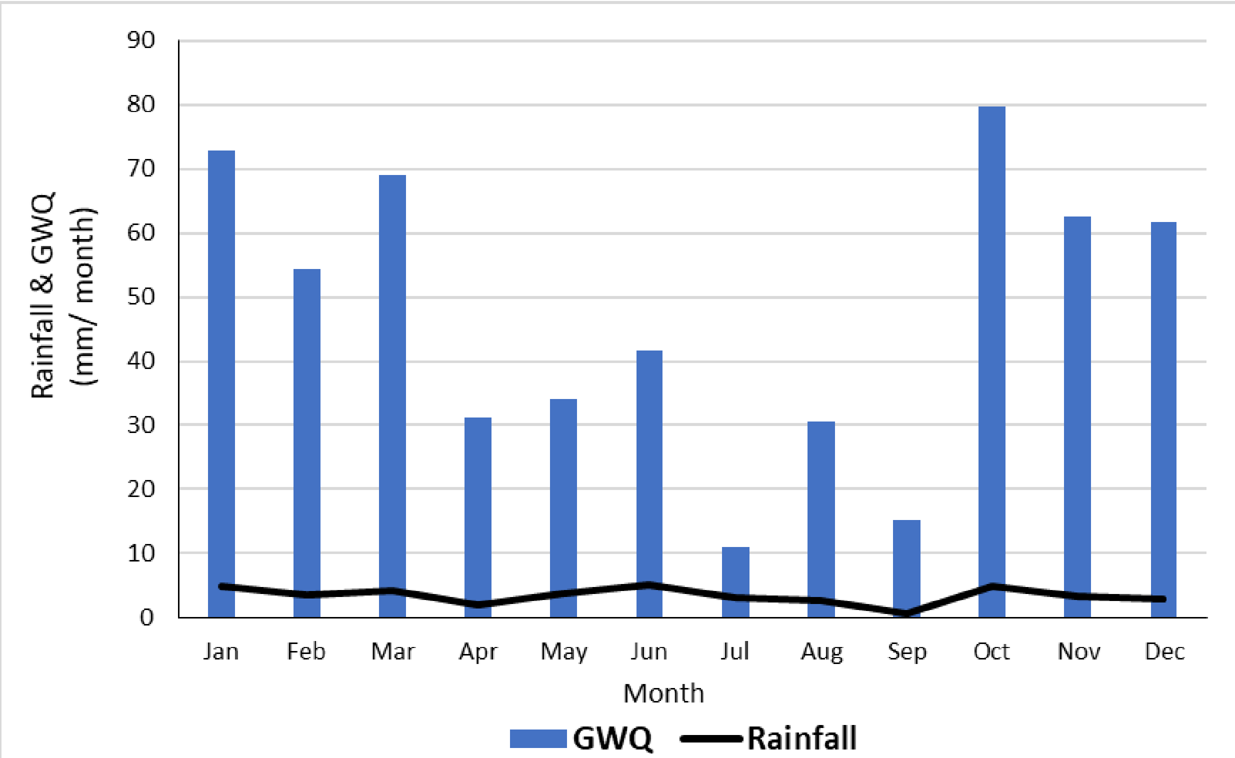

Figure 4.19. Total monthly rainfall and GWQ (2015)

Overall, groundwater flow represented 6.25% of the total rainfall, consistent with other studies. For instance, Colvin et al. (2016) reported a national average of 4% for South Africa, while Nakwafila (2015) found 5% in a study conducted in Namaqualand.

5. CONCLUSION AND RECOMMENDATIONS

5.1. Study Focus

This study analysed the water balance in the Caledon catchment, which spans Lesotho and South Africa, using the SWAT model, a physically based distributed parameter model designed to predict runoff, erosion, sediment, and nutrient transport from agricultural watersheds under various management practices. The model successfully predicted water balance components (WBCs) such as rainfall, evapotranspiration, water yield, surface runoff, and direct runoff. These predictions align closely with other researchers' findings and the Lesotho State of Water Resources Report (2016), confirming the model's accuracy.

5.2. Conclusion

The temporal distribution of rainfall around the watershed is uneven, and the basin lacks sufficient gauging stations, resulting in missing data along the Caledon River. Due to these data limitations, only hydrological parameters were considered in the modelling, excluding water quality parameters. The initial step of this study involved developing the SWAT model using observed rainfall data. This setup enabled the investigation of the variables of interest and led to the following conclusions:

- Accurate data collection, catchment description, and parameterization of basin-scale models are crucial for calibration and validation to ensure model simulations align with observations.
- The study confirms that the model setup complexity was appropriate, providing meaningful estimates compared to observed values, and the model performs well with observed rainfall in large mountainous catchments.
- The SWAT model is suitable for simulating water balance in catchment scales within Lesotho and South Africa.

The study demonstrated that the SWAT model performed satisfactorily in capturing monthly streamflow hydrographs during calibration and validation periods. However, limited detailed rainfall and stream gauge availability affected the model's performance. It is recommended that data should be collected at higher frequencies, such as sub-daily intervals, to better predict peak flows. Mishra (2013) recommends using four to six rain gauges per 2500 km^2 to capture the spatial variability of rainfall effectively.

The inability of the SWAT model to capture peak flows was also noted in studies assessing water availability for competing uses in Lesotho (Maliehe and Mulungu, 2017; Bouraoui et al., 2005). Despite this, the SWAT model effectively delineates the spatiotemporal distribution of WBCs over large catchments, like the Caledon, under limited meteorological data scenarios. This study sets the stage for hydrological modelling in the Caledon catchment, especially on the Lesotho side, where no previous SWAT modelling research has been published.

5.3. Recommendations

The comprehensive water balance analysis conducted in the study area leads to several recommendations for further investigation into the water resources of the Caledon catchment:

- Assess the spatial distribution of evapotranspiration (ET), as the catchment loses significant water due to this hydrological variable.
- Study the impact of climate change and human activities on the catchment's water resources. Ongoing and proposed economic activities, such as the irrigation horticulture project by the Millennium Challenge Account Compact II, may increase water stress on the catchment's resources. Water withdrawals for irrigation increase evaporation, leading to reduced surface runoff (Erraioui et al., 2023). Assessing the impact of climate change can aid in proper planning and water resource management.

- Investigate the impacts of industrial and urban activities on the quality of water resources and the environment, as the Caledon catchment encompasses nearly all of Lesotho's industrial and urban activities.

6. REFERENCES

Abrishamchi, A, Alizadeh, H, Tajrishy, M. 2007.Water Resources Management Scenario Analysis in the Karkheh River Basin, Iran, using the WEAP Model.

Adgolign, T.B, Srinivasa, G.V.R. Abbulu, Y. 2015. WEAP modelling of surface water resources allocation in Didessa Sub-Basin, West Ethiopia. https://doi.org/10.1007/s40899-015-0041-4.

Adu, JT, Kumarasamay, MV. 2017. Assessing Non-Point Source Pollution Models: A Review. Journal of hydrology DOI: 10.15244/pjoes/76497.

Agrawal, N, Desmukh, T.S. 2016. Rainfall Runoff Modelling using MIKE 11 Nam – A Review. ISSN (Online) 2348 – 7968.

Akan, A.O, Houghtalen, R.J. 2013. Urban Hydrology, Hydraulics, and Stormwater Quality: Engineering Application and Computer Modelling. John Wiley & Sons, Inc. USA.

Alexander, W.J.R. 1985. Hydrology of low latitude Southern hemisphere land masses. Hydrobiologia 125.

Arnold, J.G, Allen, P.M. 1996. Estimating hydrologic budgets for three Illinois Watersheds. Journal of Hydrology.

Arnold, J.G, Kiniry, J.R, Srinivasan, R, Williams, J.R, Haney, E.B, Neitsch, S.L. 2011. Soil and Water Assessment Tool Input-Output File Documentation. Soil and Water Research Laboratory, Agricultural Research Service, Grassland, 808 East Black Land Road, Temple, Texas.

Arranz, R, McCartney, M. 2007. Application of the Water Evaluation and Planning (WEAP) model to assess future water demands and resources in the Olifants catchment, South Africa. International Water Management Institute, Southern Africa, Pretoria.

Ayivi, F, Jha, M.K. 2018. Estimation of water balance and water yield in the Reedy Fork-Buffalo Creek Watershed in North Carolina using SWAT. International Soil and Water Conservation Research. https://doi.org/10.1016/j.iswcr.2018.03.007.

Bao-quig, S, Cheng, Q, Xia-hui, W. 2004. Control of Diffuse P-pollutants by Multiple Buffer/Detention Structures by Yuquiao Reservoir, North China. Journal of Environmental Science 16(4): ISSN 616-620.

Bartley, R, Buddemeier, W, Renwick, W.H, Smith, S.V. 2002. Distribution and significance of small, artificial water bodies across the United States landscape. The Science of the Total Environment 299: 21-36.

Baumer, O.W, Wenberg, R.D, Rice, J.F. 1987. The Use of Soil Water Retention Curves in DRAINMOD. In: Proceedings of the 3rd International Workshop on Land Drainage Department of Agricultural Engineering, Ohio State University, Columbus. pp. Al–A10.

Bennie, A.T.P., Hensley, M., 2001. Maximizing precipitation utilization in dryland agriculture in South Africa-a review. *Journal of Hydrology, 241 (1).*

Bhudu, M. 2000. Soil Mechanics and Foundations. John Wiley & Sons, Inc. Arizona, USA.

Black, P.E. 1970. Runoff from Watershed Models. Water Resources Reserve, 6(2):465-477.

Bouma, J. 1986. Using Soil Survey Information to Characterize the Soil Water State. J. Soil Sci.37:1–7.

Bouraoui, F, Benabdallah, S, Jrad, A, Bidoglio, G. 2005. Application of the SWAT Model on the Medjerda River Basin (Tunisia). https://doi.org/10.1016/j.pce.2005.07.004.

Burgher, Heyns, P.J, Hoffman, E, Kleynhans, E.P.J, Koegelenberg, F.H, Lategan, M.T, Stimie, C.M, Inulder, D.J, Uys. W.J, Van Der Merwe, F.P, Van Der Stoep, I. 2013. Irrigation Manual. ARC- Institute for Agricultural Engineering. Pretoria, RSA.

Busacca AJ, Sweeney MR. 2004. Earth systems and environmental science. Washington State University, Pullman, WA, USA. https://doi.org/10.1016/B0-12-348530-4/00009-6

Byakod, K, Shivapur, AV, Venktesh, B. 2017. Application of SWAT model for generating surface runoff and estimation of water availability for Balehonnuru catchment area for Badhra Riverbasin. *Journal of hydrology e*-ISSN 2395-0056.

Chai, T, Draxler, R.R. 2014. Root mean square error (RMSE) or mean absolute error (MAE) - Arguments against avoiding RMSE in the literature. Geoscientific Model Development 7(3). https://doi.org/ 10.5194/gmd-7-1247-2014.

Choudhari, K, Panigrahi, B, Jagadish, C. P. 2014. Simulation of rainfall-runoff process using HEC-HMS model for Balijore Nala watershed, Odisha, India. ISSN 0976 – 4380.

Chow, V.T. 2010. Applied Hydrology. Tata McGraw-Hill Education. USA. ISBN: 007070242X, 9780070702424.

Chu, X, Steinman, A, 2009. Event and Continuous Hydrologic Modelling with HEC-HMS. Journal of Irrigation Drainage Engineering 135, 119–124. https://doi.org/10.1061/(ASCE)0733-9437(2009)135:1(119).

Coleman, T, Van Niekerk, A. 2007. Water Quality in the Orange River. Orange Senqu River Commission. Midrand, RSA.

Colvin C, Muruven D, Lindley D, Gordon H, Schachtschneider K. 2016. Water facts and futures: rethinking South Africa’s water future. WWF-SA 2016 Water Facts and Futures.

Das, B.M. 2006. Principles of Geotechnical Engineering. 5th Edition. Thomson. California, USA.

Davis, M.L, Cornwell ,D.A. 2013. Introduction to Environmental Engineering. Fifth Edition. McGraw-Hill International. New York, USA.

Delleur, J.W. 1999. The Handbook of Groundwater Engineering. CRC Press. USA.

Demetriou, C, Punthakey, J.F. 1999. Evaluating sustainable groundwater management options using the MIKE SHE integrated hydrogeological modelling package. Environmental Modelling and Software 14(2): 129-140.

Demirel, M.C, Venancio, A, Kahya, E. 2009. Flow forecast by SWAT model and ANN in Pracana basin, Portugal. Advances in Engineering Software 40: ISSN 467–473.

Devito, K, Creed, I, Gan, T, Mendoza, C, Petrone, R, Silins, U. 2005. A framework for broad- scale classification of hydrologic response units on the boreal plain: Is topography the last thing to consider? Hydrological Processes.

Dimova, G, Tzanov, E, Ninov, P.L, Ribarova, I, Kossida, M. 2013. Complementary Use of the WEAP Model to Underpin the Development of SEEAW Physical Water Use and Supply Tables, Procedia Engineering. ISSN (Online) 70, 563-572.

Erraioui, L, Soufiane, T, Eddine, K.T, Chao, J, Mansouri, B.E. Hydrological Modelling in the Ouergha Watershed by Soil and Water Analysis Tool. https://doi.org/10.3390/geographies3010001.

Food and Agricultural Organization. Digital Soil Map of the World. https://data.apps.fao.org/map/catalog/srv/eng/catalog.search#/metadata/cc45a270-88fd-11da-a88f-000d939bc5d8. Accessed on 9 September 2022.

Gerbert, W.A. 1971. Hulburt Greek Hydrology. US Geological Survey Open File Report. Wisconsin, USA.

Gibbs, A, Gibbs, T .2002. A water supply and pollution crisis in Lesotho's textile factories: The problems of footloose investment. Centre for civil society and school of development studies report, University of Natal, Durban.

Golmohammadi, Prasher, S, Madani, A, Rudra, R. 2013. Evaluating Three Hydrological Distributed Watershed Models: MIKE-SHE, APEX, SWAT. Journal of Hydrology. doi:10.3390/hydrology1010020

Gumindoga, W, Makurira, H, Phiri, M, Nhapi, I. 2016. Estimating runoff from ungauged catchments for reservoir water balance in the Lower Middle Zambezi Basin. http://dx.doi.org/10.4314/wsa.v42i4.15

Gupta, H, Sorooshian, S, Yapo, P. 1999. Status of Automatic Calibration for Hydrologic Models: Comparison with Multilevel Expert Calibration. International Journal Hydrologic Engineering (4(2)).

Halwatura, D, Najim, M. 2013. Application of the HEC-HMS model for runoff simulation in a tropical catchment. Environmental Modelling Software 46, 155–162. Doi.org/10.1016/j.envsoft.2013.03.006.

Hamdan, A.N.A, Almuktar, S, Scholz, M. 2021. Rainfall-Runoff Modeling Using the HEC-HMS Model for the Al-Adhaim River Catchment, Northern Iraq. Doi.org/10.3390/hydrology8020058.

Hattingh, L. 2008. Water Quality in the Orange River. Orange Senqu River Commission. Midrand, RSA.

Heath, R and Brown, C. 2007. Environmental Considerations Pertaining to the Orange River. Orange Senqu River Commission. Midrand, RSA.

Hiddema, U, Erasmus, G. 2007. Legislation and Legal Issues Surrounding the Orange River Catchment. Orange Senqu River Commission. Midrand, RSA.

Hussainzada W, Lee H.S. 2021. Hydrological Modelling for Water Resource Management in a Semi-Arid Mountainous Region Using the Soil and Water Assessment Tool: A Case Study in Northern Afghanistan. https://doi.org/10.3390/hydrology8010016.

Irvem, A, El-Sadek, A. 2018. Evaluation of streamflow simulation by SWAT model for the Seyhan River Basin. Journal of hydrology Cukurova J. Agric. Food Sci. 33(2) 99-110.

Ivezic, V et al. 2017. A review of procedures for water balance modelling. Journal of hydrology

JIANG, L, CHEN, Y, WANG, H. 2015. Urban flood simulation based on the SWMM model. Doi:10.5194/piahs-368-186-2015

Kangsabanik, S, Murmu, S. 2017. Rainfall-runoff modelling of Ajay River catchment using SWAT model. Doi :10.1088/1755-1315/67/1/012033

Kateb, A.Z, Bouchelkia, H, Benmansour, A, Belarbi, F. 2019. Hydrological modeling using the SWAT model based on two types of data from the watershed of Beni Haroun dam.https://DOI.org/10.2478/jwld-2019-0065

Kim, H, Jung, M, Mallari, K. J. B, Pak, G, Kim, S, Kim, S, Kim, L, Yoon, J. 2015. Assessment of porous pavement effectiveness on runoff reduction under climate change scenarios. Desal. Water Treat. 53 (11), ISSN 3142–3147.

Krause, P, Boyle, D, Base, F. 2005. Comparison of different efficiency criteria for hydrological model assessment. SRef-ID: 1680-7359/adgeo/2005-5-89.

Kruger, E.J, Van Vuuren, S.J, Pienaar W.J, Van Dijk, M, Smither, J.C, Rooseboom, A, Pienaar, P.A. 2013. Drainage Manual. 6 th Edition. The South African National Roads Agency SOC Limited. Pretoria, RSA.

Kurbah, S, Jain, M. 2017. Rainfall Runoff modelling of a river basin using SWAT model. Journal of hydrology ISSN: 2278-0181.

Lazaro, T.R. 1990. Urban Hydrology: A Multidisciplinary Perspective. Technomic Publishing. Pennsylvania, USA.

Legates, D.R, McCabe, G.J. 1999. Evaluating the use of “good-of-fit” measures in hydrologic and hydroclimatic model validation. Water Resources Research. Vol. 35. Iss. 1.

Loague, K, Green, R.E. 1991. Statistical and graphical methods for evaluating solute transport models: Overview and application. Journal of Contaminant Hydrology 7: 51-73.

Maharjan, B, Pachel, K, Loigu, E. 2017. Modelling stormwater runoff quality and pollutant loads in a large urban catchment. Proc. Est. Acad. Sci. 2017, 66, 225–242. https://doi.org/10.3176/proc.2017.3.02

Mahasa, P.S, Xulu, S, Mbatha, N. 2023. Characterization of Evapotranspiration in the Orange River Basin of South Africa-Lesotho with Climate and MODIS Data. https://doi.org/10.3390/w15081501.

Majidi, A, Shahedi, K, 2012. Rainfall-Runoff simulation, HEC-HMS, Green-Ampt, Abnama Watershed, Iran. International Journal of Hydraulics Engineering. Doi.org/10.5923/j.ijhe.20120101.02.

Maliehe, M, Mulungu, D.M.M. 2017. Assessment of Water Availability for Competing Uses Using SWAT and WEAP in South Phuthiatsana Catchment, Lesotho. Phys. Chem. Earth Parts ABC 2017, 100, 305–316. https://doi.org/10.1016/j.pce.2017.02.014.

Mango, L.M, Melesse, A.M, McClain, M.E, Gann, D, Setegn, S.G. 2011. Land use and climate change impacts on the hydrology of the upper Mara River Basin, Kenya: results of a modeling study to support better resource management. Hydrology and Earth System Science 15:2245–2258

Mare, H. 2007. Review of Surface Hydrology in the Orange River Catchment. Orange Senqu River Commission. Midrand, RSA.

Mays, L.W. 2001. Water Resources Engineering. John Wiley & Sons, Inc. New York, USA.

Mckenzie, R, Seago, C. 2007. Current Analytical Methods and Technical Capacity of the Four Orange Basin States. Orange Senqu River Commission. Midrand, RSA.

Metobwa, O.G.M, Mourad, K.A, Ribbe, L. 2018. Water Demand Simulation Using WEAP21: A case of the Mara River Basin, Kenya. Int. J. Nat. Res. Ecol. Manag. 3, 9–18.

Midgley, D, Pitman, W.V, Middleton, B. 1994. Surface water resources of South Africa 1990 No. 298/1/94). Pretoria, South Africa: Water research commission.

Ministry of natural resources. 2002. *Industrial wastewater management policy*. Ministry of Natural Resources publication, Lesotho.

Ministry of water affairs. 2014. *Long term water and sanitation strategy: volume II*. Ministry of water affairs, Lesotho.

Ministry of water affairs. 2016. *State of water resources report 2016/2017*. Ministry of water affairs, Lesotho.

Mishra, A. 2013. Effect of rain gauge density over the accuracy of rainfall: A case study over Bangalore, India. Springer-Plus.

Moeletsi, M.E, Walker, S, Hamandawana, H. 2013. Comparison of the Hargreaves and Samani equation and the Thornthwaite equation for estimating dekadal evapotranspiration in the Free State Province, South Africa. https://doi.org/10.1016/j.pce.2013.08.003.

Moriasi, D.N, Arnold, J.G, Van Liew, M.W, Bingner, R.L, Harmel, R.D, Veith, T.L. 2007. Model evaluation guidelines for systematic quantification of accuracy in watershed simulations. Transactions of the ASABE 50: 885–900

Nakwafila A.N. 2015. *Salinisation source (s) and mechanism (s) in shallow alluvial aquifers along the Buffels River, Northern Cape Province, South Africa (PhD Thesis)*. Stellenbosch University, Stellenbosch, South Africa.

National Oceanic and Atmospheric Administration. Daily wind speed data. https://www.noaa.gov/. Accessed on 9 September 2022.

Nash, J.E, Sutcliffe, J.V. 1970. River flow forecasting through conceptual models' part I – A discussion of principles. Journal of Hydrology. Vol. 10. Iss. 3.

Ndomba, P, Mtalo, F, Killingtveit, A. 2008. SWAT model application in a data scarce tropical complex catchment in Tanzania. Physics and Chemistry of the Earth 33: 626–632

Neitsch, S.L, Arnold, J.G, Kiniry, J.R, Srinivasan, R, Williams, J. R. 2005. Soil and Water Assessment Tool Theoretical Documentation. Texas Water Resources Institute, Collage Station, Texas. http://www.swat.tamu.edu.

Neitsch, SL, Arnold, JG, Kiniry, JR, Williams, JR. 2009. Soil Water Assessment tool: theoretical documentation. Agricultural research services, Texas, USA.

Nusser, M. 2002. Pastoral utilization and land cover change: A case study from the Sanqabethu Valley, Eastern Lesotho. Erdkunde.

Patil, NS, Raikar, RV, Manor, S. 2014. Runoff modelling for Bhima River using SWAT hydrological model. Journal of hydrology ISSN: 2278-0181.

Pegram, GC, Bath, AJ. 1995. Role of non-point source in development of a water quality management plan for Mgeni river catchment. Journal of hydrology Wat. Sci. Tech 32.

Pohlert, T, Huisman, AJ, Breuer, L, Frede, HG. 2005. Modelling of point and non-point source pollution of nitrate with SWAT in the river Dill, Germany. Journal of Hydrology SRef-ID: 1680- 7359/adgeo/2005-5-7.

Prasad, N.B.N. Groundwater Hydrology. Centre for Water Resources Development and Management. Technical Report, https://www.researchgate.net/publication/317328777

Puckett, W. E., Dane, J.H, Hajek, B.F. 1985. Physical and Mineralogical Data to Determine Soil Hydraulic Properties. Soil Sci. Soc. Am. J. 49: 831–836.

Raghunath, H.M. 2006. Hydrology: Principles, Analysis and design. 2nd Edition. New Age International Publishers. New Delhi, India.

Ranit, AB, Durge, PV, Ranit, SA. 2014. Overview of hydrology with hydrological models and modelling. Journal of Hydrology ISSN: 2278-0181.

Rawls, W.J., Brakensiek, D.L, Saxton, K.E. 1982. Estimation of Soil Water Properties. Trans. ASAE. 25(5):1316–1320, 1328.

Rouhani, H, Willems, P, Feyen, J. 2009. Effect of watershed delineation and areal rainfall distribution on runoff prediction using the SWAT model. Doi: 10.2166/nh.2009.042.

Ruan, H, Zou, S, Cong, Z, Wang, Y, Yin, Z, Lu, Z, Li, F, Xu, B. 2016. Runoff simulation by SWAT model using high-resolution gridded precipitation in the upper Heihe river basin, North-eastern Tibetan Plateau. Journal of Hydrology doi:10.5194/hess-2016-594.

Sahasrandudhe, S.R. 2011. Water Resources Engineering. S.K Kataria & Sons. New Delhi, India.

Sahu, S, Pyasi, S.K, Galkate, R.V. 2020. A Review on the HEC-HMS Rainfall-Runoff Simulation Model. ISSN(p): 2250–0057; ISSN(E): 2321–0087.

Sandu, M.A, Virsta, A. 2015. Applicability of MIKE-SHE to Simulate Hydrology in Argesel River Catchment. Journal Hydrology.

Sanjay K.J, Jaivir T, Vishal S. 2010. Simulation of Runoff and Sediment Yield for a Himalayan Watershed Using SWAT Model. https://doi:10.4236/jwarp.2010.23031 . Water Resource and Protection.

Shawul, A.A, Alamirew, T, Dinka, M.O. 2013. Calibration and validation of SWAT model and estimation of water balance components of Shaya mountainous watershed, Southeastern Ethiopia. Hydrology and Earth System Sciences. doi:10.5194/hessd-10-13955-2013.

Sheth, M. 2018. Review: Rainfall Runoff Modelling. International Journal of Engineering Research & Technology (IJERT) ISSN: 2278-0181.

Shruti B and Patil K. 2016. Water balance assessment using Q-SWAT. Journal of hydrology ISSN: 2319-6890.

Singh, J, Knapp, H.V, Demissie, M. 2004. Hydrologic modelling of the Iroquois River watershed using HSPF and SWAT. ISWS CR 2004-08. Illinois State Water Survey.

Singh, R, Subramanian, K, Refsgaard, J.C. 1999. Hydrological modelling of a small watershed using MIKE SHE for irrigation planning. Agricultural Water Management 41(3): 149-166.

Smith, H.J, Van Zyl, A.J, Claassens, A.S, Schoeman, J.L, Laker, M.C. 2012. Soil Loss Modelling in the Lesotho Highlands Water Project Catchment Areas. South African Geographical Journal. https://doi.org/10.1080/03736245.2000.9713694.

Temprano, J, Arango, O, Cagiao, J, Suarez, J, Tejero, I. 2006. Stormwater Quality Calibration by SWMM: A Case Study in Northern Spain. DOI:10.4314/wsa. v32i1.5240.

Tena, T.M. Mwaanga, P. Nguvul, A. 2019. Hydrological Modelling and Water Resources Assessment of Chongwe River Catchment using WEAP Model. Doi:10.3390/w11040839.

Tetsoane, ST. 2013. Evaluation of the SWAT model in simulating catchment hydrology: Case study of the Modder River basin. Department of Civil Engineering, Central University of Technology, Bloemfontein, South Africa.

Tibebe, M, Assefa, M, Melesse, Hailu, D. 2016. Rainfall-runoff relation and runoff estimation for Holetta River, Awash subbasin, Ethiopia using SWAT model. DOI: 10.5897/IJWREE2015.0601.

Tompkins, R. 2007. Institutional Structures in the Four Orange Basin States. Orange Senqu River Commission. Midrand, RSA.

UN Water. 2007.Global Water Partnership (GWP) Road-mapping for Advancing Integrated Water Resources Management (IRWM) Processes. UN Water.

UN Water. 2008. Transboundary Waters: Sharing Benefits, Sharing Responsibilities. UN Water.

UN Water. 2015. Compendium of Water Quality Regulatory Frameworks: Which Water for Which Use. UN water.

UN Water. 2016. Worldwide Assessment of Freshwater Quality: A UN Water Analytical Brief. UN Water.

United States Embassy. Millennium Challenge Corporation Approves Second Compact with the Government of Lesotho. https://ls.usembassy.gov/millennium-challenge-corporation-approves-second-compact-with-the-government-of-lesotho/. Accessed on 2 December 2024.

United State Geological Survey. Land Cover Map/Digital Elevation Model. https://earthexplorer.usgs.gov/. Accessed on 9 September 2022.

United States Geological Services. Natural Water Cycle. https://www.usgs.gov/media/images/natural-water-cycle-jpg. Accessed on 2 December 2024

Viles, A. 2007. Review of Groundwater Resources in the Orange River Catchment. Orange Senqu River Commission. Midrand, RSA.

Wang, C, McKeague, J.A, Topp, G.C. 1985. Comparison of Estimated and Measured Horizontal K-sat Values. Can. J. Soil Sci., 65:707–715.

Ward, A.D, Trimble, S.W. 2003. Environmental Hydrology. 2 nd Edition. Lewis Publishers. Washington D.C., USA.

Williams, J.R. 1969. Flood Routing With Variable Travel Time or Variable Storage Coefficients. Transactions of the ASAE, 12(1), 100-0103.

Willmott, C.J, Ackleson, S.G, Davis, R.E, Feddema, J.J, Klink, K.M, Legates, D.R, O'Donnell, J, Rowe, C.M. 1985. Statistics for the Evaluation and Comparison of Models. Journal of Geophysical Research 90(C5): ISSN 8995-9005.

Wilson, E.M. 1990. Engineering Hydrology. Pelgrave Macmillian. New York, USA.

Wu, J.Y, Thompson, J.R, Kolka, R.K, Franz, K.J, Stewart, T.W. 2013. Using the Storm Water Management Model to predict urban headwater stream hydrological response to climate and land cover change. Hydrological Earth System Science. ISSN 4743–4758.

Yang, W, Brüggemann, K, Seguya, K.D, Ahmed, E, Kaeseberg, T, Dai, H, Hua, P, Zhang, J, Krebs, P. 2020. Measuring performance of low impact development practices for the surface runoff management. Environ. Sci. Ecotechnology 2020, 1, 1–9. https://doi.org/10.1016/j.ese.2020.100010.

Yates, D, Sieber, J, Purkey, D, Lee. 2005. WEAP21—A demand- priority- and preference-driven water planning model-part 1: model characteristics. International Water Resources Association 30(4):487–500.

Zakizadeh, F, Nia, A.M, Salajegheh, A, Sañudo-Fontaneda, L.A, Alamdari, N. 2022. Efficient Urban Runoff Quantity and Quality Modelling Using SWMM Model and Field Data in an Urban Watershed of Tehran Metropolis. https://doi.org/10.3390/su14031086.

Zhang, J, Zhang, M, Song, Y, Lai, Y. 2021. Hydrological simulation of the Jialing River Basin using the MIKE SHE model in changing climate. Doi: 10.2166/wcc.2021.253.